Investigating the role of testis-mitochondrial genes in Drosophila lethal (3) malignant brain tumor

Ánxela Louzao Boado

Tesis Doctoral

UNIVERSITAT DE BARCELONA

Investigating the role of testis-mitochondrial genes in *Drosophila lethal (3) malignant brain tumor*

Memoria presentada por ÁNXELA LOUZAO BOADO para optar al grado de Doctora por la Universitat de Barcelona

Programa de Genética

Tesis doctoral realizada en el laboratorio de División celular del Institut de Reçerca Biomédica de Barcelona

Director	Tutor	Doctoranda
Dr. Cayetano González Hernández	Dr. Emili Saló Boix	Ánxela Louzao Boado

Barcelona, 2019

Investigating the role of testis-mitochondrial genes in *Drosophila lethal (3) malignant brain tumor*

Ánxela Louzao Boado

Institute for Research in Biomedicine

Universitat de Barcelona

A thesis submitted for the degree of

PhilosophiæDoctor (PhD).

Barcelona 2019

Acknowledgements

I would like to thank my PhD supervisor Dr. Cayetano González for giving me the opportunity to carry out the PhD in his laboratory. Through his critical scientific mind, broad knowledge and insightful comments, he has helped me to develop this thesis project.

I would like to express my sincere gratitude to all my laboratory colleagues, past and present, for their scientific and personal support throughout these years. Special thanks to Fabrizio Rossi, for introducing me to Drosophila research during my Master Thesis, and also to Pepe Reina, for his infinite knowledge and always available help. Vicky, Piet, Cristina, Salud, Giulia, Trini, Andrea, Judit and Madhulika, thanks for being great colleagues and for contributing to this thesis project with your scientific advises and suggestions.

I would like to thank the members of my Thesis Advisory Committee, Fátima Gebauer, Jordi Casanova and Emili Saló, for their useful comments and supervision during the development of this thesis project.

I had the pleasure to stay in the laboratory of Dr. Antonio Zorzano for my lab rotation, directly working with Juan Pablo Muñoz, who introduced me to other fields in science which I knew little about.

I am very thankful to the Spanish Ministerio de Economía y Competitividad, which granted me a fellowship for accomplishing my PhD at IRB Barcelona (Ayudas para contratos predoctorales Severo Ochoa 2014, SVP-2014-068698). I also would like to thank the members of the IRB administration and facilities for their bureaucratic and scientific support.

A huge thanks to all my friends, either from Barcelona, Galicia or abroad, for all the support and the joyful moments shared throughout these years.

E por último, e sobre todo:

Gracias ó meu compañeiro, polo extraordinario do común.

E gracias á miña familia, polo seu inmenso cariño e incondicional apoio.

Abstract

Genetically tractable models such as *Drosophila melanogaster* may help to identify new approaches to halt malignant growth. During my doctoral thesis, I performed a screen to find mitochondrial genes required for the growth of *lethal (3) malignant brain tumor*. I discovered that several testis-mitochondrial genes, i.e. genes with a mitochondrial function and a maximum expression in testes, were required for the growth of *l(3)mbt* tumors, rescuing both viability and brain anatomy traits. Nevertheless, inhibition of testis-mitochondrial genes did not affect either wild-type or *brat* tumor development. One of these testis-mitochondrial genes, *ttm2*, was found to be expressed both in wild-type and *l(3)mbt* brains. In addition, when overexpressed in an otherwise wild-type background, Ttm2 produces hyperplasia specifically in the neuroepithelial cells of the medial outer proliferative center (OPC). Yet, ectopic expression of Ttm2 in either central brain or medulla neuroblasts does not affect neuroblast division or number, suggesting that the brain cell types are differentially sensitive to mitochondrial function alteration. The data presented in this thesis project provides novel information about the critical role of mitochondria controlling both cell fate and carcinogenesis.

Resumen

Durante los últimos años, el uso de *Drosophila melanogaster* como organismo modelo ha servido para identificar nuevos mecanismos moleculares implicados en el crecimiento tumoral. Durante mi tesis doctoral, descubrí que varios genes mitocondriales son necesarios para el crecimiento del tumor cerebral causado por la falta de función del gen *lethal (3) malignant brain tumor* (*l(3)mbt*). En concreto, varios genes mitocondriales testiculares, es decir, genes con función mitocondrial y máxima expresión en el testículo de machos adultos, son imprescindibles para el desarrollo de tumores *l(3)mbt*. Sin embargo, la función de estos genes mitocondriales testiculares es prescindible tanto para el desarrollo de cerebros "wild-type" como del tumor cerebral *brat*. Uno de estos genes mitocondriales testiculares, *ttm2*, se expresa tanto en cerebros normales como en cerebros tumorales *l(3)mbt*. Además, cuando *ttm2* es sobreexpresado en el neuroepitelio del cerebro larvario, produce hiperplasia. Esta hiperplasia es específica de las células mediales del "outer proliferative center" (OPC), sin afectar ni al "inner proliferative center" (IPC) ni a los neuroblastos del cerebro. Estos resultados sugieren que los diferentes tipos celulares del cerebro de la larva de *Drosophila* tienen requerimientos metabólicos distintos y no reaccionan de igual manera a la alteración de la función mitocondrial. Los resultados presentados en esta tesis doctoral proporcionan nuevos datos que confirman el papel crítico de la mitocondria tanto en el proceso de carcinogénesis como en el mantenimiento de la identidad celular.

Contents

List of Abbreviations

The following list describes several abbreviations that will be later used within the body of the document.

a.u. Arbitrary units
AEL After Egg laying
aPKC atypical Protein Kinase C
ATP Adenosine Triphosphate
ATP5A ATP synthase subunit 5A
BCA Bicinchoninic acid
BDSC Bloomington Drosophila Stock Center
Brat Brain tumor
cAMP cyclic Adenosine Monophosphate
CB Central Brain
CD8 Cluster of Differentiation 8
cDNA complementary Deoxyribonucleic Acid
CG Cancer Germline
CNS Central nervous system
COX Cytochrome C Oxidase
CT Cancer testis
Dac Dachshund
DAPI 4,6-diamidino-2-phenylindole
DCP1 Death Caspase 1
DE-Cadh Drosophila Epithelial Cadherin
DIG Digoxigenin
Dm *Drosophila melanogaster*
DNA Deoxyribonucleic Acid
Dpn Deadpan
DTT Dithiothreitol
EDTA Ethylenediaminetetraacetic acid
EGFR Epidermal Growth Factor Receptor
EMS Ethyl methanesulfonate

LIST OF ABBREVIATIONS

FCS Fetal Calf Serum
FDR False Discovery Rate
GFP Green Fluorescent Protein
GMC Ganglion Mother Cell
GO Gene Ontology
GOF Gain Of Function
HA Hemagglutinin
HCl Hydrochloric acid
Hs *Homo sapiens*
IPC Inner Proliferative Center
L(3)mbt Lethal(3) malignant brain tumor
LC-MS Liquid Chromatography - Mass Spectrometry
LDH Lactate Dehydrogenase
LOF Loss Of Function
mbFeret Maximum brain Feret diameter
mbt-SPR Lethal(3) malignant brain tumor suppressor
MBTS Lethal(3) malignant brain tumor signature
$MgCl_2$ Magnesium Chloride
Mira Miranda
MMP Mitochondrial Membrane Potential
MRP Mitochondrial Ribosomal Protein
mtDNA Mitochondrial Deoxyribonucleic Acid
NaCl Sodium chloride
NB Neuroblast
NE Neuroepithelia
OL Optic lobe
OPC Outer Proliferative Center
OXPHOS Oxidative Phosphorylation
PBS Phosphate Buffer Saline
PBST Phosphate Buffer Saline with 0.3% Triton
PCR Polymerase Chain Reaction
PDGF Platelet-derived growth factor
PH3 Phospho Histone H3

Phall Phalloidin
PMSF Phenylmethylsulfonyl fluoride
PSM Peptide Spectrum Matches
q-RT-PCR quantitative Real-Time Polymerase Chain Reaction
RNA Ribonucleic Acid
RNAi RiboNucleic Acid interference
ROS Reactive Oxygen Species
s.d. Standard deviation
SDS Sodium Dodecyl Sulfate
SV Seminal vesicle
SWH Salvador-Warts-Hippo
Tb Tubby
TCA Tricarboxylic Acid Cycle
TRIP Transgenic RNAi Project
UAS Upstream Activation Sequence
UTR Untranslated Region
VDRC Vienna Drosophila Resource Center
VEGF Vascular endothelial growth factor
VNC Ventral Nerve Cord
WT Wild Type
YFP Yellow Fluorescent Protein

List of Figures

List of Tables

1. Introduction

1.1 *Drosophila melanogaster* as a model system

1.1.1 Discovery and establishment of *Drosophila melanogaster* as a tool for research

Drosophila melanogaster, widely known as the fruitfly or vinegar fly, is an holometabolous insect (i.e. undergoes complete metamorphosis) with four different developmental stages: embryo, larva, pupa and adult (Fig. 1.1). It was Thomas Hunt Morgan, back in 1900, the first scientist that used *Drosophila* as an animal model for genetic research. Even though *Drosophila* has limitations as any other model system, several important advantages such as its small size, short generation time and ease of maintenance in the laboratory, have strengthened its use in research ever since. In addition, *Drosophila* researchers benefit from a century of genetic tool building, allowing for a detailed dissection of the functions of genes in development and disease (Gonzalez, 2013).

Drosophila genome, with only four pairs of chromosomes (three autosomes and one sex chromosome), facilitated studies that have provided the basis of much of our conceptual understanding on fundamental aspects of eukaryotic genetics, including the chromosomal basis of sex determination, genetic linkage, and chromosomal mechanics and behavior (Rubin & Lewis, 2000). With the sequencing of the full *Drosophila* genome in the 2000 (Adams et al., 2000), researches found that around 75% of human genetic loci associated with disease have an homologue in the fruitfly (Rubin et al., 2000). *Drosophila* is now widely used as a genetic model for several human diseases, including neurodegenerative disorders, such as Alzheimer's, Huntington's or Parkinson's, and immunity disorders, diabetes, aging, as well as cancer (Vidal & Cagan, 2006; Rudrapatna et al., 2012).

1.1.2 *Drosophila melanogaster* as a model for cancer

In humans, cancer disease is a multistage process that often develops over decades. Therefore, it seems rather counterintuitive that anything similar might occur over the very short lifespan of *Drosophila*, which lasts in the order of 6 to 8 weeks. However, recent studies have found that tumors of the testis and gut are

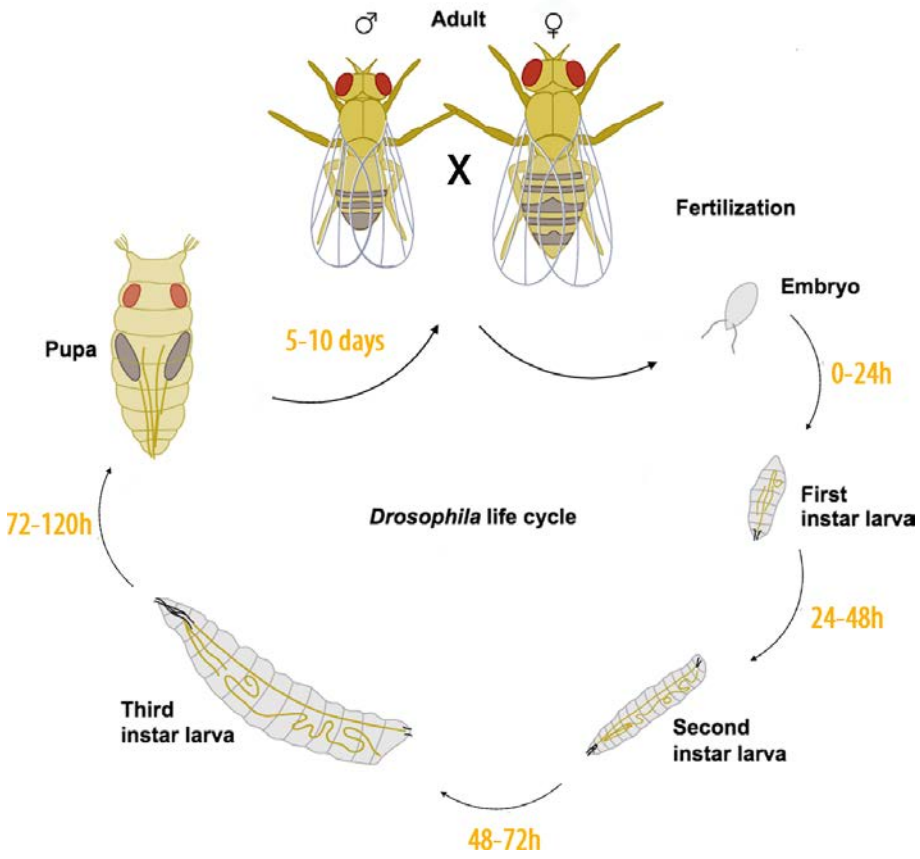

Figure 1.1: The life cycle of *Drosophila melanogaster*. The different stages of the *Drosophila* life cycle are shown. The fruitfly has a short life cycle: the minimal generation time is 10 days at 25°C. Adapted from McGraw-Hill.

frequent in wild-type laboratory strains of *Drosophila* (Salomon & Jackson, 2008). Most importantly, the incidence of these tumors increases with age, demonstrating that despite the orders of magnitude difference in lifespan, ageing is also a risk factor for tumor development in flies. Understanding the mechanisms of origin and growth of *Drosophila* natural malignant tumors might unveil principles that apply to human cancer (reviewed by Gonzalez (2013)).

Tumors are being experimentally induced in both *Drosophila* larvae and adult flies by recreating the combination of loss and gain of function conditions that are known to be causative of certain human cancers, making *Drosophila* a useful model to study multiple aspects of transformation. A pioneering screen was conducted in

1978 to find recessive lethal mutations driving tumors in *Drosophila* by Elisabeth Gateff (Gateff, 1978). The majority of these mutants were identified because they caused in situ overgrowth in imaginal discs, brain, blood cells, and gonads (reviewed by Gateff (1994)). Since then, several tumor models in *Drosophila* have been established, and can be subdivided into hyperplastic and neoplastic tumors.

Hyperplastic tumors have increased cell number, but they are not invasive and stop proliferating as they undergo terminal differentiation together with the surrounding wild-type tissue. Among this class are the tumors caused by mutations in the genes like *Pten*, *warts*, *salvador*, *hippo* and *Merlin*, most of which affect imaginal discs (Brumby & Richardson, 2005).

In contrast, neoplastic malignant tumors overproliferate without limit and do not differentiate. The best-established assay to characterize the growth potential of neoplastic tumors in *Drosophila* is the transplantation of the tumoral tissue into the adult host abdomen (allograft culture) (Rossi & Gonzalez, 2015) (Fig. 1.2). Neoplastic malignant tumors are immortal and can expand for years through successive rounds of implantation into healthy hosts, and even metastasize into different fly adult organs (Brumby & Richardson, 2005). Examples of these are the tumors caused by loss of function in *lethal (2) giant larvae* (*l(2)gl* or *lgl*), *disc large 1* (*dlg1*), *scribbled* (*scrib*), *brain tumor* (*brat*), or *lethal (3) malignat brain tumor* (*l(3)mbt*). Lgl, Dlg and Scrib mutants disrupt polarity in epithelial tissues and neuroblasts and act as human tumor suppressors (Bilder, 2004). Mutation of *brat* results in dramatic proliferation of the type II neuroblast lineage that causes massive larval brain overgrowth (Arama et al., 2000; Betschinger et al., 2006), while *l(3)mbt* mutants cause neoplastic tumors in the brain neuroepithelia (Gateff et al., 1993).

In our laboratory, we investigate the process of malignancy using different types of *Drosophila* tumor models. In my PhD thesis, I focused mainly on the study of *l(3)mbt*, that affects both the larval brain and the imaginal discs.

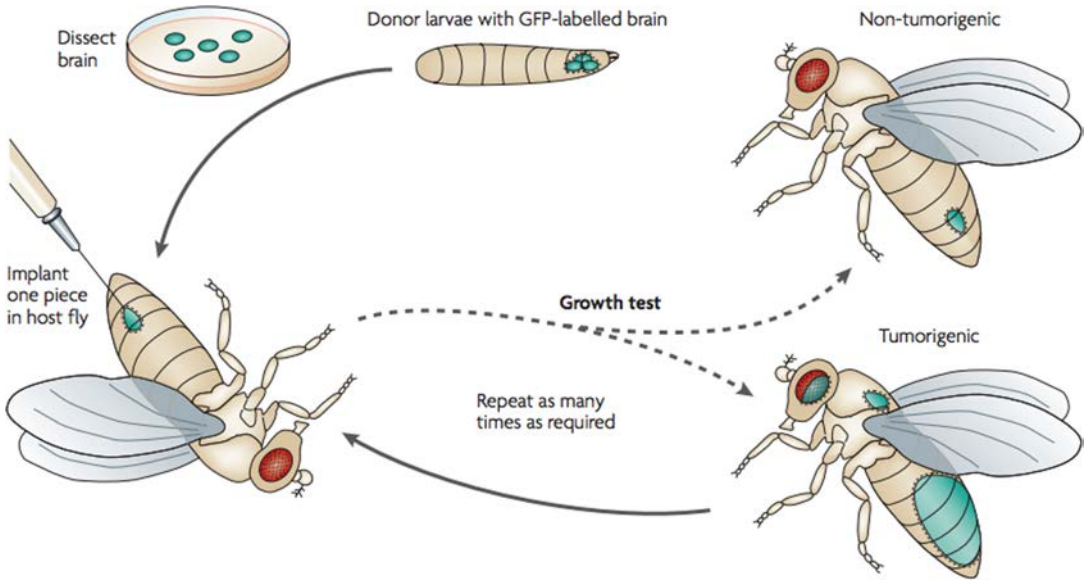

Figure 1.2: Tissue implantation into adult hosts to assay for tumor growth. First, tissue from the donor larvae -ideally labelled with a marker such as GFP- is dissected, cut into pieces and implanted into the adult host. The culture period is typically a few weeks. The growth potential of wild-type larval brains is limited, while the malignant neoplasias expand over the abdomen and, in some instances, into anatomically distant structures. These tumors can be dissected into pieces and injected again into new hosts to determine whether they can continue to grow in further transfer generations, as would be expected for malignant neoplasms. Adapted from Gonzalez (2007).

1.2 Development and organization of both wild-type and *l(3)mbt* brain and wing disc tissues

1.2.1 Wild-type larval brain

The larval brain consists on three different regions: the central brain (CB) and the optic lobes (OL), that form the brain lobes, and the ventral nerve cord (VNC). Two waves of neurogenesis can be distinguished during development. In the first one, single neuroectodermal cells delaminate from the surface epithelium and move into the interior of the embryo to form the VNC and CB neural precursor cells, called neuroblasts. Later on, during the second wave of neurogenesis, the optic lobe neuroblasts arise. Altogether, based on their position in the brain and their lineage

characteristics, we can distinguish abdominal and thoracic neuroblasts in the VNC and type I, type II, mushroom body and optic lobe neuroblasts in the brain lobes. During the first wave of neurogenesis, embryonic neuroblast divisions produce all the neurons that will form the larval central nervous system (CNS) but only 10% of the cells in the adult CNS. Then, at late first and early second instar larval stages, during the second wave of neurogenesis, the neuroblasts continue dividing and produce the remaining 90% of adult neurons (Homem & Knoblich, 2012; Yasugi & Nishimura, 2016).

Approximately 90 type I and eight type II neuroblasts can be found in each brain lobe. Type I neuroblasts constitute the majority of CB and VNC neuroblasts and are located in both ventral and dorsal sides of the brain. They divide to produce another type I neuroblast and a ganglion mother cell (GMC). The GMC divides again to generate two neurons or glia. By contrast, type II neuroblasts are located only in the dorsal side of the CB and are characterized by a different lineage. They undergo asymmetric cell divisions to produce intermediate neural progenitors (INPs) that can self-renew and divide several times to generate GMCs. INPs are therefore recognized as transit amplifying neuroblasts (Bello et al., 2008; Boone & Doe, 2008; Bowman et al., 2008) (Fig. 1.3). The regulation of asymmetric neuroblast division has been studied extensively and most of the components involved in regulating this process have been identified (reviewed in Knoblich (2008)). In addition, the study of CB and VNC neuroblasts has provided key insights into the mechanisms underlying asymmetric cell division and tumor formation (Januschke & Gonzalez, 2008).

The OL of the *Drosophila* brain is the visual processing center, and contains four neuropils: lamina, medulla, lobula and lobula plate. It develops from two proliferation centers: the outer proliferation center (OPC) and the inner proliferation center (IPC). The OPC gives rise to lamina and medulla neurons, whereas the IPC generates the lobula complex. During early larval development, neuroepithelial cells of the OPC and IPC proliferate by symmetric division, thereby expanding the stem cell pool (Bate & Martinez Arias, 1993). Both OPC and IPC remain in contact with each other until the end of the second instar, when they become separated by newly generated cells that penetrate into the space between the IPC and OPC (Nériec & Desplan, 2016) (Fig. 1.4). At late second instar, the

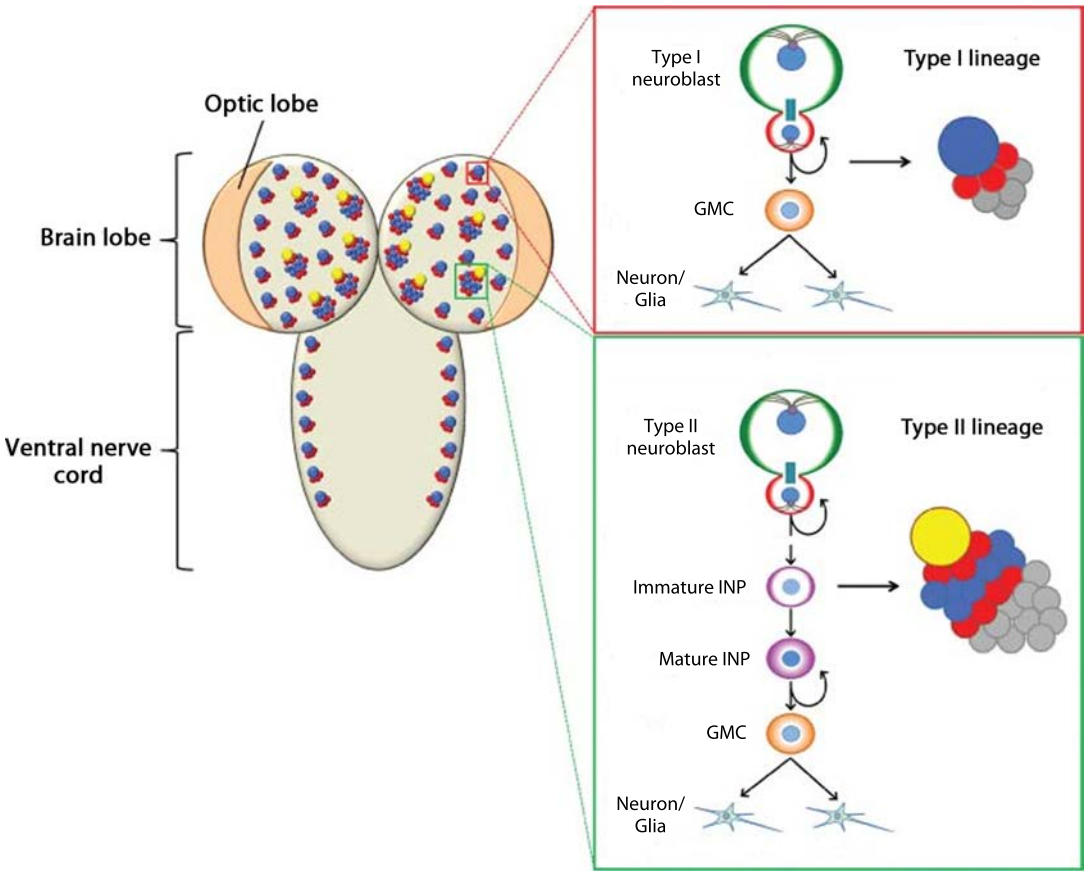

Figure 1.3: Larval brain organization and neuroblast lineages. Dorsal view of *Drosophila* third instar larval brain. Type I neuroblasts (in blue) are located in the central brain and the ventral nerve cord, while type II neuroblasts (in yellow) are exclusive of the central brain. Type I neuroblasts divide asymmetrically to self-renew and produce a ganglion mother cell (GMC). The GMC divides one more time to generate neurons or glial cells. Type II neuroblasts divide to generate a self-renewing neuroblast and an immature intermediate neural progenitor (INP). After maturation, the INP divides asymmetrically to self-renew and generate a GMC that will give rise to neurons or glial cells. Adapted from Koe & Wang (2016).

neuroepithelial cells on the medial edge of the OPC begin to differentiate into medulla neuroblasts. These neuroblasts undergo asymmetric division producing a daughter neuroblast and a smaller GMC that divides once to generate two medulla neurons. Situated between the neuroepithelium and the neuroblasts, there is a group of cells referred to as the transition zone that transiently expresses the proneural gene *lethal of scute* (*l'sc*). *l'sc* expression sweeps across the epithelium as

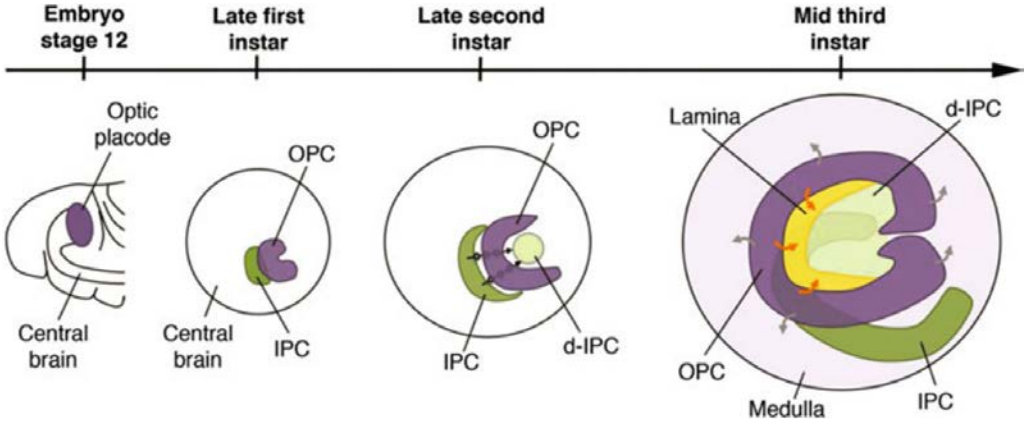

Figure 1.4: Optic lobe development. The optic lobe derives from an optic placode (purple) formed during embryonic stage 12. At the end of the first larval instar, the optic placode becomes subdivided into the Outer Proliferation Center (OPC, purple) and the Inner Proliferation Center (IPC, green). By the end of the second larval stage, the OPC and the IPC adopt a crescent shape and become separated by newly generated cells (black arrows). These cells form the distal IPC (d-IPC, light green). During the third larval instar, the lateral side of the OPC (orange arrows) generates lamina neurons (yellow) while its medial side (grey arrows) generates medulla neurons (light purple). The IPC produces lobula and lobula plate neurons. Adapted from Bertet (2017).

a proneural wave, in which cells ahead of the wave divide symmetrically and those behind divide asymmetrically (Yasugi et al., 2008) (Fig. 1.5). During late third instar larval stage, the OPC neuroepithelium is characterized by densely packed cells expressing DE-cadherin, and gives rise to medulla neuroblasts medially and to lamina neurons laterally (Egger et al., 2007). The lamina cells, that are characterized by the expression of the transcription factor Dachshund (Dac), are separated by the neuroepithelial cells through an indentation called the lamina furrow (LF). As cells exit the LF, they are contacted by incoming retinal axons that trigger the lamina differentiation program (Selleck & Steller, 1991) (Fig. 1.6).

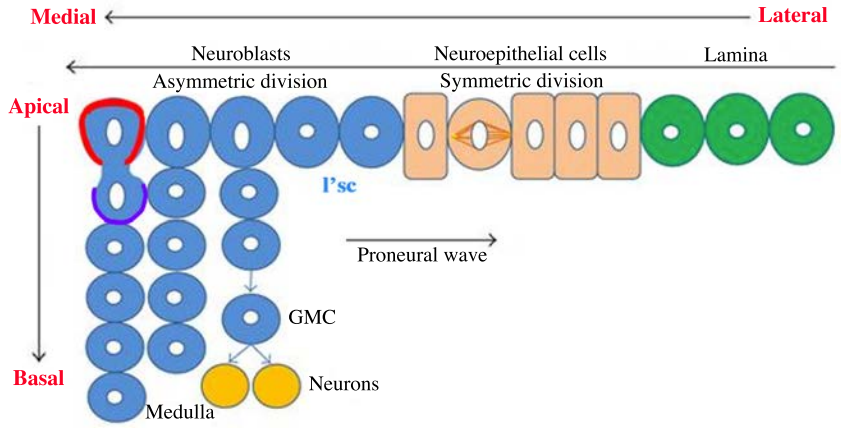

Figure 1.5: OPC neuroepithelial to neuroblast transition. During larval development, transition from neuroepithelial (NE, orange) to neuroblast (NB, blue) takes place. NE cells undergo symmetric proliferation with a horizontal spindle orientation to expand the pool of precursor cells and give rise to asymmetrically dividing NB. This is in response to the proneural wave of lethal of scute (l'sc). The NB divides asymmetrically with a vertical spindle orientation, owing to the clear subcellular localization of the apical (polarity proteins, red boundary) and basal (cell-fate determinants and their adaptor proteins, purple boundary) complex, to give rise to the Ganglion mother cells (GMCs) and medulla neurons. Adapted from Saini & Reichert (2012).

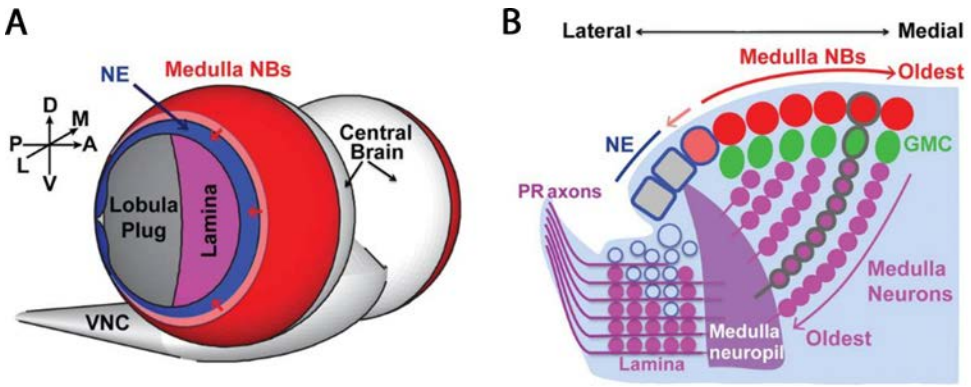

Figure 1.6: The developing neuroepithelia. A) Model of a larval brain showing that the neuroepithelium (NE) (blue) gives rise to the lamina (purple) on the lateral (L) side and to the medulla (red) on the medial (M) side. VNC: ventral nerve cord. B) Cross-section model showing NBs (red), GMCs (green), and neurons (purple). A wave of neurogenesis (light red) converts NE cells (blue) into neuroblasts (NBs) (red). A single NB clone is shown by grey thick outlines. Adapted from Li et al. (2013).

The proliferation and differentiation pattern in the transition from neuroepithelial to neuroblast cells closely resembles that of neural progenitor cells in the developing vertebrate brain. In the past few years, a number of researchers have used the *Drosophila* optic lobe as a model to analyze the key signaling mechanisms controlling neural stem cell maintenance and the transition from symmetric to asymmetric division (Chen et al., 2014). Several master regulators have been identified that regulate the maintenance and differentiation of neuroepithelial stem cells, including the JAK/STAT, Notch, Fat/Hippo and EGFR pathways (Egger et al., 2010; Ngo et al., 2010; Wang et al., 2011; Weng et al., 2012; Yasugi et al., 2010, 2008).

1.2.2 Wild-type imaginal wing discs

Each imaginal disc arises from a cluster of few cells in the embryo, whose morphology matures throghout the larval stages. The wing imaginal disc is a sac-like structure composed of two opposing layers surrounding the disc lumen. One side of the imaginal disc is a single pseudostratified columnar epithelial layer, while the other is a squamous epithelium formed by flat cells called the peripodial membrane. Imaginal discs become patterned during development, under the concerted action of signaling pathways and morphogens. At the end of the larval period, the wing disc is subdivided into different territories by the restricted expression of selector genes, which confer specific cell identity. These selector genes encode transcription factors and are thought to regulate genes required for cell-type-specific differentiation as well as genes that control cell interactions between territories (García-Bellido, 1975).

The larval wing disc is subdivided into anterior and posterior regions by the activity of Engrailed (En) transcription factor in posterior cell, thus conferring the posterior identity and establishing the anterior-posterior (A-P) boundary. En directs expression of the secreted short-range signaling molecule, Hedgehog (*Hh*), which can cross the A-P boundary and induce expression of Decapentaplegic (*Dpp*). Dpp is expressed along the A-P boundary, and its secretion permits long-range signaling to direct patterning of a wider disc region. The wing disc is also subdivided into dorsal and ventral territories by the localized expression of the selector gene *apterous* in the dorsal cells. Wingless (Wg) is produced at the dorsal-ventral (D-V) boundary. Finally, the wing disc is also subdivided into

proximal (notum) and distal (wing) regions (Fig. 1.7). The A-P and the D-V subdivisions constitute developmental compartments, groups of cells that do not mix with adjacent cells of other compartments most probably as a consequence of the compartment specific expression of adhesion molecules. At the border between two adjacent compartments, specific signaling pathways, such as Hedhehog, Notch, Wingless and Decapentaplegic, are activated and play fundamental roles in wing growth and patterning (Garcia-Bellido & Merriam, 1971; Lawrence & Struhl, 1996; Vincent, 1998).

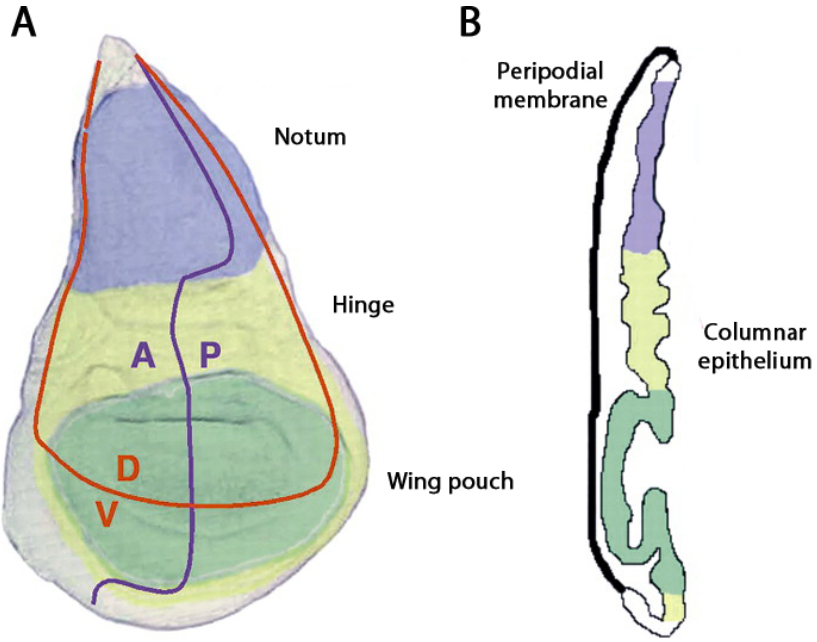

Figure 1.7: *Drosophila* wing disc organization. A) Fate map of the wing disc showing the anterior-posterior (A-P) and dorsal-ventral (D-V) boundaries and major regions in the disc. In the adult, the wing pouch (green) gives rise to the wing blade, while the hinge (yellow) constricts to form a mobile link to the body wall. B) There are two cell layers in the wing disc: the peripodial membrane and the columnar epithelium, that will give rise to the adult epidermis. Adapted from Butler et al. (2003).

1.2.3 *l(3)mbt* tumors

L(3)mbt is a 1477 amino acid protein that is ubiquitously expressed in *Drosophila* and is conserved from worms to humans. L(3)mbt harbors three MBT repeats that bind methylated histone tails in vitro. Together with *Sfmbt* and *Scm*, *l(3)mbt* forms

a family of three genes coding for proteins containing MBT domains. Sfmbt is a subunit of PhoRC, a polycomb group (PcG) complex, and Scm is a component of a distinct PcG complex, PRC1. Both complexes function to maintain tissue specific repression of genes throughout *Drosophila* development (Bonasio et al., 2010). L(3)mbt is enriched at the promoters of repressed genes, suggesting a direct role in transcriptional repression, but its binding sites overlap with insulator elements, indicating that L(3)mbt might also function as an insulator accessory factor (Richter et al., 2011). There are several homologues of *l(3)mbt* in the human genome, that are known to have functions in different gene regulatory pathways, including RB/E2F and polycomb mediated repression (Bonasio et al., 2010).

L(3)mbt was purified in two non-enzymatic repressive chromatin complexes: the dREAM-MMB complex and the LINT complex. *L(3)mbt* is a substoichiometric component of the dREAM-MMB complex, which also includes the two *Drosophila* retinoblastoma proteins (RBF and E2F2) and the Myb- MuvB (MMB) complex. The dREAM-MMB complex controls gene expression throughout the cell cycle but also represses developmental genes (Lewis et al., 2004). The LINT complex is composed of L(3)mbt, the transcriptional repressor Lint-1 and the co-repressor CoREST, and has been shown to silence developmental genes in cultured cells. Interestingly, the dREAM and LINT complexes repress overlapping sets of genes in somatic cells, including genes that are normally expressed in the germline (Coux et al., 2018; Meier et al., 2012).

The first link between *l(3)mbt* and cancer was observed by the strong brain tumorigenic phenotype and epithelial overgrowth in imaginal discs of *l(3)mbt* mutant larvae. A temperature sensitive *l(3)mbt* mutant *(l(3)mbt*^{ts1}*)*, was isolated in a genetic screen for malignant transformations in the developing fly. When shifted to the restrictive temperature during the first 6 hours of embryonic development, *l(3)mbt* mutants develop malignant overgrowth of the larval brain with 100% penetrance and die at the end of the third instar larva phase, without ever giving rise to an adult. Imaginal discs are also hyperplastic and their single-layer epithelium is abnormally folded. In contrast with the brain, the transformation of the imaginal discs is not malignant because the transformed cells do not give rise to secondary tumors upon transplantation (Gateff, 1994; Gateff et al., 1993). Other *l(3)mbt* alleles were found in a screen for germ cell formation, where loss of function of *l(3)mbt* was

found to affect the synchronous mitotic divisions and nuclear migration of the early embryo and this results in a reduction in germ-cell formation (Yohn et al., 2003).

The *l(3)mbt* brain tumor (henceforth referred to as mbt tumor) is initiated by the overproliferation of neuroepithelial cells during late second instar larval stages. As development progresses, the neuroepithelia of both OPC and IPC are massively expanded and the number of optic lobe neuroblasts increased. (Richter et al., 2011). In *l(3)mbt* mutants, there is an upregulation of Salvador-Warts-Hippo (SWH) target genes that are essential for mbt tumorigenesis, however, overactivation of the SWH-pathway can not recapitulate the tumor phenotype seen in *l(3)mbt* mutants (Richter et al., 2011). Therefore, similar to the multifactorial origin of mammalian tumors, the combined deregulation of several signaling pathways could be required. The Notch pathway could be involved as it regulates the formation of optic lobe neuroblasts from the neuroepithelia and moreover, Notch pathway genes are bound by L(3)mbt. In addition, an increased activity of the Jak/STAT pathway, a major regulator of OL development, has also been observed in *l(3)mbt* tumors (Richter et al., 2011).

Gene expression profiling studies have revealed that mbt tumors up-regulate hundreds of genes and have helped to define a mbt tumor signature (MBTS) that uniquely identifies these tumors away from other larval brain tumor types (Janic et al., 2010). A significant fraction of the MBTS consists of germline genes that are normally required for germline stemness, fitness and longevity, thus revealing a soma-to-germline transformation of the brain tissue. Interestingly, inactivation of any of the germline genes *nanos*, *vasa*, *piwi* or *aubergine* is able to suppress *l(3)mbt* malignant growth (Janic et al., 2010). Unscheduled expression of germline genes in somatic tumors is not unique to *Drosophila*; it has been abundantly reported in human oncology studies where such genes are collectively referred to as Cancer/Testis (CT) or Cancer/Germline (CG) genes (Simpson et al., 2005; Almeida et al., 2009). Remarkably, some of the germline genes up-regulated in mbt tumors are orthologs of cataloged human CT genes. Moreover, meta-analysis of expression profiles shows that up-regulation of the human orthologs of *l(3)mbt* tumor-associated germline genes is common in human cancers (Feichtinger et al., 2012).

In humans, alterations in L3MBTL may have a role in tumor development and progression. The human homolog, L3MBTL1 maps to region 20q12, which is

frequently deleted in myeloid malignancies. Moreover, 20q deletions have also been linked to central nervous system germinomas (Schneider et al., 2006). In addition, a significant rate of hemy- and homozygous deletions of L3MBTL2, L3MBTL3 and SCML2 is reported to occur in patients with medulloblastoma (Northcott et al., 2009).

1.3 Mitochondria and cancer

1.3.1 The multifaceted role of mitochondria during tumorigenesis

Out of a screen conducted in our laboratory to identify targets whose depletion severely curtails *l(3)mbt* tumor growth, it was found that *l(3)mbt* tumors might be more sensitive than wild-type tissues to loss of mitochondria-related functions (Rossi et al., 2017).

The first observations of mitochondrial metabolism in cancer were first done by Otto Warburg 70 years ago, who claimed that tumors produce excess lactate in the presence of oxygen (Warburg, 1956; Weinhouse, 1956). This became known as aerobic glycolysis or the "Warburg effect", which he interpreted as mitochondrial dysfunction, an incorrect assumption that *de facto* relegated mitochondria to a role of mere bystanders of the oncogenic process for decades. However, it is now clear that mitochondrial function is essential for cancer cell viability, as cancer cells without mtDNA (ρ° cells) have reduced growth rates, decreased colony formation and markedly reduced tumor formation in nude mice (Morais et al., 1994; Cavalli et al., 1997). Thus, although different cancer cell types undergo different bioenergetic alterations, some to more glycolytic and others to more oxidative, mitochondrial function is essential for cancer cells (Wallace, 2012).

A major function of mitochondria is ATP production, hence its nickname "powerhouse of the cell". However, mitochondria perform many roles beyond energy production, including the generation of reactive oxygen species (ROS), redox molecules and metabolites, regulation of cell signaling and cell death, and biosynthetic metabolism. These multifaceted physiological functions of mitochondria make them key players in tumorigenesis (Vyas et al., 2016) (Fig. 1.8).

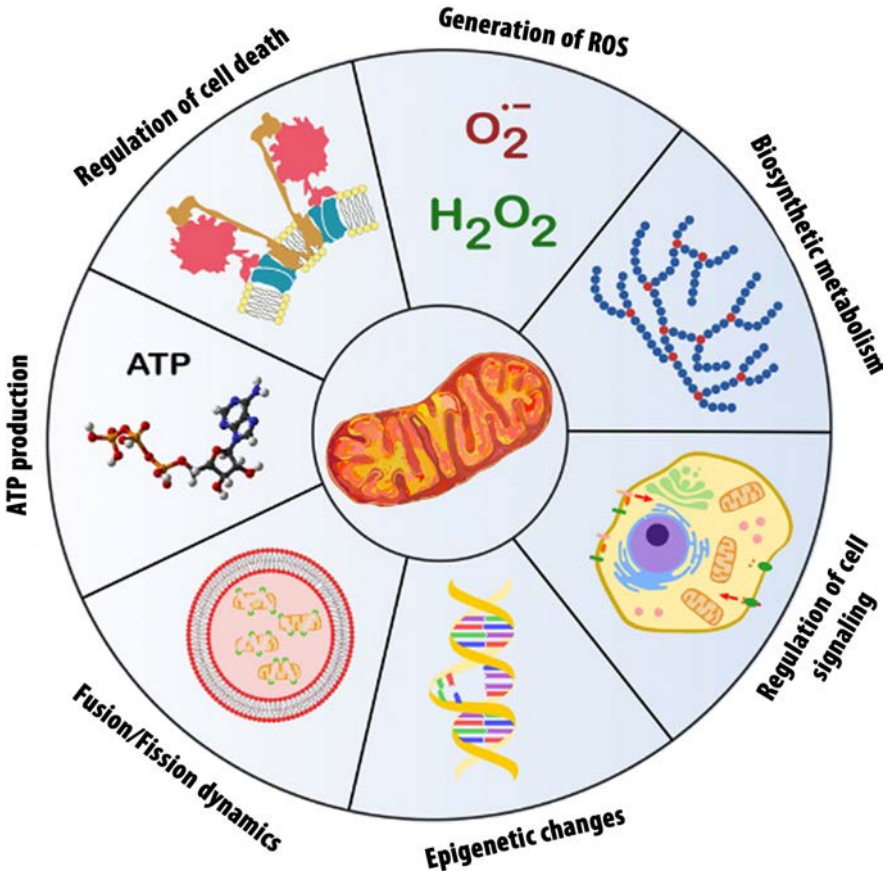

Figure 1.8: The mulitfaceted role of mitochondria during tumorigenesis. Esquematic representation of different biological processes involved in tumorigenesis in which mitochondria play a crucial role. Adapted from Masgras et al. (2017).

Mitochondrial network remodeling is important in tumorigenesis. Mitochondria are extremely dynamic organelles and might exist as either tubular networks or as fragmented granules depending on the cellular state, where mitochondrial metabolism, respiration, and oxidative stress regulate the fission/fusion machinery. Multiple studies have demonstrated an imbalance of fission and fusion activities in cancer, with elevated fission activity and/or decreased fusion resulting in a fragmented mitochondrial network. Importantly, restoration of fused mitochondrial networks in these studies, through either *Dinamin related protein 1* (*Drp1*) knockdown or *Mitofusin 2* (*Mfn2*) overexpression, impaired cancer cell

growth. Increased Drp1 expression is associated with a migratory phenotype in multiple cancer types, further highlighting the role of mitochondrial dynamics in metastasis (Senft & Ronai, 2016; Vyas et al., 2016).

In addition, mitochondria are major contributors to cellular ROS (reactive oxygen species) and have multiple antioxidant pathways to neutralize ROS including superoxide dismutase, glutathione, thioredoxin, and peroxiredoxins. The early observation that cancer cells have high ROS levels led to an overly simple hypothesis that inhibiting ROS could be a successful therapeutic strategy. However, a more complex picture is emerging, in which ROS stimulate signaling and proliferation, and the concomitant upregulation of antioxidant pathways prevents ROS-mediated cytotoxicity and may even enhance tumor survival (Sullivan & Chandel, 2014; Shadel & Horvath, 2015; Vyas et al., 2016).

Mitochondrial biology and tumorigenic signaling intersect at multiple levels. Classical oncogenic signaling pathways can alter mitochondrial functions to support tumorigenesis, but also direct signals from mitochondria can affect cellular physiology and tumor growth. For example, c-MYC, K-RAS, mTOR, and p53 signaling pathways regulate key mitochondrial mechanisms. Through transcriptional regulation, c-Myc induces mitochondrial biogenesis and metabolism in addition to its stimulation of cell-cycle progression and glycolysis. mTOR promotes mitochondrial biogenesis both transcriptionally and translationally. Loss of p53 promotes survival not only via transcriptional regulation of cell death programs, but also through direct interactions with Bcl-2 proteins at the mitochondria. p53 can also induce mitochondrial respiration to promote tumorigenesis by allowing for metabolic flexibility. Oncogenic K-Ras mutations result in a coordinated program of mitochondrial regulation, reprogramming mitochondrial metabolism through multiple mechanisms as well as promoting mitochondrial fission and mitophagy (Vyas et al., 2016).

Furthermore, the conditions within the tumor microenvironment have profound effects on the metabolism of a cancer cell. Tumors are often faced with nutrient- and oxygen-poor surroundings and develop various nutrient-scavenging strategies to bypass these limitations. Moreover, hypoxia impedes the ability of cells to carry out oxidative phosphorylation and other reactions that require oxygen and disrupts the redox balance, affecting cellular signaling and transcriptional programs. Taken

together, reciprocal interactions between cancer cells and their microenvironment impose a selective pressure that further shapes cancer cell metabolism and actively contributes to the emergence of a more aggressive state (Pavlova & Thompson, 2016). Thus, it is critical to study cancer metabolism in models comparable to the in vivo disease. For example, while glutamine fuels Tricarboyxlic Acid Cycle (TCA) cycle anaplerosis in vitro, this is not necessarily true of all tumors in vivo. Studies comparing the fate of labeled glucose and glutamine in mouse models of K-Ras-driven non-small-cell lung cancer showed minimal contribution of glutamine to TCA cycle intermediates (Davidson et al., 2016). Furthermore, primary patient-derived glioma stem-like cells grew independently of glutamine supplementation. These studies highlight the importance of understanding in vivo metabolic requirements of tumor cells when designing therapeutic strategies (Vyas et al., 2016).

In conclusion, there is no simple canon for the role of mitochondria in cancer development. The lack of knowledge of basic mitochondrial biology and genetics, together with the fact that mitochondrial functions in cancer vary depending upon genetic, environmental, and tissue-of-origin differences, are some of the reasons for this somewhat confusing picture of the mitochondrial role during tumorigenesis that still requires much research.

1.3.2 *Drosophila* as a model to study the link between mitochondria and cancer

In the last years, *Drosophila* is emerging as a model to study how metabolism affects tumorigenesis and malignant transformation. Indeed, several studies using larval imaginal discs have shown how different aspects of mitochondrial metabolism contribute to cancer (reviewed in Herranz & Cohen (2017).

Both *Pvr* and *Notch* oncogenes promote a shift towards the "Warburg effect" metabolism in epithelial tumors. Activation of the PDGF/VEGF-receptor (*Pvr*) in the imaginal discs causes metabolic reprogramming by affecting glycolysis and mitochondrial respiration. Pvr activation leads to the formation of epithelial tumors that upregulate the *Lactate Dehydrogenase* (*LDH*) and show aerobic glycolysis (Wang et al., 2016). *Notch* behaves as an oncogene in the *Drosophila* imaginal discs, in which Notch activation leads to tissue hyperplasia and tumor formation. Notch activation induces a switch towards increased

glycolysis and reduced TCA cycle and mitochondrial respiration in the imaginal epithelia (Slaninova et al., 2016). In addition, it was recently shown that LDH enzyme is a critical factor in driving transition from benign hyperplastic growth to neoplasia and metastasis in an EGFR-dependent *Drosophila* epithelial tumor model (Eichenlaub et al., 2018). Altogether, these studies have shed light on the molecular mechanisms regarding the shift from oxidative to glycolytic metabolism in tumorigenesis.

The connection between mitochondrial function and the Hippo pathway has been recently discovered in both flies and mammalian cells. Overexpression of *Yki* or *YAP2* leads to the expansion of mitochondria due to increased mitochondrial function, in addition to cell proliferation. Further genome-wide microarray analysis revealed that many genes associated with mitochondrial function are upregulated by Yki overexpression, including the two mitochondrial fusion genes *optic atrophy 1-like* (*Opa1*) and *mitochondria assembly regulatory factor* (*Marf*). RNAi knockdown of *Opa1* or *Marf* suppresses the mitochondrial fusion phenotype in Yki-overexpressing cells and also partially inhibits cell proliferation (Nagaraj et al., 2012). These data indicate that the Hippo pathway influences mitochondrial structure and function, which in turn may affect cell proliferation.

Drosophila epithelial cells defective in mitochondrial function and expressing Ras^{V12} produce ROS, which activates the JNK stress-response pathway. The cooperation of oncogenic RAS with JNK inactivates the SWH pathway, leading to the upregulation of the interleukin-6 and WNT homologues *Unpaired* and *Wingless*. Activation of Unpaired and Wingless induces cell proliferation and benign hyperplasia of the neighboring tissue. Interestingly, when Ras^{V12} is active in the surrounding cells, activation of the Unpaired and Wingless pathways promotes malignant tumors and metastasis (Ohsawa et al., 2012). These observations suggest that mitochondrial defects, rather than being a consequence of the increase in the glycolytic flux observed in cancer cells, can play an instructive role in cancer progression.

As in humans, the presence of malignant tumors in *Drosophila* impairs muscle function and causes systemic wasting. The induction of neoplastic tumors in flies leads to metabolic reprograming in the muscle that results in mitochondrial degeneration and a reduction in ATP levels in muscle cells. Moreover, the tumors

produce ImpL2, an homolog of the secreted insulin growth factor-binding protein, that promotes a systemic insulin signaling reduction. Notably, suppression of ImpL2 alleviates some wasting phenotypes associated with these tumors, suggesting a potential therapeutic approach to cachexia (Figueroa-Clarevega & Bilder, 2015; Kwon et al., 2015).

In conclusion, in the last decades *Drosophila* has emerged as a very useful tool to investigate malignancy thanks to the several models available that recapitulate various aspects of human cancer, and it can further contribute to reveal different aspects of how metabolism affects tumorigenesis and malignant transformation. My thesis project is focused on the identification and study of genes required for the growth of the malignant larval brain tumor type *l(3)mbt*, and more specifically, to the contribution of a specific set of testis-mitochondrial genes to the process of malignancy.

2. Objectives

The rational behind my thesis project is to advance in the understanding of the carcinogenesis process using *Drosophila melanogaster* as a model. My work is focused on the identification and study of genes required for the growth of *lethal (3) malignant brain tumor*. In this line, we specifically aimed:

- To identify mitochondrial genes whose inhibition specifically affects the growth of *lethal (3) malignant brain tumor*.
- To study the contribution of one of the identified mitochondrial candidates to the process of malignancy.

3. Materials and methods

3.1 *Drosophila* strains

The following fly strains were used: UAS-RNAi lines were obtained from Bloomington *Drosophila* Stock Center (BDSC) or Vienna *Drosophila* Resource Center (VDRC). UAS-brat-RNAi (TRiP line, 28590, BDSC), mbt^{ts1} (Yohn et al., 2003), $ttm2^{C205}$ (16303, BDSC), insc-Gal4 (8751, BDSC), c855a-Gal4 (6990, BDSC), c253-Gal4 (6980, BDSC), UAS-ttm2 (F002672, FlyORF), UAS-CD8:GFP (108068, Kyoto Stock Center), nub-Gal4 (Calleja et al., 1996), salEPv-Gal4 (Cruz et al., 2009), hh-Gal4 (Tanimoto et al., 2000). Recombinants *l(3)*mbt^{ts1} *ttm2*^{C205} were generated by standard genetic techniques. The wild-type strain is w^{1118}. Mbt tumor crosses were maintained at 29°C.

3.2 Genetic manipulation

For targeting gene expression, we used the binary Gal4-UAS system (Brand & Perrimon, 1993). This induction system is based on two components: (i) the yeast transcription activator gene Gal4, placed downstream of a promoter/enhancer, and (ii) the Gal4 target sequences named as UAS (Upstream Activation Sequence), placed 5' of the gene of interest. When a cell has both of these elements - typically achieved by standard genetic crossing - the promoter activates Gal4 expression, which in turn binds to the UAS elements to induce transgene expression in a temporally and spatially precise manner (Brand & Perrimon, 1993; Brand et al., 1994) (Fig. 3.1).

3.3 Screen strategy

The Gal4-UAS system (Brand et al., 1994) was used to drive the expression of both UAS-l(3)mbt-RNAi and each of the UAS-RNAi lines to be screened. Lines were obtained from Bloomington *Drosophila* Stock Center (BDSC) or Vienna *Drosophila* Resource Center (VDRC) (Dietzl et al., 2007). The stock to induce mbt tumor in *Drosophila* carries the UAS-l(3)mbt-RNAi line (v12709,VDRC), a pUbi-Gal4, an UAS-Dicer2 (24650, BDSC) to further enhance the phenotype, the *l(3)*mbt^{ts1} allele, a PiggyBac insertion carrying DsRed (140131, Kyoto stock center) as chromosome

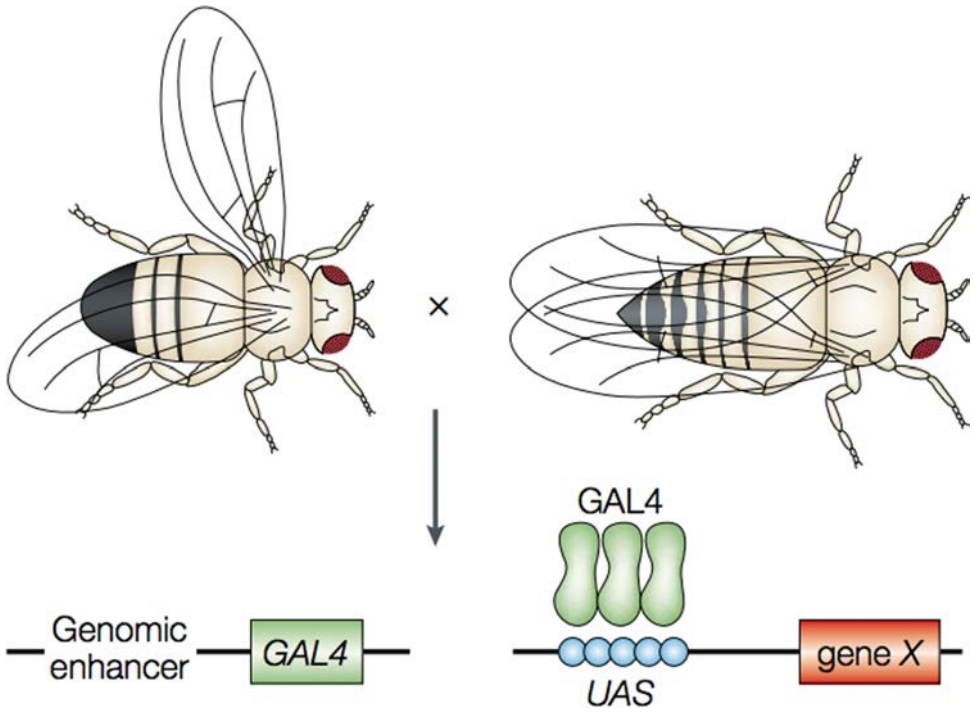

Figure 3.1: The GAL4-UAS system for directed gene expression. The expression of a gene x can be driven in the desired pattern by crossing the appropriate GAL4 enhancer trap line to flies that carry the UAS-gene x transgene. Adapted from St Johnston (2002).

marker, a Y-chromosome carrying heat shock-inducible hid (Yhs-hid, 24638, BDSC) to facilitate the collection of virgins, and a Gal80 expressing balancer (9490, BDSC) to repress UAS-transgene expression in the parental flies. The final genotype of the stock is: w^{1118}/Yhs-hid; Ubi-Gal4, UAS-Dcr2; UAS-l(3)mbt-RNAi, DsRed, mbt^{ts1}/TM6B, tubP-Gal80, Tb.

Females from this stock were crossed to males carrying each of the transgenic UAS-RNAis to be tested. Eggs were collected for 0 to 24 hours and were let to develop up to 7-8 days after egg laying (AEL) at 29°C. (Fig. 3.2).

3.4 Brain size measurement

Wandering Tb+ larvae were selected and brains were dissected in PBS. An image of larval brains from each cross was taking using a LEICA EC3 camera coupled to a NIKON SMZ800 stereoscope. Ventral ganglions were either dissected out

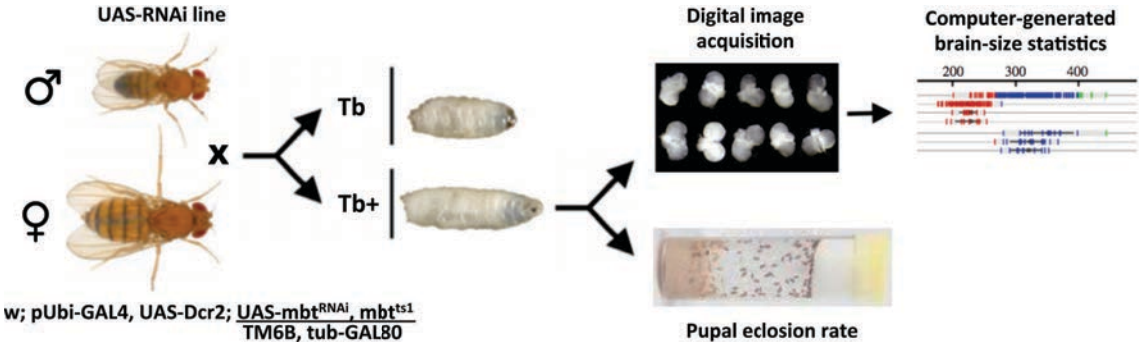

Figure 3.2: Screen strategy. Females from w; pUbi-GAL4, UAS-Dcr2; UAS-mbtRNAi, mbt^{ts1}/TM6B, tubP-GAL80 are crossed to males carrying each of the transgenic UAS-RNAi lines. Brains from Tb+ larvae are disected for automated classification of mbFeret and then pupae eclosion rates are calculated from the same crosses. Adapted from Rossi et al. (2017).

prior to image acquisition or digitally masked before measurement. The wild-type strain w^{1118} was used as a control to determine wild type brain sizes. The images were analyzed by a purpose made macro written in ImageJ software that classifies the effect of the corresponding RNAi by working out the statistics of mbFerets from a micrograph of dissected brains. Based on pooled mbt-RNAi and wild-type populations, brains smaller than 190 a.u.(arbitrary units), between 190 and 300 a.u., or bigger than 300 a.u. are classified as smaller than wild-type (gray), wild-type (red) or mbt size (blue), respectively. Samples in which the fraction of brains smaller than wild type is lower than 0.6 are classified as gray and samples in which the fraction of brains smaller than mbt is lower than 0.6 are classified as red (mbt-SPR). Mbt-like size samples are classified as blue.

3.5 Pupal eclosion rate measurement

Pupal eclosion was calculated by measuring the number of empty pupae divided by the total number of pupae at 15 days after egg laying for both Tb and Tb+ pupae.

3.6 Immunohistochemistry

Immunostaining of larval brains and imaginal wing discs was performed as described (Gonzalez & Glover, 1993). Briefly, the tissue was dissected in PBS, fixed for 20 min in 3.7 % Formaldehyde in PBS and incubated in blocking solution (0.3% Triton X-100, 10% Fetal Calf Serum (FCS) in PBS) for 1 hour at room temperature. Primary antibodies were diluted in blocking solution and incubated overnight at 4°C, washed three times with PBST (0,3% Triton X-100 in PBS) for 20 min, incubated with the secondary antibodies in blocking solution for 1 h in the dark at room temperature, washed again three times with PBST for 20 min, incubated with DAPI (1μg/ml) in PBS for 30 min to counterstain the DNA and washed with PBS. Finally, the samples were mounted in Vectashield with DAPI (Vector Laboratories, Inc).

The following primary antibodies and dilutions were used: Rabbit anti-aPKC (1:1000, Sigma), Rat anti-PH3 (1:1000, Abcam), Rabbit anti-HA (1:500, Cell Signaling Technology), Mouse anti-ATP5A (1:500, Abcam), Rabbit anti-Miranda (1:1000, Mollinari et al. (2002)), Mouse anti-Dachshund (1:50, DSHB), Mouse anti-Fasciclin III (1:5, DSHB), Mouse anti-DCP1 (1:100, Cell Signaling Technology), Rat anti-Deadpan (1:100, Abcam) and Alexa Fluor 633 anti-Phalloidin (1:1000, Molecular probes). Alexa conjugated secondary antibodies (Molecular probes) were used at 1:1000 dilution.

3.7 Mass spectrometry

3.7.1 Protein extraction and subcellular fractionation

200 adult testes were dissected in PBS and transferred immediately to a 1.5 ml tube in dry ice. The tissue was homogenized on ice-cold homogenization buffer (10mM Tris-HCl (ph 7.5), 10mM NaCl, 1.5mM $MgCl_2$) using a dounce instrument. The mitochondrial stabilization buffer (525mM mannitol, 175mM sucrose, 2.5mM EDTA, 12.5mM Tris-HCl) was added and mixed thoroughly by inversion. The sample was centrifugated at 1000g for 5 min at 4°C. The supernatant was transfered to a clean microfuge tube and centrifugated at 17000g for 30 min at 4°C. Both the pellet (that contains the mitochondria) and the supernatant were homogenized in lysis buffer (20mM Tris-HCl (pH 7,8), 0.4NaCl, 15% glycerol, 1mM DTT, 1mM

PMSF and 1,5%Triton X-100) and sonicated for 2 min at 30% intensity. Finally, all cell lysates were centrifugated at 9000g for 30 min and the supernatants were recovered. Protein concentration was measured using the Pierce BCA protein assay kit (Thermo scientific).

3.7.2 Protein extraction and gel separation

50 brains per genotype were lysed in 150μl of lysis buffer (4% SDS, 100mM Tris/HCl pH 7.6, 0.1M DTT) followed by an incubation at 95°C for 3 min. The sample was sonicated to shear the DNA to reduce the viscosity of the sample. The lysate was centrifugated at 16000g for 5 min before loading. Total protein extracts were run on precast Bolt 12%-4% Bis-Tris Plus Gels (Thermo NW04120BOX) following the instructions of the supplier. After electrophoresis, the gel was stained with Brilliant Blue G (Sigma B8522) and cut in four pieces <30Kd, 30-60 Kd, 60-90Kd, >90Kd using a clean scalpel blade.

3.7.3 Liquid chromatography–mass spectrometry (LC-MS)

The nano-LC-MS/MS set up was as follows. 2μL of samples were loaded to 100 μm x 2 cm Acclaim PepMap100, 5 μm, 100 Å, C18 (Thermo Scientific) at a flow rate of 15 μL/min using a Thermo Scientific Dionex Ultimate 3000 chromatographic system (Thermo Scientific). Peptides were separated using a C18 analytical column (Acclaim PepMap® RSLC (75 μm x 75 cm, nanoViper, C18, 2 μm, 100Å, Thermo Scientific) with a 300 min run, comprising four consecutive steps with linear gradients from 1% to 35% of B in 267 min, from 35% to 50% in 5min and from 50% to 85 in 2 min, followed by isocratic elution at 85% B in 5 min and stabilization to initial conditions (A= 0.1% FA in water, B= 0.1% FA in CH3CN). The column outlet was directly connected to an Advion TriVersa NanoMate (Advion) fitted on an Orbitrap Fusion LumosTM Tribrid (Thermo Scientific). The mass spectrometer was operated in a data-dependent acquisition (DDA) mode. Survey MS scans were acquired in the orbitrap with the resolution (defined at 200 m/z) set to 120,000. The lock mass was user-defined at 445.12 m/z in each Orbitrap scan. The top speed (most intense) ions per scan were fragmented in the CID cell and detected in the linear ion trap. The ion count target value was 400,000 for the survey scan and 10,000 for the MS/MS scan. Target ions already selected for MS/MS were

dynamically excluded for 15 s. Spray voltage in the NanoMate source was set to 1.70 kV. RF Lens were tuned to 30%. Minimal signal required to trigger MS to MS/MS switch was set to 5000 and activation Q was 0.250. The spectrometer was working in positive polarity mode and singly charge state precursors were rejected for fragmentation.

3.7.4 Database searching

A database search was performed with Proteome Discoverer software v1.4 (Thermo) using Sequest HT search engine and UniProt database *Drosophila melanogaster* release 2016 04 database. Searches were run against targeted and decoy databases to determine the false discovery rate (FDR). Search parameters included trypsin enzyme specificity, allowing for two missed cleavage sites, carbamidomethyl in cysteine as static modification and methionine oxidation as dynamic modifications. Peptide mass tolerance was 10 ppm and the MS/MS tolerance was 0.6 Da. Peptides with a q-value lower than 0.1 and a FDR $< 1\%$ were considered as positive identifications with a high confidence level.

3.8 qRT-PCR

RNA isolation, cDNA synthesis, library preparation and amplification were performed as described by Gonzalez-Roca et al. (2010). Basically, a piece of tissue was disected in PBS, immediately introduced in lysis buffer (20 mM DTT, 10 mM Tris.HCl ph 7.4, 0.5% SDS, 0.5μg/μl proteinase K) and incubated 15 min at 65^{o}C. Subsequently, RNA was purified using RNA Clean XP bead suspension (Agencourt Bioscience). Analysis of RNA Isolation sample integrity was done using the Bioanalyzer Pico Assay. The cDNA generated by reverse transcription from each sample was added to an amplification mix and the cDNA:mix was divided in 3 equivalent parts for PCR amplification. A sample without RNA was included in the amplification experiment. Amplification was performed for 13 cycles. Subsequently, cDNA was purified on PureLink Quick PCR Purification Kit (Invitrogen) and eluted in 40 μl. cDNA concentration was determined using the Nanodrop 1000 spectrophotometer (Thermo Scientific).

qRT-PCR was performed in Applied Biosystems^{TM}QuantStudio^{TM}6 Flex Real-Time PCR System termocycler (Thermo Scientific). Initial activation was performed

at 95°C for 3 min, followed by 39 cycles of: 95°C for 5 s, 60°C for 5 s, 70°C for 10 s. The following primers were used:

RP49-Forward 5' ATCGGTTACGGATCGAACA 3',

RP49-Reverse 5' GACAATCTCCTTGCGCTTCT 3', s

ttm2-Forward 5' GGCGGAGCAAGGAGTTACTGTGTTC 3',

ttm2-Reverse 5' CGACAACCACTCGCTTTAGGTCTCG 3'.

Measurements were performed on biological triplicates, with technical triplicates of each biological sample. ttm2 RNA levels were normalized to RP49 (RpL32 – FlyBase). The relative transcript levels were calculated using the $2-\Delta\Delta CT$ method (Livak & Schmittgen, 2001).

3.9 In situ hybridization

In situ hybridization with RNA probes was carried out as described previously for larval brains (Hevia & de Celis, 2013). Basically, brains were dissected, fixed by treatment in 4% paraformaldehyde for 20 min at room temperature and washed three times in PBST (PBS, 0,1% Tween-20). Proteinase K treatment (4 min at 30μg/ml) was introduced after fixation to improve probe penetration in larval brains. Then, brains were treated for 20 min at room temperature with 4% paraformaldehyde, 0.1% Tween, prehybridized, and hybridized at 55°C overnight, using digoxigenin (DIG) labeled probes. After hybridization, brains were washed and incubated for 2 hr at room temperature with anti-DIG antibody (Roche) conjugated to alkaline phosphatase. After alkaline phosphatase activity detection, brains were washed in PBST, dehydrated and mounted in glycerol 70%.

The probes were synthesized from LP16167 cDNA (*Drosophila* Genomics Resource Center, DGRC) using the following primers:

5' CCCTGGCGTTGACGTGTTTTTGAAA 3', and

5' TAATACGACTCACTATAGGGGGTAGACATTGAAGAATGCTAGGAA 3'

3.10 Statistical analysis

p-values were calulated using Unpaired Student's t-test with GraphPad Prism software.

4. Results

4.1 Depletion of mitochondrial translation impairs *lethal (3) malignant brain tumor growth*

In order to identify genes that are required for *Drosophila lethal (3) malignant brain tumor* growth (henceforth referred to as mbt tumors), our laboratory performed an untargeted screen in vivo using transgenic RNAi technology (Rossi et al., 2017). As a result of the screen, in which over 4000 genes were screened, we found several candidates required for the growth of mbt tumors (henceforth referred to as mbt-SPRs, short for mbt suppressors), among which we noticed an overrepresentation of mitochondrial genes. While the percentage of mitochondria-related genes (Flybase search: mitochondria OR mitochondrial) represents approximately an 8% of the total screened genes, 17% of the mbt-SPRs are mitochondria-related genes. Using the Generic Gene Ontology (GO) Term Finder from Princeton University (https://go.princeton.edu/cgi-bin/GOTermFinder), even though mitochondria-related genes represent a 6% of the total genes screened, they increase upon a 16% regarding genes found as mbt-SPR. This finding suggests that mbt tumors might be more sensitive than wild-type tissues to the loss of mitochondrial-related functions, and that a certain threshold might exist in which normal development can proceed while tumor growth is severely curtailed when mitochondrial function is inhibited (Rossi et al., 2017). This observation is consistent with numerous reports published over the last century in which mitochondria have been described to play a central and multifunctional role in malignant tumor progression (Warburg, 1956; Wallace, 2012). Besides exerting central bioenergetic functions, mitochondria provide as well building blocks for tumor anabolism, control redox and calcium homeostasis, participate in transcriptional regulation, and govern cell death. Thus, mitochondria constitute promising targets for the development of novel anticancer agents (Porporato et al., 2018). Considering this, we decided to take advantage of the *l(3)mbt Drosophila* tumor model to further investigate the role of mitochondrial genes in malignancy.

The group of mitochondrial ribosomal protein (MRP) or mitoribosome genes stands out among the list of mitochondrial mbt-SPRs. MRPs are responsible for the translation of the mRNAs transcribed from the mtDNA and conform both the small

and large subunits of the mitochondrial ribosomes (Greber & Ban, 2016). Indeed, several MRPs found to be overexpressed in some human cancers have been proposed as predictors for poor prognosis (Kim et al., 2017). In order to confirm the sensitivity of mbt tumors to mitochondrial ribosome depletion, I screened 10 different MRPs, which included the ones previously found as mbt-SPRs -*mRpL48, mRpS6, mRpS11* and *mRpL21*-, plus *mRpL3, mRpS29, mRpL20, mRpL46, mRpL48* and *mRpL50*. As a readout for tumor suppression I measured larval brain size. To this end I took advantage of a purpose-made macro that measures the maximum brain Feret diameter (henceforth referred to as mbFeret) of the optic lobe pair (see Materials and Methods). I found that depletion of any of the mitoribosome subunits mRpS11, mRpL3, mRpL20 and mRpL46 results in much reduced mbt mutant brains that do not even reach the size of wild-type brains. However, depletion of mRpL49 or mRpS6 results in a distribution of brain sizes in which some of them are within the wild-type range (Fig. 4.1).

From these results we conclude that, on the one hand, mbt tumors are sensitive to the depletion of mitoribosome components, and, on the other hand, that mitoribosome inhibition might also affect wild-type development because the size of the mbt brains depleted for MRPs is below the wild-type range. There might exist the possibility that mitoribosome inhibition at a certain dosage impairs tumor growth without being deleterious for the wild-type. Indeed, many novel compounds that target mitochondrial metabolism with potent anticancer activity both in vitro and in vivo have been identified in the recent years (Wen et al., 2013; Weinberg et al., 2015).

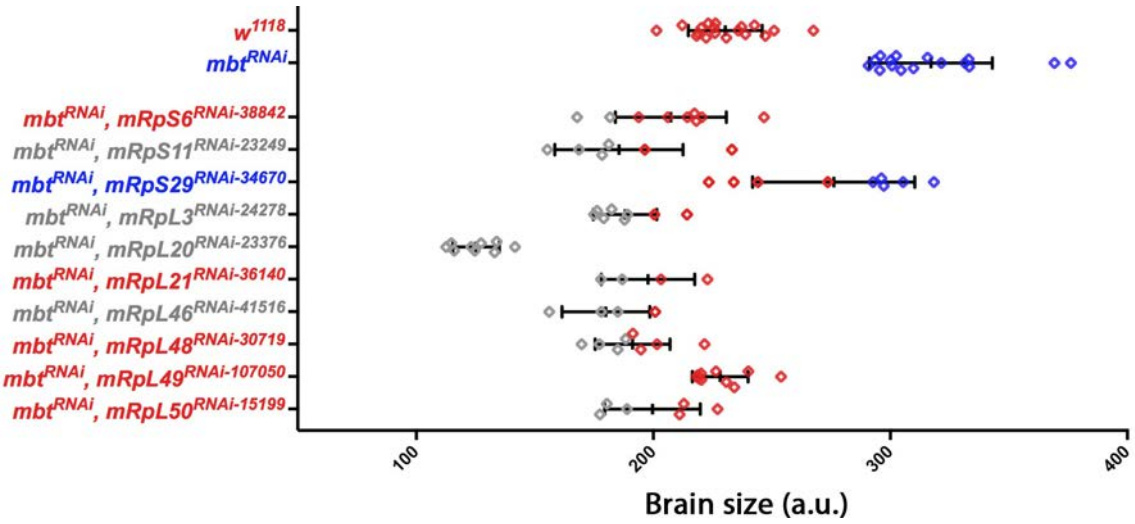

Figure 4.1: RNAi inhibition of mitochondrial ribosomal protein (MRP) genes impairs mbt tumor growth. Plot showing mbFerets (mean and s.d) for each larval brain sample in which the indicated MRP gene is inhibited in an mbt tumoral background. Brains are disected at 7-8 days AEL, except for w^{1118} disected at 5-6 days AEL. Each point represents a single brain. Color code indicates brain-size class: smaller than wild-type (grey), wild-type like size or mbt-SPR (red) and mbt like size (blue) (see Materials and Methods). a.u. arbitrary units.

4.2 *l(3)mbt* tumor development is dependent on mitochondrial testis-specific functions

Out of the mitochondrial mbt-SPRs genes, one remarkable exception to the general cytostatic effect of depletion of mitochondrial genes (i.e. depletion being deleterious for both tumor and wild-type tissues) is *CG1409*. I found that depletion of *CG1409* appears to exert a rather specific impact on mbt tumor growth but allows for wild-type brain development. RNAi inhibition of *CG1409* in mbt-RNAi background results in brains within the range of wild-type and mbt sizes (Fig. 4.2A). Furthermore, mbt tumors lacking *CG1409* function show an increased adult viability rate (Fig. 4.2B) and a remarkable brain anatomy rescue (Fig. 4.2C).

The function of *CG1409* is unknown, but it is very similar in sequence to *Drosophila black pearl* gene. Both *CG1409* and *black pearl* are predicted orthologs of the human gene *magmas* (*timm16*, *pam16*) (Becker et al., 2001). Magmas is an inner membrane-associated protein and an essential component of the mitochondrial protein translocation machinery. Moreover, Magmas regulates cellular ROS by enhancing the activity of electron transport chain complexes (Srivastava et al., 2014). Like human *magmas*, *Drosophila black pearl* is ubiquitously expressed, and it is required for larval growth and survival (Becker et al., 2001). Black pearl also regulates ROS and enhances the activity of the mitochondrial electron transport chain (Roy et al., 2012). The peculiarity of *CG1409* compared to *magmas* and *black pearl* is that its expression is restricted to testis. The fact that it does not contain introns, together with its high similarity to *black pearl* sequence, suggests that *CG1409* is a retrogene that was originated by the insertion of a cDNA in the genome that later acquired a specific function in testes (Bai et al., 2007).

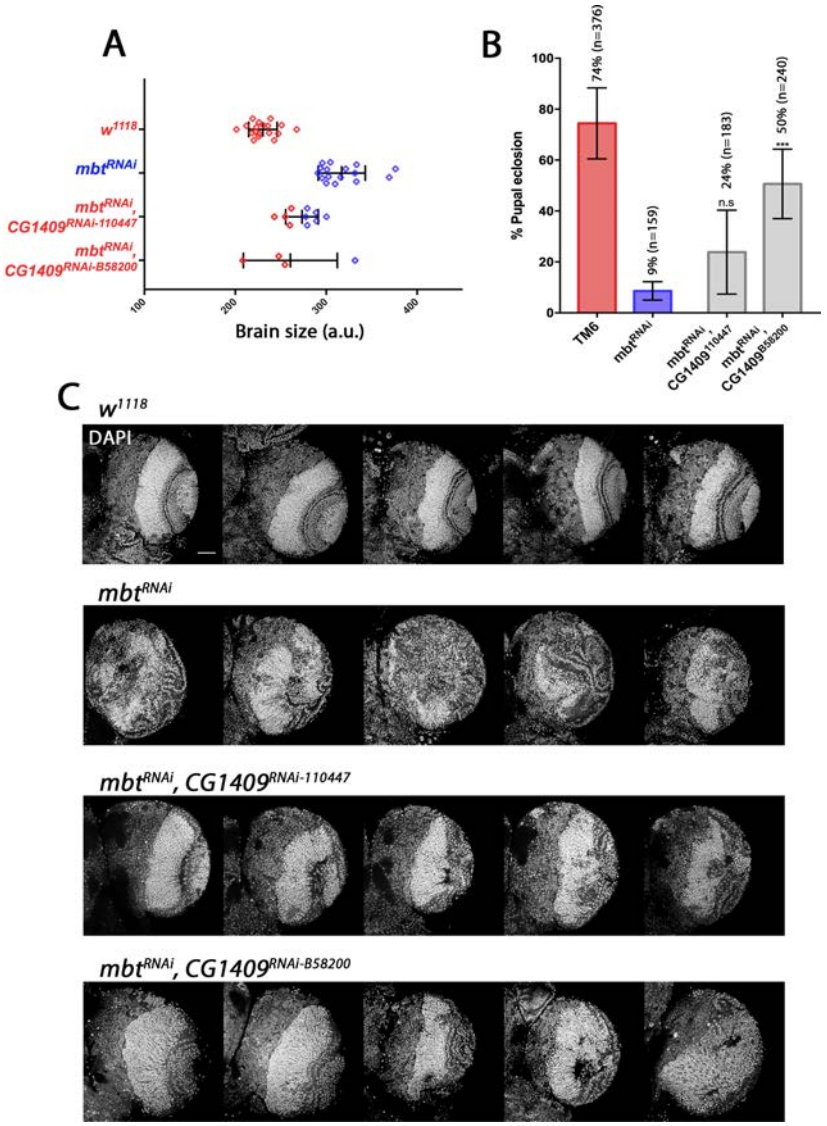

Figure 4.2: *CG1409* is required for mbt tumor growth. A) Plot showing mbFerets (mean and s.d) for w^{1118} (5-6 days AEL) and mbt-RNAi (7-8 days AEL) controls, and two independent *CG1409* RNAi lines expressed in an mbt-RNAi background (7-8 days AEL). Each point represents a single brain. Color code indicates brain-size class: wild-type like size or mbt-SPR (red) and mbt like size (blue) (see Materials and Methods). a.u. arbitrary units. B) Graph showing average pupal eclosion rates. TM6 and mbt-RNAi controls are depicted as red and blue bars respectively, while *CG1409* RNAi lines expressed in mbt-RNAi background are depicted in grey. Average pupal eclosion rate and total number of pupae are specified for each condition. Error bars indicate s.d. (n.s. not significant, $***p < 0.005$). C) Array of confocal ventral sections of five DAPI stained optic lobes from w^{1118} (5-6 days AEL), mbt^{RNAi} and *CG1409* RNAi lines expressed in mbt-RNAi background (7-8 days AEL). Scale bar 50μm.

Lead by our observations regarding the role of *CG1409* in mbt tumor growth, we wondered whether other genes with a testis-enriched expression and a putative mitochondrial function were also required for mbt tumor development. The *Drosophila* genome contains an important fraction of mitochondrial genes that were duplicated and have acquired testis-specific expression. Thus, two or more copies of several mitochondrial genes exist in the genome of *Drosophila*, and while one is mostly expressed in the soma, the other is expressed in the testis. These mitochondrial-duplicated genes participate in a variety of mitochondrial processes: electron transport chain, mitochondrial membrane transport, tricarboxylic acid cycle or the voltage-dependent anion channel transport (Tripoli et al., 2005; Bai et al., 2007; Gallach et al., 2010).

Based on previously published gene duplication studies and expression data publicly available, I searched for genes related to *CG1409*. Taking advantage of the FlyAtlas project on gene expression, I first pre-selected mitochondrial genes whose expression is 9-fold higher in testes compared to the whole fly tissue. This specific expression enrichment was selected because it includes most of the genes described in Tripoli et al. (2005) and Gallach et al. (2010) studies, that investigate *Drosophila* nuclearly-encoded mitochondrial duplicates. The definitive list of testis-mitochondrial genes related to *CG1409* contains those retrieved by the specified FlyAtlas search and a few others only included in the studies mentioned above. In addition, ModEncode expression data confirms the testis-enriched expression of the selected genes. Thus, the candidate list of testis-mitochondrial genes is composed of 32 genes, 22 involved in the oxidative phosphorylation (OXPHOS) process and 10 in the mitochondrial membrane transport machinery, both gene ontologies related to the putative function of *CG1409* (Table 4.1).

For each gene on the list, I used RNAi stocks from the VDRC (Vienna *Drosophila* Resource Center) collection, selecting those without off-targets when available. Putative mbt-SPRs were confirmed with an independent RNAi line either from the VDRC or the BDSC (Bloomington *Drosophila* Stock Center) collections if available. Out of the 44 RNAi lines analyzed, I found 3 that caused early onset lethality (*ATPsynbetaL* VDRC-22112, *ATPsynepsilonL* VDRC-28600 and *COX4L* VDRC-1482). Out of the 41 RNAi lines that allowed for larval viability -including *CG1409*-, 8 produced mbt brains that grew to sizes within the-wild-type range and

	GENES		SELECTION CRITERIA		
	Annotation Symbol	Gene Name	FlyAtlas expression	Tripoli et al.	Gallach et al.
OXIDATIVE PHOSPHORYLATION	CG5389	ATPsynbetaL		X	
	CG12027	ATPsynCF6L	X	X	X
	CG31477	ATPsynepsilonL		X	X
	CG7211	ATPsynGL	X	X	
	CG10396	COX4L		X	X
	CG11043	COX5BL	X	X	
	CG30093	COX6AL	X	X	
	CG14077		X		
	CG18193	COX7AL	X	X	X
	CG13263	Cyt-c-d		X	X
	CG14508	Cyt-c1L	X	X	X
	CG2014	ND-20L	X	X	X
	CG6485	ND-24L	X	X	X
	CG11913	ND-49L	X	X	X
	CG11423	ND-51L1	X	X	X
	CG8102	ND-51L2	X	X	X
	CG6914	ND-B14.5AL	X	X	
	CG5718	SdhAL	X	X	X
	CG7349	SdhBL	X	X	X
	CG6629		X		
	CG30354	UQCR-11L	X	X	
	CG17856	UQCR-14L	X	X	X
MITOCHONDRIAL TRANSPORT	CG10090	Tim17a1	X		X
	CG14666	Tim17a2			X
	CG1158	Tim17b1	X		X
	CG15257	Tim17b2	X		X
	CG1724		X		X
	CG14690	tomboy20	X		X
	CG8330	tomboy40	X		X
	CG12313	ttm2	X		
	CG6691	ttm3	X		
	CG1409		X		

Table 4.1: Selected testis-mitochondrial genes. Table showing the selection criteria for each candidate of the testis-mitochondrial gene list related to *CG1409*. A cross is depicted when the gene was retrieved in the following searches: FlyAtlas expression, Tripoli et al. (2005) and Gallach et al. (2010) studies.

were therefore classified as mbt-SPRs, while 33 had no effect on mbt brain size (Fig. 4.3).

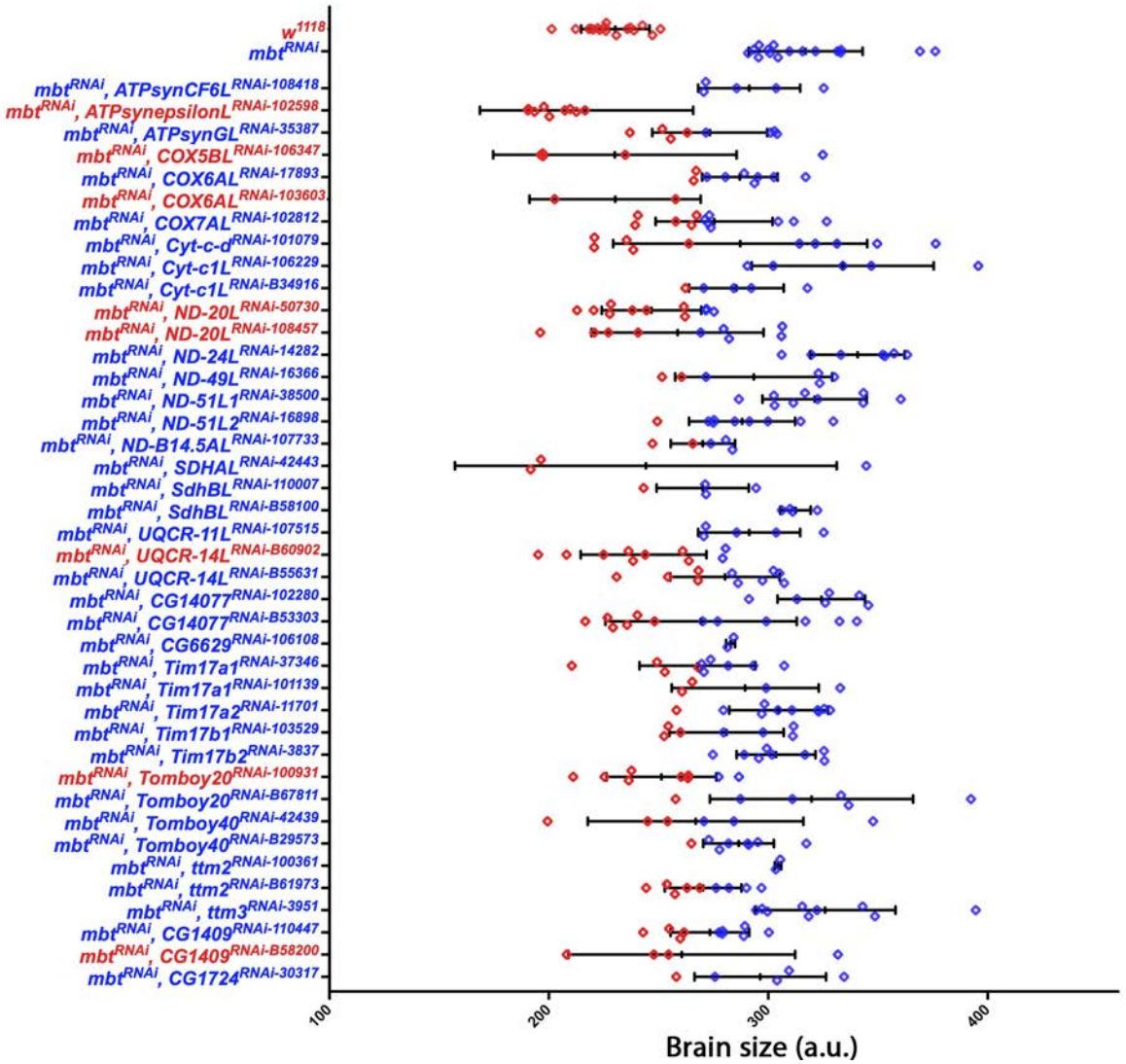

Figure 4.3: RNAi inhibition of several testis-mitochondrial genes impairs mbt tumor growth. Plot showing mbFerets (mean and s.d.) for each larval brain sample in which the indicated testis-mitochondrial gene is inhibited in mbt-RNAi tumoral background. Brains are disected at 7-8 days AEL, except for w^{1118} disected at 5-6 days AEL. Each point represents a single brain. Color code indicates brain-size class: wild-type like size (red) and mbt like size (blue) (see Materials and Methods). a.u. arbitrary units.

Wild-type and mbt samples cluster well, with most of the brains included within a narrow distribution. However, while some mbt-SPRs are also well clustered, such as *ND-20L* VDRC 50730 or *Tomboy20* BDSC 29573, most of them show a broad size distribution, in which brains from the same sample range from wild-type like to mbt sizes.

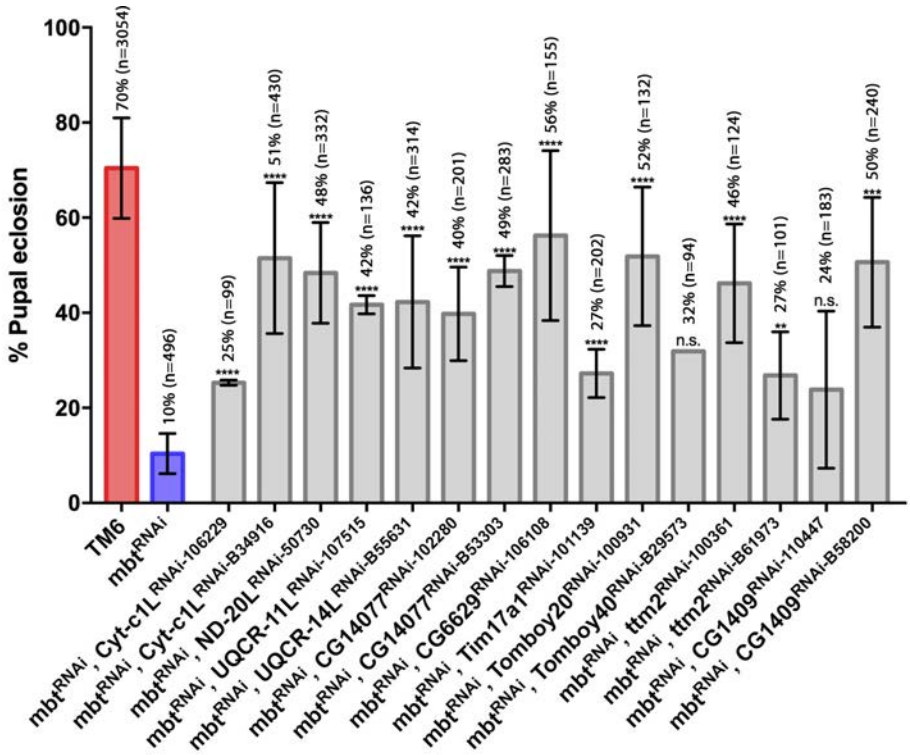

Figure 4.4: RNAi inhibition of several testis-mitochondrial genes improves mbt viability. Graph showing average pupal eclosion rates. TM6 and mbt-RNAi controls are shown as red and blue bars, respectively. All mbt-SPRs that increase pupal eclosion rate are depicted (grey bars). Average pupal eclosion rate and total number of pupae are specified for each condition. Error bars indicate s.d. $^{****}p < 0.001$; $^{***}p < 0.005$; $^{**}p < 0.01$; $^{*}p < 0.5$; n.s. not significant.

In addition, 12 RNAi lines increased pupae eclosion rates to a variable extent (Fig. 4.4). Only 3 RNAi lines (*ND-20L* VDRC-50730, *Tomboy20* VDRC-100931 and *CG1409* BDSC-B58200) rescue both size and viability. A possible explanation might be that the penetrance of the suppression is not complete, and individuals in which tumor growth has been suppressed pupariate around day 6 while only those in which

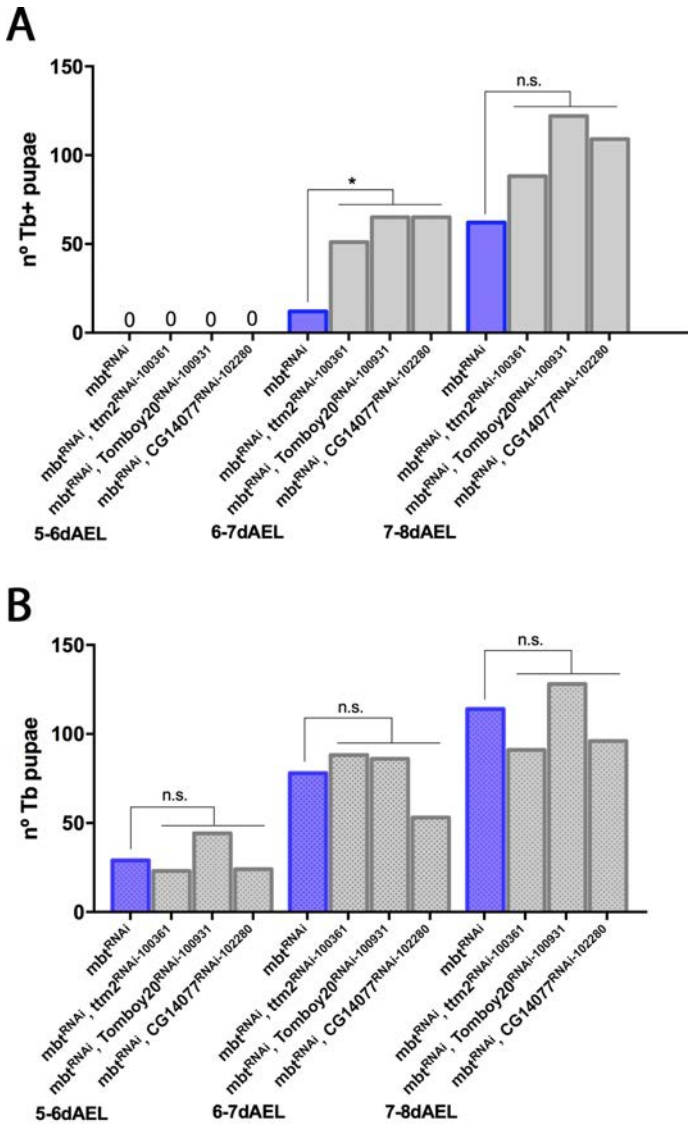

Figure 4.5: mbt-SPRs improve mbt pupariation delay. Out of the cross to test tumor suppression, two populations arise: the experimental condition (Tb+) and the control flies (Tb) (see Materials and Methods). A) Graph showing the number of pupae at 5-6, 6-7 and 7-8 days AEL for mbt^{RNAi} and three mbt-SPRs that rescued mbt viability. While at 6-7dAEL few mbt larvae have pupated, there is a significant increase in pupariation in the mbt-SPRs. B) In the control Tb larvae, the number of pupae is not statistically different between mbt and mbt-SPR conditions. * $p < 0.5$; n.s. not significant.

the tumor develops reach day 7 to 8. Indeed, in those cases in which viability was improved, the number of larvae that reached day 7-8 was much reduced (ex. *ttm2* VDRC-100361). In addition, I have observed that pupariation starts earlier when viability is increased (Fig. 4.5), further suggesting that two populations might exist and while one is rescued, the other one still develops the mutant mbt phenotype.

I focused my work on those mbt-SPRs that can be depleted to levels that inhibit tumor growth and rescue viability. These include *Cyt-c-1L, ND-20L, UQCR-11L, UQCR-14L, CG14077* and *CG6629*, which belong to the OXPHOS gene ontology; and *Tim17a1, Tomboy20, Tomboy40, ttm2* and *CG1409* of the mitochondrial transport group. To gain insight into the effect that these mbt-SPRs exert on mbt tumor growth, I examined the gross organization of the brain as revealed by DAPI staining at 5 days AEL, just before pupariation. At 5 days AEL, mbt brain lobes are clearly distinguishable from those of the wild-type as they already present a convoluted neuroepithelium that reaches medially and invades most of the brain lobe including the central brain. For every gene for which at least one RNAi line increased mbt viability, I checked brain morphology for one, or two when available, RNAi lines. In Fig. 4.6 and 4.7, a representation panel of 5 brains per condition is shown both for the Oxidative phosphorylation and Mitochondrial transport mbt-SPRs respectively. Concerning brain anatomy phenotype, I found that the penetrance of tumor suppression can be rather variable for any given RNAi line, which was only to be expected given the wide expressivity range of the mbt tumor phenotype alone. However, several testis-mitochondrial mbt-SPRs allow mbt mutant brains to develop such that they very closely resemble wild-type brains (like *CG14077* VDRC-102280 or *ttm2* VDRC-100361).

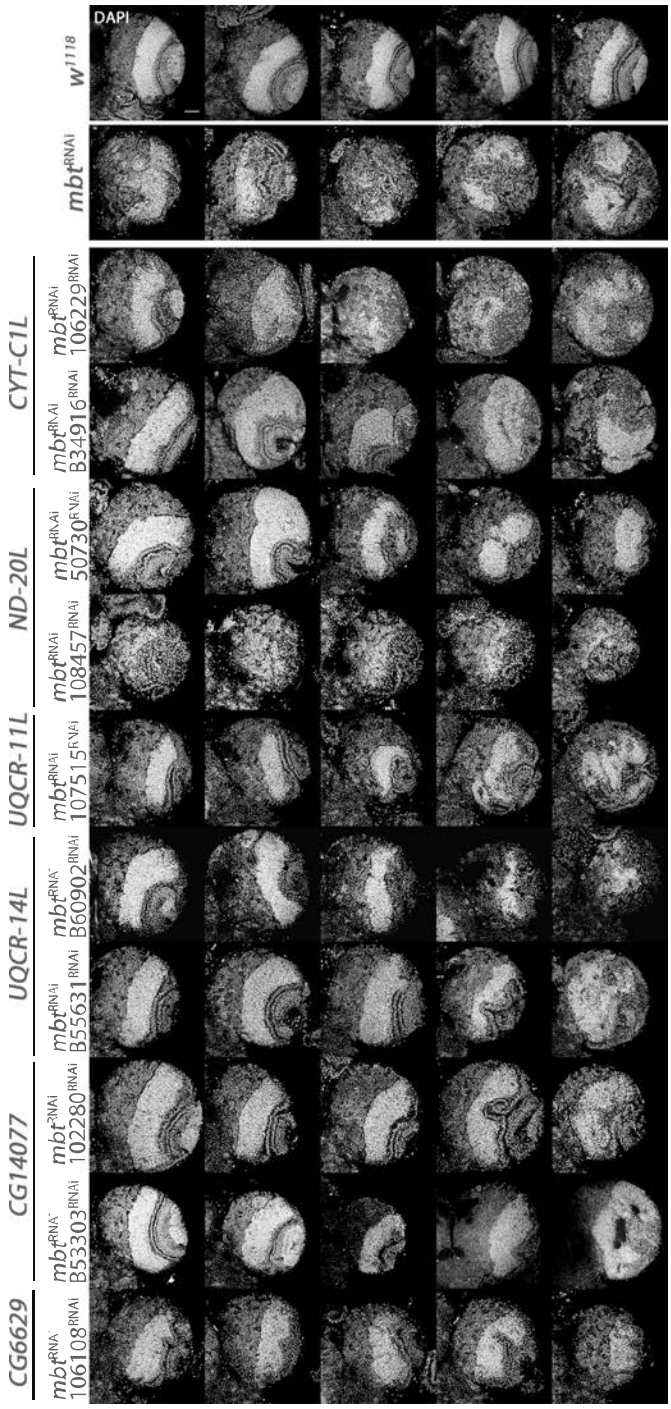

Figure 4.6: Some oxidative phosphorylation mbt-SPRs rescue wild-type brain anatomy traits. Array of confocal ventral sections of five DAPI stained optic lobes in which the corresponding mbt-SPR is inhibited in mbt-RNAi background at 5 days AEL. Those mbt-SPRs that increase viability are shown. w^{1118} and mbt^{RNAi} brains are shown above. Scale bar 50μm.

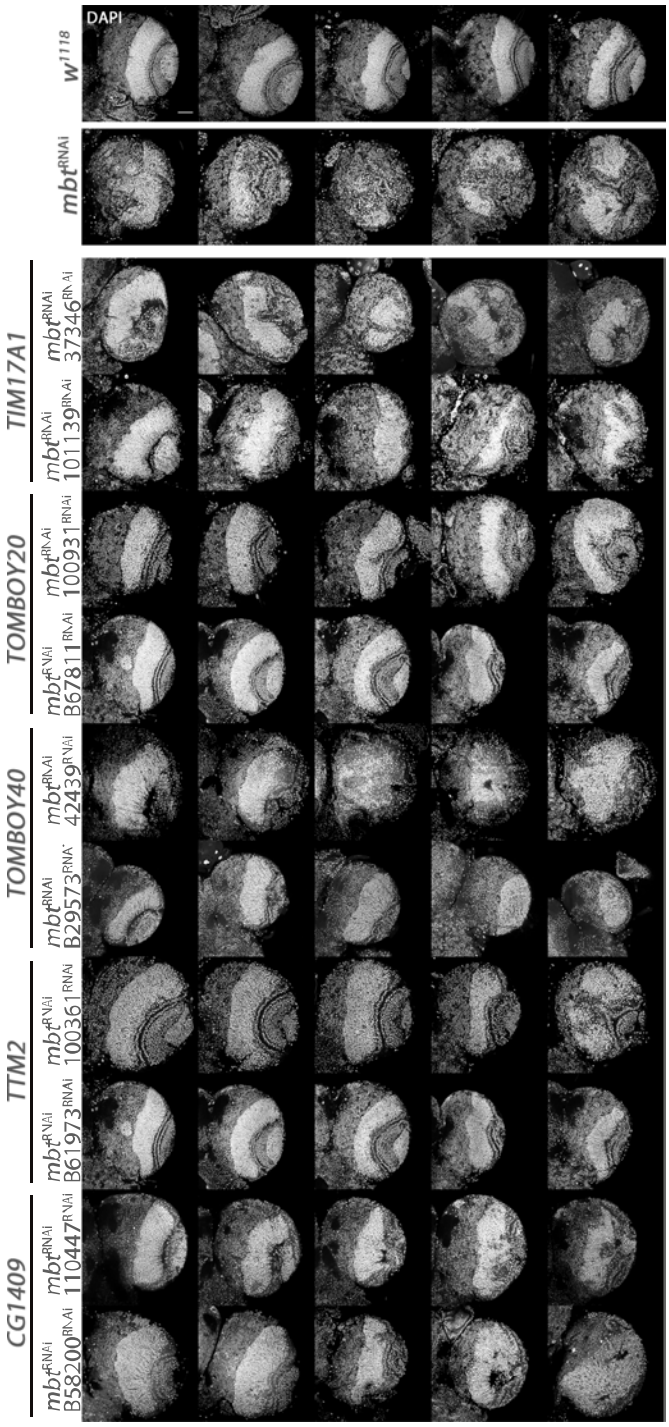

Figure 4.7: Some mitochondrial transport mbt-SPRs rescue wild-type brain anatomy traits. Array of confocal ventral sections of five DAPI stained optic lobes in which the corresponding mbt-SPR is inhibited in mbt-RNAi background at 5 days AEL. Those mbt-SPRs that increase viability are shown. w^{1118} and mbt$^{\mathrm{RNAi}}$ brains are shown above. Scale bar 50μm.

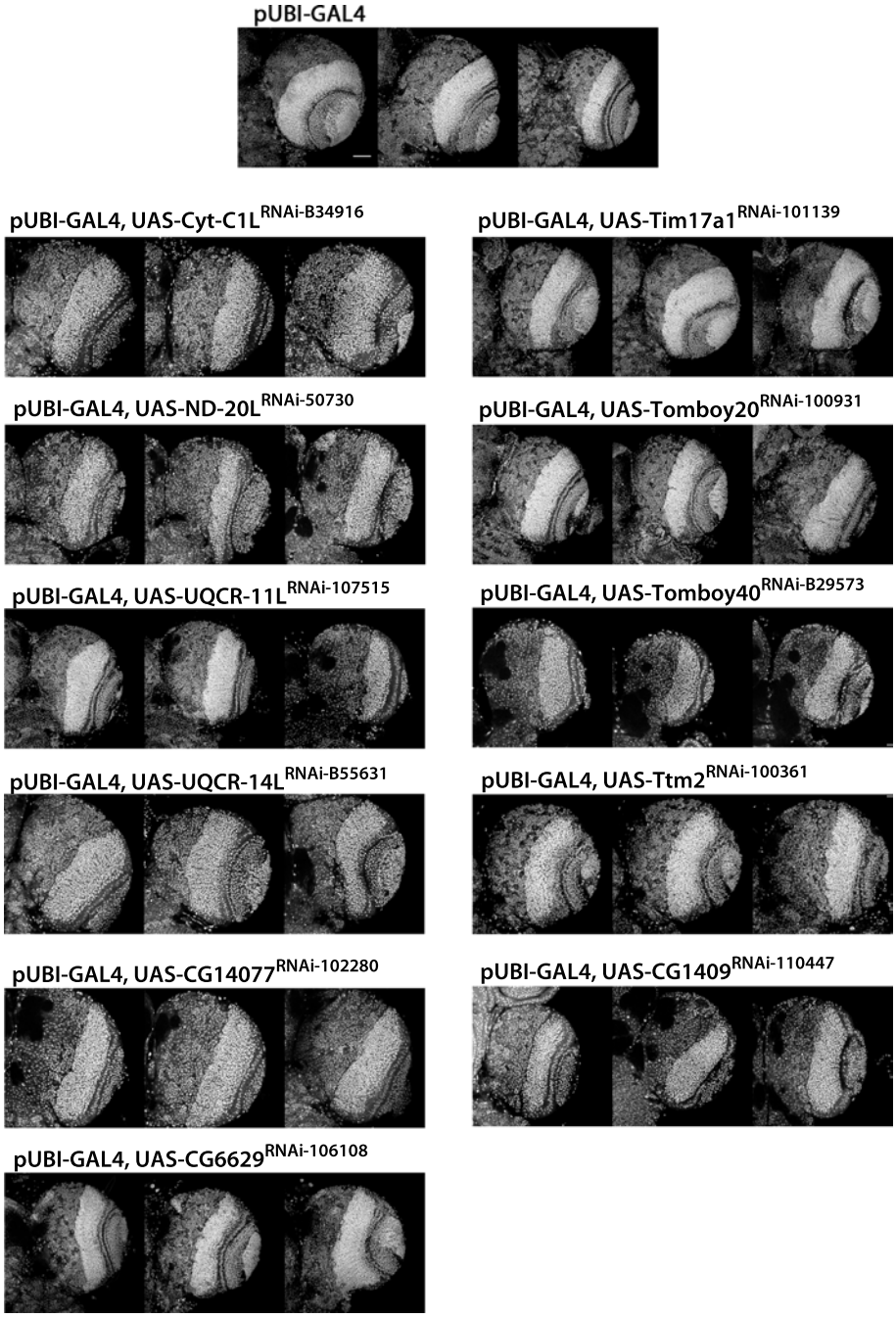

Figure 4.8: RNAi inhibition of mbt-SPRs does not affect brain lobe anatomy. Array of confocal ventral sections of five DAPI stained optic lobes in which the corresponding mbt-SPR is inhibited in wild-type background at 5 days AEL. Those mbt-SPRs that increase viability are shown. w^{1118} brains are shown above. Scale bar 50μm.

In addition, to assess the level of specificity of the mbt-SPRs, I tested the effect of expressing the best candidate RNAi lines in both wild-type and *brat*, a different larval brain tumoral background. Brat is a post-transcriptional regulator and functions as a differentiation factor that, when mutated, causes a dramatic proliferation of central brain type II neuroblasts (Bello et al., 2006; Sonoda & Wharton, 2001). Neither brain anatomy (Fig. 4.8) nor adult viability were affected upon inhibition of the selected mbt-SPRs in wild-type background. In addition, the growth of *brat* brain tumors was not perturbed by mbt-SPR RNAi depletion, as measured by brain size (Fig. 4.9), with the exception of *UQCR-14L* BDSC-B55361. Altogether, these results strongly suggest that testis-mitochondrial genes specifically contribute to mbt malignant growth.

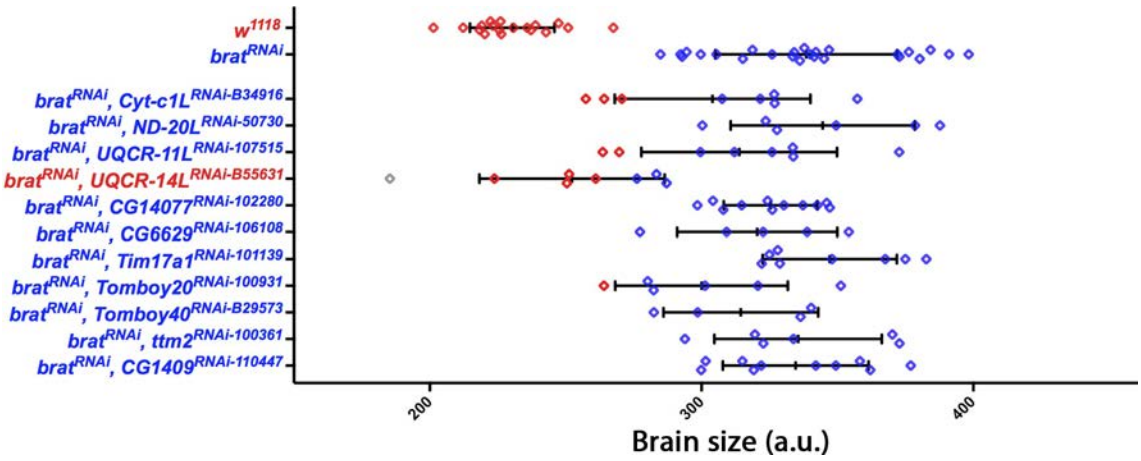

Figure 4.9: RNAi inhibition of mbt-SPRs does not affect brat tumor growth. Plot showing mbFerets (mean and s.d) from brat-RNAi larval brains depleted for the best mbt-SPR candidates. Brains are disected at 7-8 days AEL, except for w^{1118} disected at 5-6 days AEL. Each point represents a single brain. Color code indicates brain-size class: smaller than wild-type (grey), wild-type like size or mbt-SPR (red) and mbt like size (blue) (see Materials and Methods). a.u. arbitrary units.

To summarize, table 4.2 represents the results obtained for each gene concerning all criteria assessed: brain size rescue, viability rescue, brain anatomy rescue, and effect in either wild-type or *brat* backgrounds. There is a group of mbt-SPRs that affect tumor size without improving viability (*ATPsynepsilonL, COX5BL, COX6AL* or *Cyt-c-d*). Nevertheless, the most interesting mbt-SPRs are those that increase viability rates, improve brain anatomy and its effect is specific of *l(3)mbt*, without affecting the growth of a different larval brain tumor or wild-type development. These mbt-SPRs are *Cyt-c-1L, ND-20L, UQCR-11L, UQCR-14L, CG14077, CG6629, Tim17a1, Tomboy20, Tomboy40, Ttm2* and *CG1409*.

In conclusion, I have found several genes that are normally mostly expressed in testes and are critical for the growth of mbt larval brain tumors. This result could be linked to the previously reported observation that mbt tumors present a soma-to-germline transformation by the overexpression of numerous germline specific genes (Janic et al., 2010). Moreover, the putative mitochondrial role of the mbt-SPRs, as predicted by homology when compared with their respective somatic paralogs, suggests the existence of a specific mitochondrial requirement for mbt tumor development.

				MBT			WT	BRAT
	ANNOTATION SYMBOL	GENE NAME	RNAi LINE	BRAIN SIZE RESCUE?	VIABILITY RESCUE?	BRAIN ANATOMY RESCUE?	BRAIN ANATOMY DEFECT?	BRAIN SIZE RESCUE?
OXIDATIVE PHOSPHORYLATION	CG5389	ATPsynbetaL	22112	lethal				
	CG12027	ATPsynCF6L	108418	NO	NO			
	CG31477	ATPsynepsilonL	102598	YES	NO			
	CG31477	ATPsynepsilonL	28600	lethal				
	CG7211	ATPsynGL	35387	NO	NO			
	CG10396	COX4L	1482	lethal				
	CG11043	COX5BL	106347	YES	NO			
	CG30093	COX6AL	103603	YES	NO			
	CG30093	COX6AL	17893	NO	NO			
	CG18193	COX7AL	102812	NO	NO			
	CG13263	Cyt-c-d	101079	YES	NO			
	CG14508	Cyt-c1L	106229	NO	YES	NO	NO	NO
	CG14508	Cyt-c1L	B34916	NO	YES	NO		
	CG2014	ND-20L	50730	YES	YES	YES	NO	NO
	CG2014	ND-20L	108457	YES	NO	NO		
	CG6485	ND-24L	14282	NO	NO			
	CG11913	ND-49L	16366	NO	NO			
	CG11423	ND-51L1	38500	NO	NO			
	CG8102	ND-51L2	16898	NO	NO			
	CG6914	ND-B14.5AL	107733	NO	NO			
	CG5718	SDHAL	42443	NO	NO			
	CG7349	SDHBL	110007	NO	NO			
	CG7349	SDHBL	B58100	NO	NO			
	CG30354	UQCR-11L	107515	NO	YES	NO	NO	NO
	CG17856	UQCR-14L	B60902	YES	NO	NO		
	CG17856	UQCR-14L	B55631	NO	YES	YES	NO	YES
	CG14077		102280	NO	YES	YES	NO	NO
	CG14077		B53303	NO	YES	NO		
	CG6629		106108	NO	YES	NO	NO	NO
MITOCHONDRIAL TRANSPORT	CG10090	Tim17a1	37346	NO	NO	NO		
	CG10090	Tim17a1	101139	NO	YES	NO	NO	NO
	CG14666	Tim17a2	11701	NO	NO			
	CG1158	Tim17b1	103529	NO	NO			
	CG15257	Tim17b2	3837	NO	NO			
	CG14690	Tomboy20	100931	YES	YES	YES	NO	NO
	CG14690	Tomboy20	B67811	NO	NO	NO		
	CG8330	Tomboy40	42439	NO	NO	NO		
	CG8330	Tomboy40	B29573	NO	YES	YES	NO	NO
	CG12313	ttm2	100361	NO	YES	YES	NO	NO
	CG12313	ttm2	B61973	NO	YES	YES		
	CG6691	ttm3	3951	NO	NO			
	CG1409		110447	NO	YES	NO	NO	NO
	CG1409		B58200	YES	YES	NO		
	CG1724		30317	NO	NO			

Table 4.2: Summary results from the screen of testis-mitochondrial genes. Table summarizing the outcome of brain size, adult viability and brain anatomy rescue for each of the testis-mitochondrial RNAi lines analyzed in mbt-RNAi background. RNAi effect in wild-type (WT) and *brat* backgrounds is also specified when required. Positive results are highlighted in red.

4.3 Testis-mitochondrial proteins are not among the 4000 most expressed proteins in mbt brains

Previous transcriptomic expression data from our laboratory did not detect the upregulation of testis-mitochondrial genes in mbt tumors (Janic et al., 2010). Nevertheless, the fact that the inhibition of several testis-mitochondrial genes impaired mbt tumor growth made us hypothesize that these testis-mitochondrial proteins might be expressed in mbt brains. To test this hypothesis, I analyzed the proteome of mbt brain tumors.

Protein symbol	Ensembl ID	% Coverage	# PSMs	# Peptides
RpS5b	FBpp0082465	57,4	52	18
dhd	FBpp0311766	49,5	7	7
vas	FBpp0401446	46,6	40	27
CG15930	FBpp0291095	43,1	52	21
Pxt	FBpp0082932	42,6	23	19
CG31373	FBpp0081794	41,8	7	5
CG9925	FBpp0082339	41,7	36	26
CG31997	FBpp0311450	33,1	6	6
cona	FBpp0083044	31,4	5	4
GNBP3	FBpp0076237	27,6	14	10
SkpB	FBpp0087127	27,3	3	3
TrxT	FBpp0070722	24,8	3	3
fs(1)Yb	FBpp0070462	20,1	20	15
CG32483	FBpp0072504	16,4	6	6
piwi	FBpp0079755	15,3	9	9
CG14036	FBpp0078666	12,9	1	1
CG11674	FBpp0073743	6,1	1	1
CG13741	FBpp0087713	6,0	1	1
CG9961	FBpp0077420	5,8	3	2
yellow-h	FBpp0088184	5,0	2	2
HP1D3csd	FBpp0074441	3,9	2	1
zpg	FBpp0303218	3,5	1	1
krimp	FBpp0086333	3,2	2	2
CG4753	FBpp0075179	2,6	1	1
SoYb	FBpp0300444	2,5	3	3
CG42255	FBpp0304441	0,3	1	1

Table 4.3: Mbt tumor signature (MBTS) proteins detected in mbt brains. 26 out of the total 100 MBTS proteins included in the MBTS were detected in the proteomic profile. Table showing the corresponding coverage and number of peptide spectrum matches (PSM), peptides and unique peptides quantified for each protein. The coverage displays the percentage of the protein sequence covered by the identified peptides. The number of PSM displays the total number of identified peptide sequences for the protein, including those redundantly detected. The number of peptides displays the number of identified distinct peptide sequences for the protein group. The number of unique peptides displays the number of identified peptide sequences that are unique for the protein group.

First, I conducted a pilot experiment to check whether the technique was sensitive to the detection of our proteins of interest. I dissected testes with seminal vesicles from previously isolated adult males and performed a subcellular fractionation experiment to also test whether a simple protocol would allow us to increase the rate of mitochondrial proteins detected. In this first approach, I was able to detect 4947 proteins, including most of our proteins of interest (Table 4.4A), improving the results from previous sperm proteome studies (Dorus et al., 2006; Wasbrough et al., 2010). However, subcellular fractionation did not help to positively discriminate for mitochondrial proteins (data not shown).

Next, I analyzed protein expression in wild-type and mbt brains, separating the proteins in 4 different fractions by molecular weight in a polyacrylamide gel in order to increase the rate of detected proteins. Similarly, in this second experiment I also obtained a significant amount of detected proteins (3052 in wild-type and 4384 in mbt samples). I first validated the results by checking the expression of the mbt signature (MBTS) proteins. The MBTS comprises the 100 most upregulated transcripts in mbt tumors, from which a substantial fraction consists of germline genes, thus revealing a soma-to-germline transformation of the brain tissue (Janic et al., 2010). In our proteome experiment, I was able to detect nearly one fourth of the MBTS proteins (Table 4.3), validating for the first time that the germline transformation of mbt tumors also occurs at the protein level. However, the testis-mitochondrial proteins were not among the 4000 proteins detected in mbt tumors (Table 4.4A). This negative result is not caused by an underrepresentation of mitochondrial proteins, because many of the somatic counterparts of the testis-mitochondrial proteins were indeed detected (Table 4.4B).

In conclusion, testis-mitochondrial proteins were not detected by our proteomic profiling among the most expressed proteins in mbt tumors. Yet, these results do not discard their presence in mbt tumors, as they could be expressed at a very low rate or be only expressed in a small subset of cells. In fact, there are more examples of genes whose expression is not upregulated but that are essential for the development of mbt tumor, such as *mei-w68* (Rossi et al., 2017). Another possible scenario is that testis-mitochondrial proteins are not expressed in the brain and that the observed mbt tumor suppression phenotype is caused by a systemic effect.

A

			MASS SPECTROMETRY DECTECTION				
	TESTIS PARALOGS		SPERM	SPERM	OUR RESULTS		
	Annotation Symbol	Gene Name	(Dorus et al.)	(Wasbrough et al.)	Testes & SV	WT Brain	MBT Brain
OXIDATIVE PHOSPHORYLATION	CG5389	ATPsynbetaL			x	x	x
	CG12027	ATPsynCF6L	x		x		
	CG31477	ATPsynepsilonL				x	
	CG7211	ATPsynGL	x		x		
	CG10396	COX4L			x		
	CG11043	COX5BL	x	x	x		
	CG30093	COX6AL		x	x		
	CG14077	CG14077		x	x		
	CG18193	COX7AL	x	x	x		
	CG13263	Cyt-c-d			x		
	CG14508	Cyt-c1L	x	x	x		
	CG2014	ND-20L			x		
	CG6485	ND-24L		x	x		
	CG11913	ND-49L	x		x		
	CG11423	ND-51L1		x	x		
	CG8102	ND-51L2	x		x		
	CG6914	ND-B14.5AL			x		
	CG5718	SdhAL	x	x	x		
	CG7349	SdhBL	x	x	x		
	CG6629	SdhCl	x		x		
	CG30354	UQCR-11L					
	CG17856	UQCR-14L		x	x		
MITOCHONDRIAL TRANSPORT	CG10090	Tim17a1		x	x		
	CG14666	Tim17a2					
	CG1158	Tim17b1			x		
	CG15257	Tim17b2			x		
	CG1724	CG1724					
	CG14690	tomboy20			x		
	CG8330	tomboy40			x		
	CG12313	ttm2			x		
	CG6691	ttm3					
	CG1409	CG1409			x		

B

		MASS SPECTROMETRY DECTECTION				
SOMATIC PARALOGS		SPERM	SPERM	OUR RESULTS		
Annotation Symbol	Gene Name	(Dorus et al.)	(Wasbrough et al.)	Testes & SV	WT Brain	MBT Brain
CG11154	ATPsynbeta		x	x		
CG4412	ATPsynCF6	x		x	x	x
CG9032	sun					
CG6105	ATPsynG	x		x	x	x
CG10664	COX4			x	x	x
CG11015	COX5B			x	x	x
CG17280	levy				x	x
CG9603	COX7A					
CG17903	Cyt-c-p			x	x	x
CG4769	Cyt-c1			x	x	x
CG9172	ND-20			x		x
CG5703	ND-24	x		x	x	x
CG1970	ND-49			x	x	x
CG9140	ND-51			x	x	x
CG3621	ND-B14.5A			x	x	x
CG17246	SdhA	x	x	x	x	x
CG3283	SdhB			x	x	x
CG6666	SdhC			x	x	x
CG41623	UQCR-11					x
CG3560	UQCR-14			x	x	x
CG40451	Tim17b			x	x	x
CG7654	Tom20			x	x	x
CG12157	Tom40			x	x	x
CG2713	ttm50			x	x	x
CG5268	blp			x		

Table 4.4: Testis-mitochondrial and somatic paralogs protein expression in mbt tumors. Table summarizing protein expression profiles from: A) testis-mitochondrial genes and B) their respective somatic counterparts, in both previous published sperm proteome data (Dorus et al., 2006; Wasbrough et al., 2010) and our mass spectrometry experiments in testes & seminal vesicle (SV) and w^{1118} and $l(3)mbt^{ts1}$ larval brains.

4.4 Loss of function of the testis-mitochondrial *ttm2* gene in *l(3)mbt*^{ts1} mutant condition confirms *ttm2* requirement for mbt tumor growth

As a final step in our study of the role of mitochondrial genes in mbt tumor growth I focused on *ttm2*, which is one of the mbt-SPRs whose loss of function has a most dramatic effect on viability and larval brain anatomy in mbt-RNAi individuals. Moreover, *Tim50*, *ttm2* human homologue, has been described as overexpressed in breast cancer and non-small cell lung carcinoma cell lines and its depletion reduced cellular growth rate (Sankala et al., 2011; Gao et al., 2016).

Because all data obtained so far was based on RNAi depletion, I first reassessed *ttm2* function in mbt tumors using classical mutant alleles: *l(3)mbt*^{ts1} and *ttm2*^{C205}. *l(3)mbt*^{ts1} is an EMS-induced, temperature-sensitive (ts), recessive-lethal mutation in *l(3)mbt* that can be propagated at the permissive temperature of 22°C in the homozygous state, but causes malignant transformation of the optic lobe neuroepithelia at the restrictive temperature of 29°C (Gateff et al., 1993). *ttm2*^{C205} is a P-element insertion (PBac{3Hpy+}C205) in the 5′UTR of the gene that causes male sterility in the homozygous condition (Englund et al., 2006).

I first checked the effect of *ttm2*^{C205} loss of function in wild-type brain development. Upon co-staining with Phalloidin (that labels actin-membrane filaments) and DAPI (DNA labelling), I found that *ttm2* loss of function has no effect in optic lobe development (Fig. 4.10A), which is consistent with our previous *ttm2* RNAi knockdown results. Moreover, the number of mitotic cells as revealed by PH3 staining (Goto et al., 1999) in the neuroepithelia -the region in which mbt tumors arise and where *ttm2* has also been published to be expressed (Southall et al., 2013)- was the same in wild-type and in *ttm2*^{C205} mutants (Fig. 4.10B).

Then, I generated a recombinant chromosome containing both *ttm2*^{C205} and *l(3)mbt*^{ts1} alleles and checked the development of mbt tumors in this condition. *l(3)mbt*^{ts1} *ttm2*^{C205} homozygous mutants die as larvae or early pupae around day 8 AEL. Depletion of *ttm2* significantly reduces the growth of mbt brain tumor (Fig. 4.11A), although brain lobe anatomy rescue is only partial (Fig. 4.11B). These results are consistent with our previous results using RNAi technology and strongly substantiate the importance of *ttm2* for mbt tumor growth.

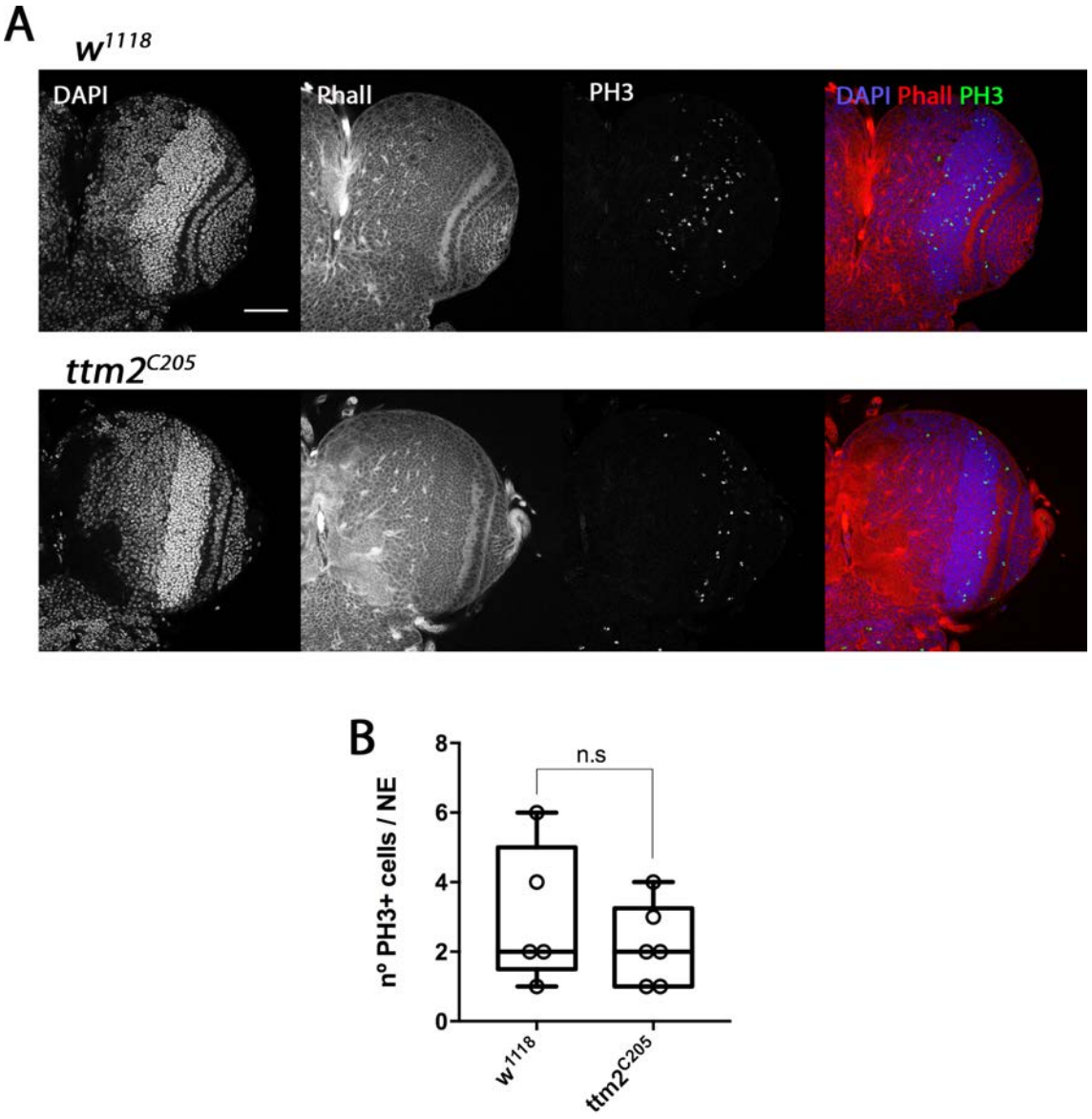

Figure 4.10: *ttm2*^{C205} brains have wild-type brain anatomy traits. A) Immunostaining of w^{1118} and *ttm2*^{C205} third instar larval brains with DAPI (blue) to stain DNA, Phalloidin (red) to stain actin-membrane filaments, and PH3 (green) to stain dividing cells. B) Boxplot showing the quantification of PH3+ cells per neuroepithelium in a single slice (n=5) Error bars indicate s.d. Scale bar 50μm.

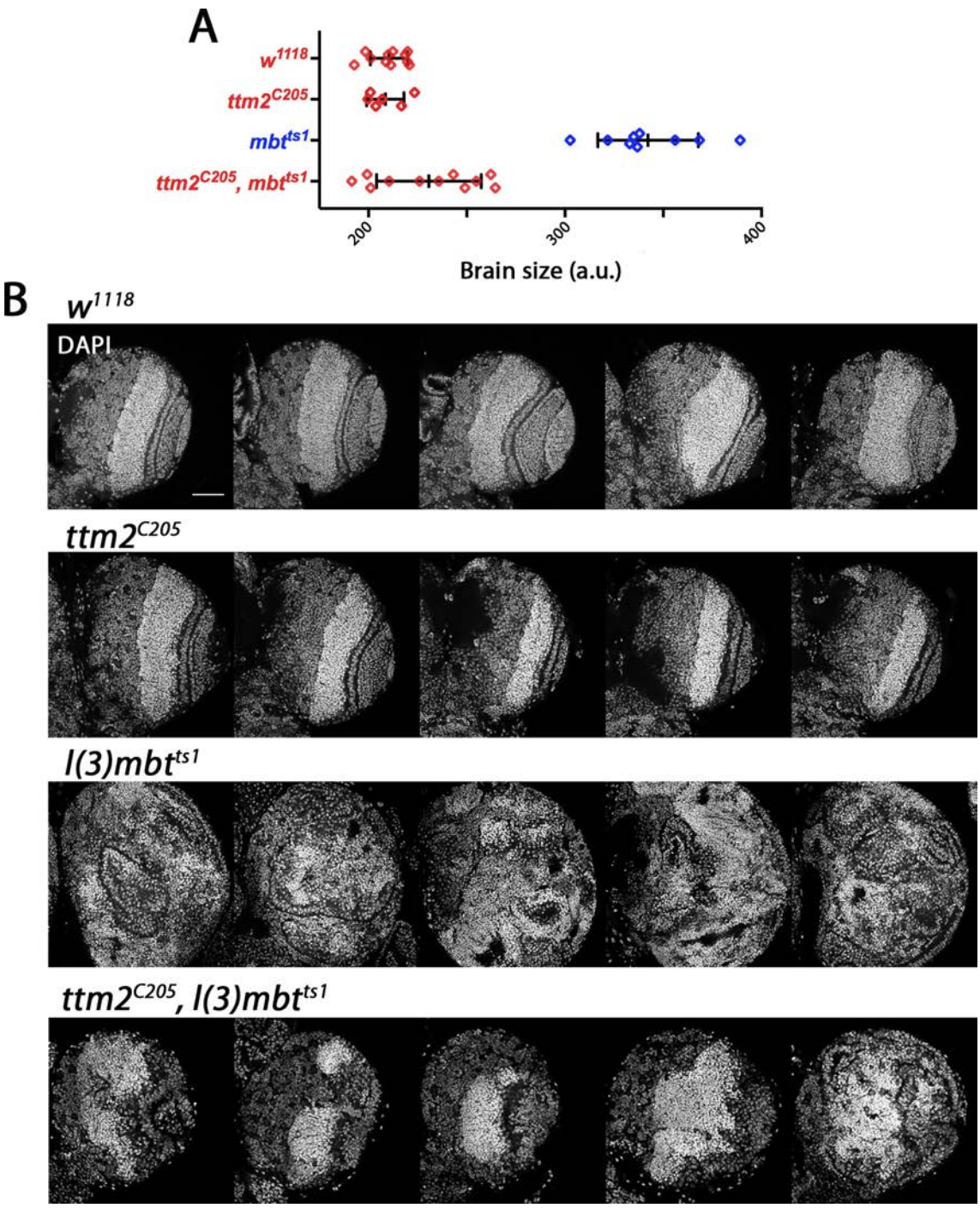

Figure 4.11: homozygous *ttm2*^{C205} *l(3)mbt*^{ts1} brains present wild-type size. A) Plot showing brain size (mean and s.d.) for w^{1118} and *ttm2*^{C205} at 5 days AEL, and *l(3)mbt*^{ts1} and double mutant *ttm2*^{C205} *l(3)mbt*^{ts1} at 7-8 days AEL. B) Array of confocal ventral sections of five DAPI stained optic lobes from each genotype. Scale bar 50μm.

4.5 Ttm2 protein localizes to the mitochondria

tiny tim 2 (*ttm2*) is a 1,5kb gene that has the cytological map location 61B3, in the left arm of the 3rd chromosome. *ttm2* is very similar in sequence to *Drosophila ttm3* and *ttm50* genes. While *ttm50* is ubiquitously expressed, *ttm2* and *ttm3* appear to be testes-specific (Sugiyama et al., 2007). However, a different study has found *ttm2* to be also expressed in neuroepithelial and neuroblast cells of the larval brain (Southall et al., 2013), challenging the testes specificity of *ttm2*. Hence, *ttm2* mutants are male sterile (Englund et al., 2006), supporting a role for Ttm2 in *Drosophila* male fertility.

Both *ttm2* and *ttm3* were probably originated by retropositional events, because they are intronless, so they are likely to have been inserted into the genome after a duplication event (Bai et al., 2007). Ttm50, Ttm2 and Ttm3 sequences contain a putative, positively charged presequence at the N-terminal end and a putative transmembrane domain, suggesting that all gene products translocate into the mitochondria and are embedded in the inner membrane (Fig. 4.12A). Ttm50 was indeed proved to localize to the mitochondria by co-staining with a mitochondrial marker (Sugiyama et al., 2007). The subcellular localization of Ttm2 remains unconfirmed.

To check Ttm2 subcellular localization I expressed an HA-tagged Ttm2 protein using the GAL4/UAS system (Brand & Perrimon, 1993). I used a UAS-ttm2-HA transgene available at the FlyORF stock collection and expressed it under the control of two different brain cell promoters, insc-GAL4 and c855a-GAL4, that are expressed in neuroblast and neuroepitelial brain cells respectively. The localization of Ttm2-HA was observed in a reticulated pattern in the cytoplasm of the NE and NB cells. Moreover Ttm2-HA colocalizes tightly with the inner membrane mitochondrial protein ATP5A (Fig. 4.12). I therefore concluded that, as predicted from sequence homology, Ttm2 localizes to mitochondria.

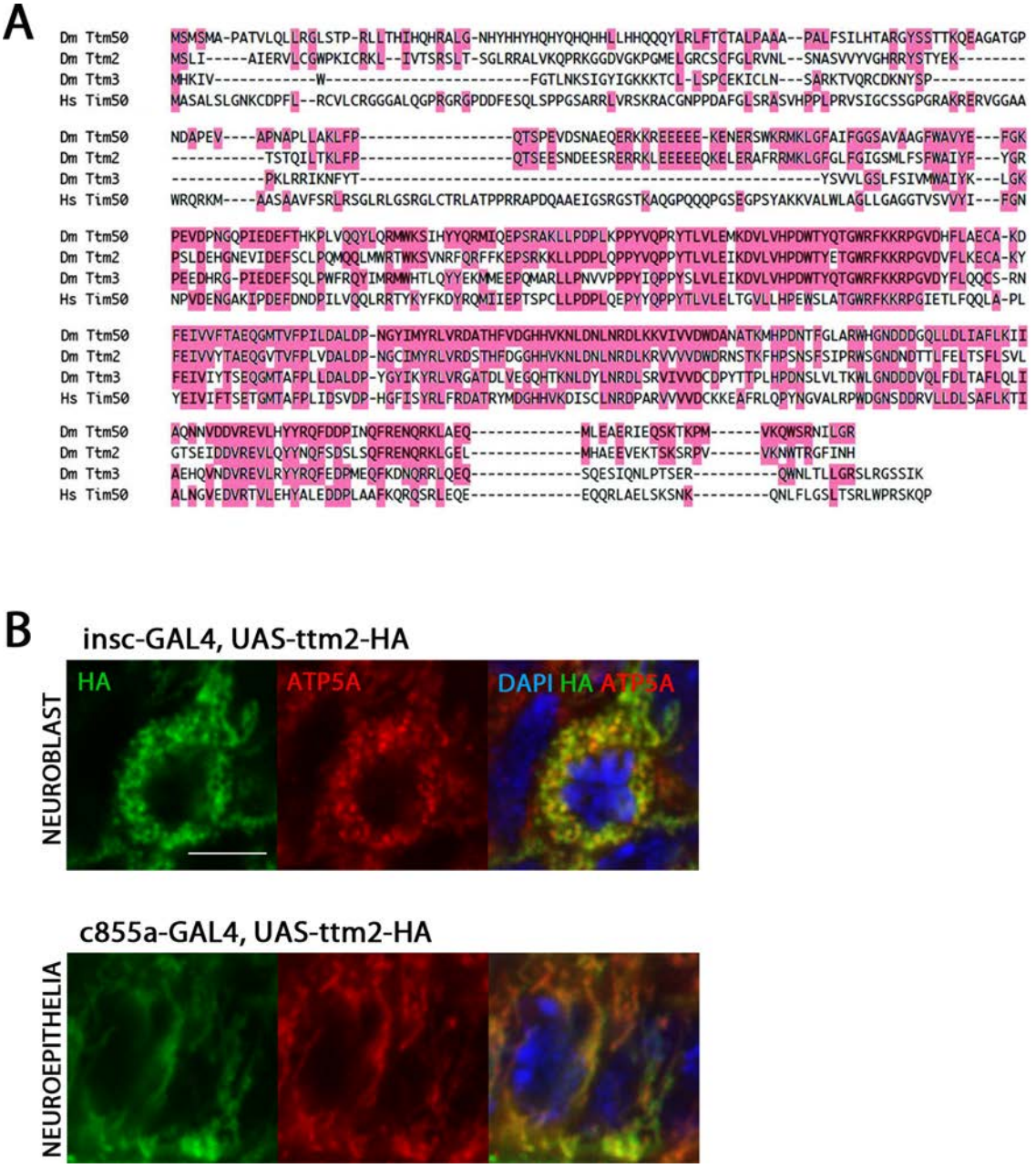

Figure 4.12: Ttm2 is a paralog of *Drosophila* ttm50 and human Tim50 and localizes to the mitochondria. A) Amino acid sequence comparison between *Drosophila* (Dm) Ttm50, Ttm2 and Ttm3 proteins and Human (Hs) Tim50 protein. Amino acid residues identical to Dm Ttm50 are highlighted in pink and gaps are indicated by dashes. Adapted from Sugiyama et al. (2007). B) Expression of the UAS-ttm2-HA construct with the NB specific driver insc-GAL4 and the NE specific driver c855a-GAL4. DAPI (blue) stains the DNA, HA (green) shows Ttm2 expression and ATP5A (red) was used to stain the mitochondria. Scale bar 5μm.

4.6 *ttm2* is expressed in both wild-type and *l(3)mbt*^{ts1} larval brains

Our transcriptome and proteome-wide profiles did not detect *ttm2* expression in either wild-type or mbt brains, even though *ttm2* has been reported to be expressed in NE and NB cells of the wild-type larval brain (Southall et al., 2013). We therefore decided to re-assess ttm2 mRNA expression using two different approaches: RNA in situ hybridization and quantitative real-time PCR (qRT-PCR).

I generated two different probes for RNA in situ hybridization, an antisense probe that is specific for ttm2 mRNA and a sense probe as a negative control. I confirmed that UAS-ttm2 overexpressed in the neuroepithelium with the c855a-GAL4 driver is detected by our antisense probe, while the sense probe generates no signal. Using these probes I found that, *ttm2* is expressed indeed, albeit at low levels, in *l(3)mbt*^{ts1} larval brain tumors as well as in wild-type larval brains in the NE area (Fig. 4.13A). qRT-PCR assays confirmed that *ttm2* expression is low but significant in both wild-type and *l(3)mbt*^{ts1} brains (Fig. 4.13B). As a positive control for the qRT-PCR assays I used testes. Consistent with FlyAtlas and ModEncode data, I found that *ttm2* is expressed at very high level in testes. Thus, in summary, using two independent techniques I was able to confirm ttm2 mRNA expression in both wild-type and mbt brains.

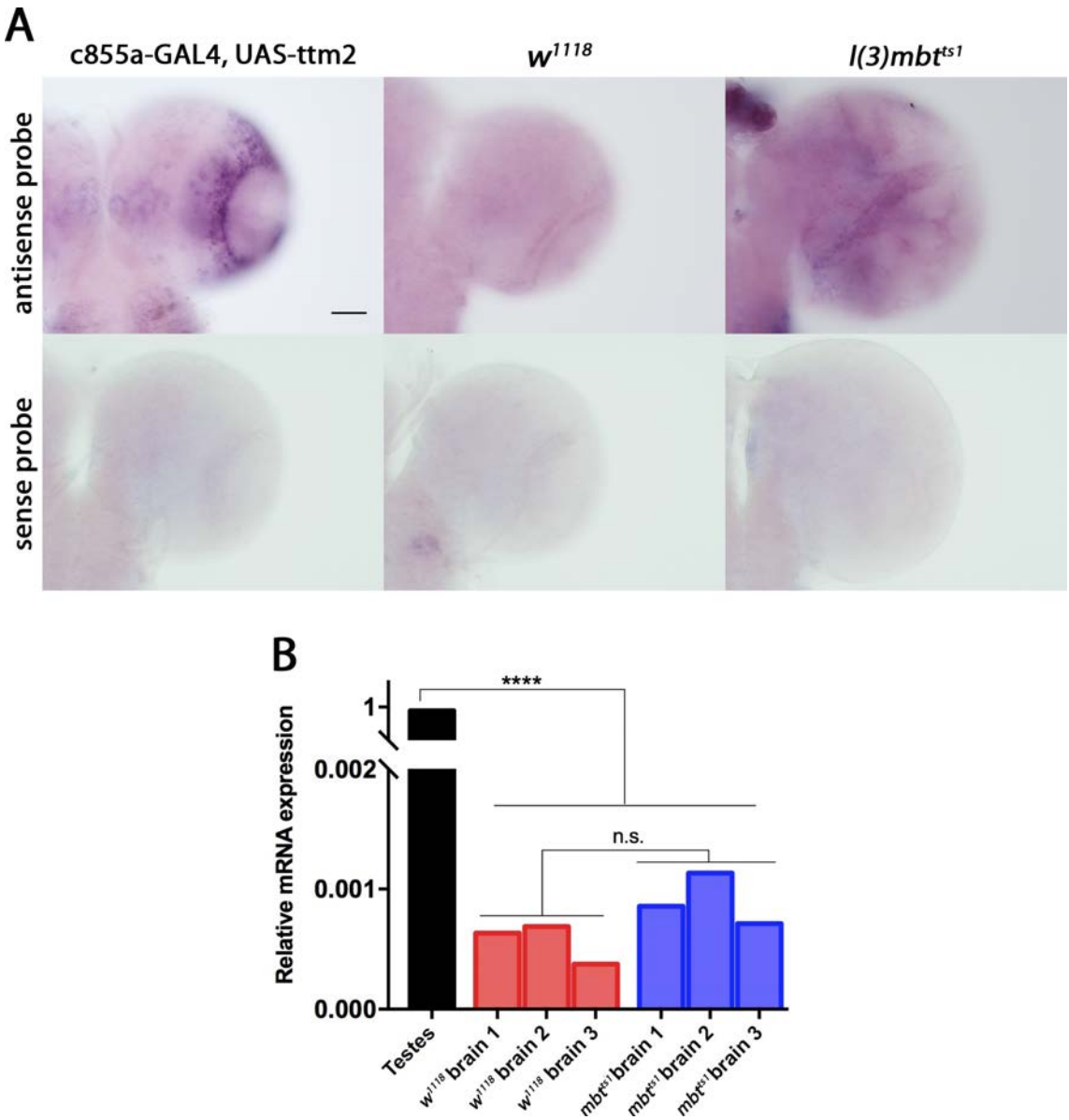

Figure 4.13: *ttm2* is expressed in wild-type and *l(3)mbt*^{ts1} larval brains. A) RNA in situ hybridization showing the expression of ttm2 mRNA in both w^{1118} and *l(3)mbt*^{ts1} brains. Overexpression of *ttm2* in the neuroepithelia (c855a-GAL4, UAS-ttm2) was used as a positive control. No signal is observed with the sense probe (negative control). Scale bar 50μm. B) Graph showing ttm2 mRNA relative expression levels compared to RP49 measured by qRT-PCR in w^{1118} testes and both w^{1118} and *l(3)mbt*^{ts1} larval brains. Error bars indicate s.d. ****$p < 0.001$; n.s. not significant.

4.7 Ectopic expression of Ttm2 is sufficient to induce hyperplasia in the medial OPC neuroepithelia

Given *ttm2* essential contribution to overgrowth in mbt brain tumors, we wondered whether *ttm2* could on its own cause overproliferation in the larval brain. To test this hypothesis I started by expressing an UAS-ttm2 transgene using the ubiquitous pUbi-GAL4 driver and found that *ttm2* gain of function (ttm2-GOF) caused lethality at early larval stages (data not shown).

Next, I expressed *ttm2* in either the NE or NBs, the two brain cell types in which *ttm2* expression was previously reported (Southall et al., 2013). For NB cells, I used specific drivers for both type I and type II NB (insc-GAL4) and medulla NB (c253-GAL4). Overexpressing *ttm2* with either insc-GAL4 or c253-GAL4 did not affect fly viability. Measurement of the respective compartments of the brain in which *ttm2* was ectopically expressed showed that neither the central brain nor the medulla relative areas were increased (Fig. 4.14A, B and C). In addition, NB asymmetric division was not impaired as checked by the proper segregation of the cell fate determinant Miranda during mitotic division (Fig. 4.14A′ and A″).

In contrast, using c855a-GAL4 to drive *ttm2* expression in the NE, caused developmental delay and flies died as third-instar larvae or early pupae. Keeping the larvae at 25°C the first 4 days AEL and then switching them to 29°C, there is a severe developmental delay that enables the flies to stay in the larval stage for much extended periods of time, in extreme cases up to day 20 AEL, while wild-type larvae pupariate around day 5. I found that in these larvae, *ttm2* overexpression produced neuroephitelial hyperplasia, progressively increasing the relative area of the OPC region, while the relative medulla area was subsequently reduced (Fig. 4.15A). Yet, neither IPC nor lamina regions were affected (Fig.4.15B and C). These results suggest that the hyperplasia is restricted to the medial layer of OPC neuroepithelial cells -those that will produce medulla neuroblasts- affecting neither the OPC lateral cells nor the IPC cells. The quantification of the relative areas of the different brain lobe compartments is shown in Fig 4.16.

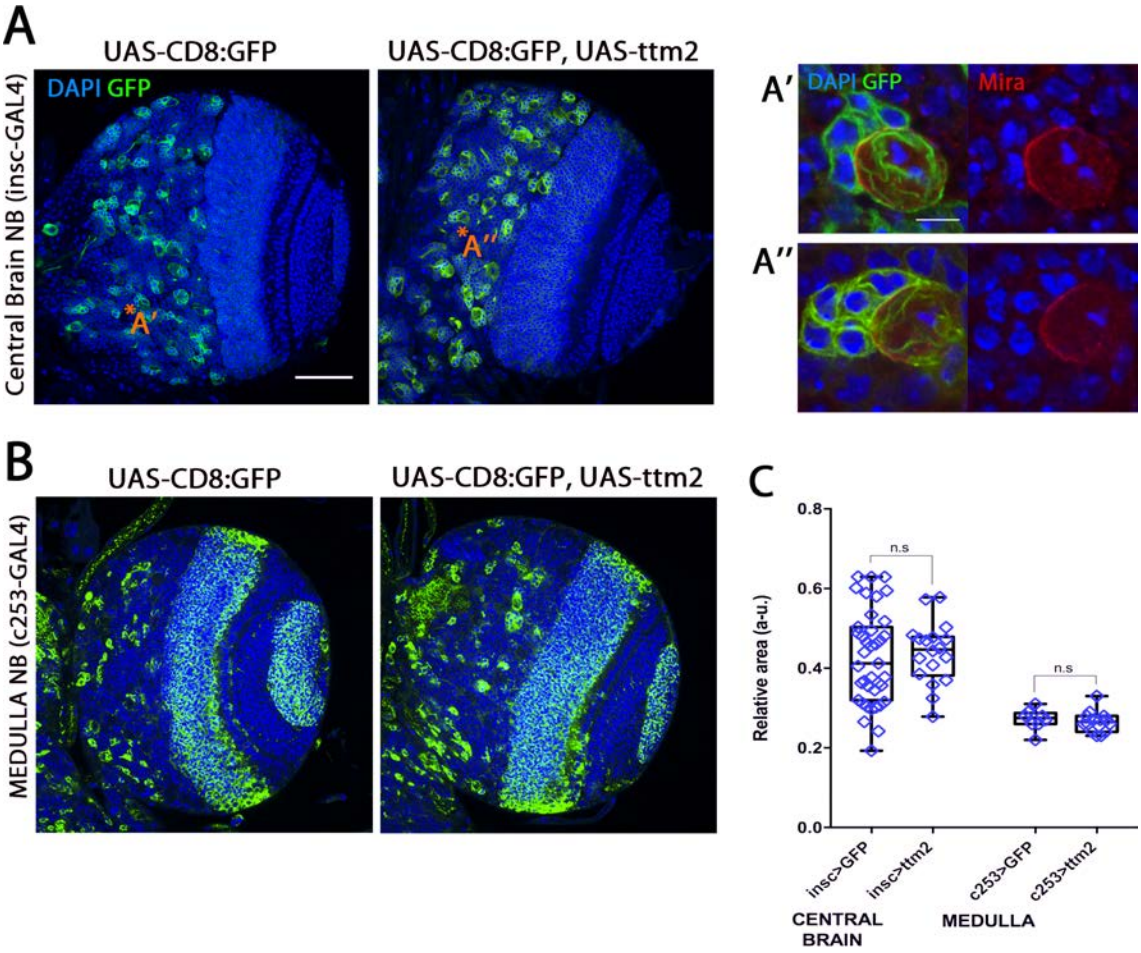

Figure 4.14: *ttm2* overexpression does not affect NB development. A) Confocal ventral section of insc-GAL4 brains expressing either UAS-CD8:GFP or UAS-CD8:GFP and UAS-ttm2. DAPI stains the DNA and central brain NB and their GMC progeny are labeled with GFP. An inset of control and *ttm2* expressing NBs during cell division (A′ and A″ respectively) stained with Miranda (red) is shown. B) Confocal ventral section of c253-GAL4 brains expressing either UAS-CD8:GFP or UAS-CD8:GFP and UAS-ttm2. DAPI stains the DNA and medulla and few CB NBs and are labeled with GFP. C) Boxplot representing CB relative area in the insc-GAL4 condition and medulla relative area in the c253-GAL4 condition. Error bars indicate s.d. Scale bars: in toto brains 50μm; NB inset 5μm. n.s. not significant.

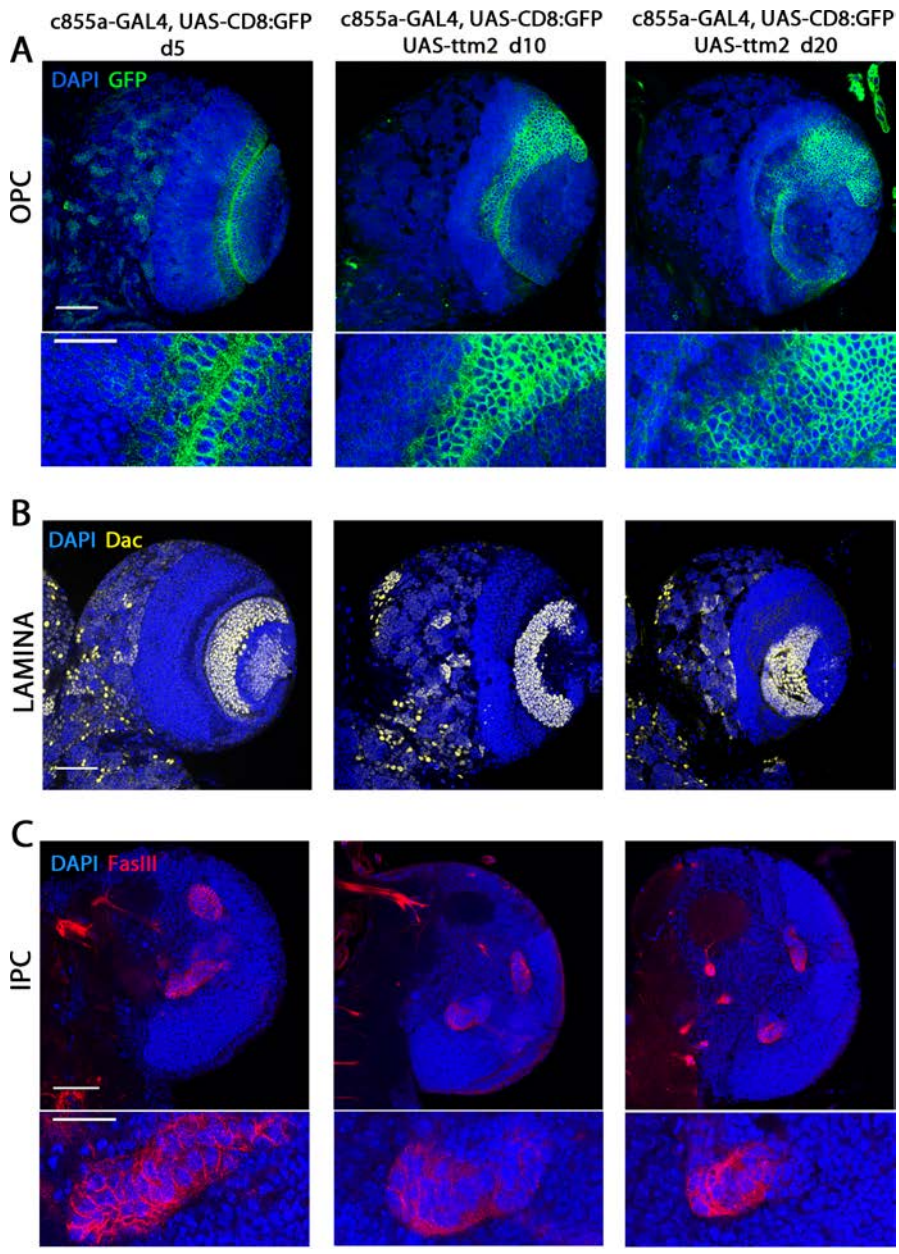

Figure 4.15: *ttm2* overexpression causes hyperplasia in the OPC. UAS-ttm2 and UAS-CD8:GFP were overexpressed in the NE using c855a-GAL4 driver. Brains were disected at 5 days AEL in the control experiment and at 10 and 20 days AEL in the *ttm2* overexpression condition. A) Ventral OL section showing the NE region stained with GFP. An inset of the OPC cells is shown. B) Ventral OL section showing the lamina region stained with Dachshund (yellow). C) Medial OL section showing the IPC stained with Fasciclin III (red). An inset of the IPC cells is shown. Scale bars: in toto brains 50μm; OPC and IPC insets 20μm.

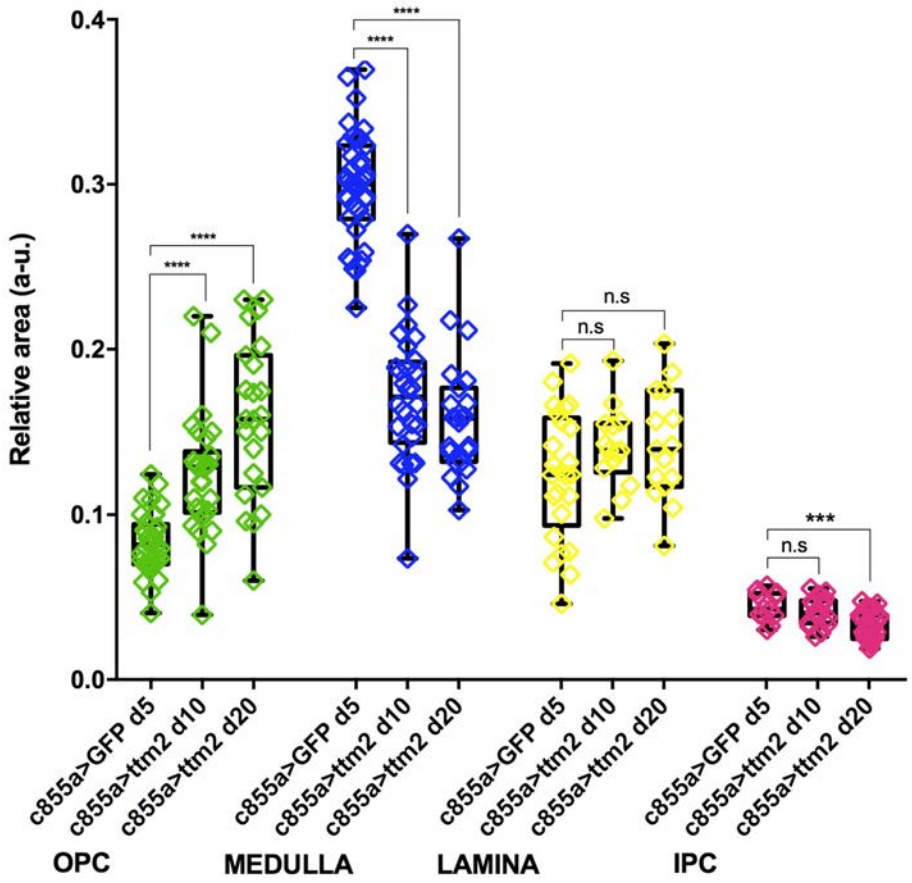

Figure 4.16: *ttm2* overexpression increases relative OPC area. Boxplot showing the relative area of the outer proliferative center (OPC), Medulla, Lamina and inner proliferative center (IPC) regions compared to the total OL area. Error bars indicate s.d. $^{****}p < 0.001$; $^{***}p < 0.005$; n.s. not significant.

To assess whether the amplified set of cells corresponds to either neuroepithelial cells or to cells transitioning from the neuroepihtelial to the neuroblast stage, I checked NB cell fate determinants and NE identity markers. The amplified cell pool does not express either Miranda or Deadpan NB cell fate determinants, suggesting that these cells have not entered the neuroepithelial to neuroblast transition yet (Fig. 4.17). In addition, both atypical Protein Kinase C (aPKC) and *Drosophila* E-Cadherin (DE-Cadh), that label epithelial apical cortex and adherens junctions respectively, are correctly localized in the amplified cell pool, suggesting that these cells retain the neuroepithelial identity and that, furthermore, polarity is not perturbed. Centrosomal labeling using the asl-YFP transgene revealed that the centrosomes are also apically localized as in the wild-type neuroepithelia (Fig. 4.18).

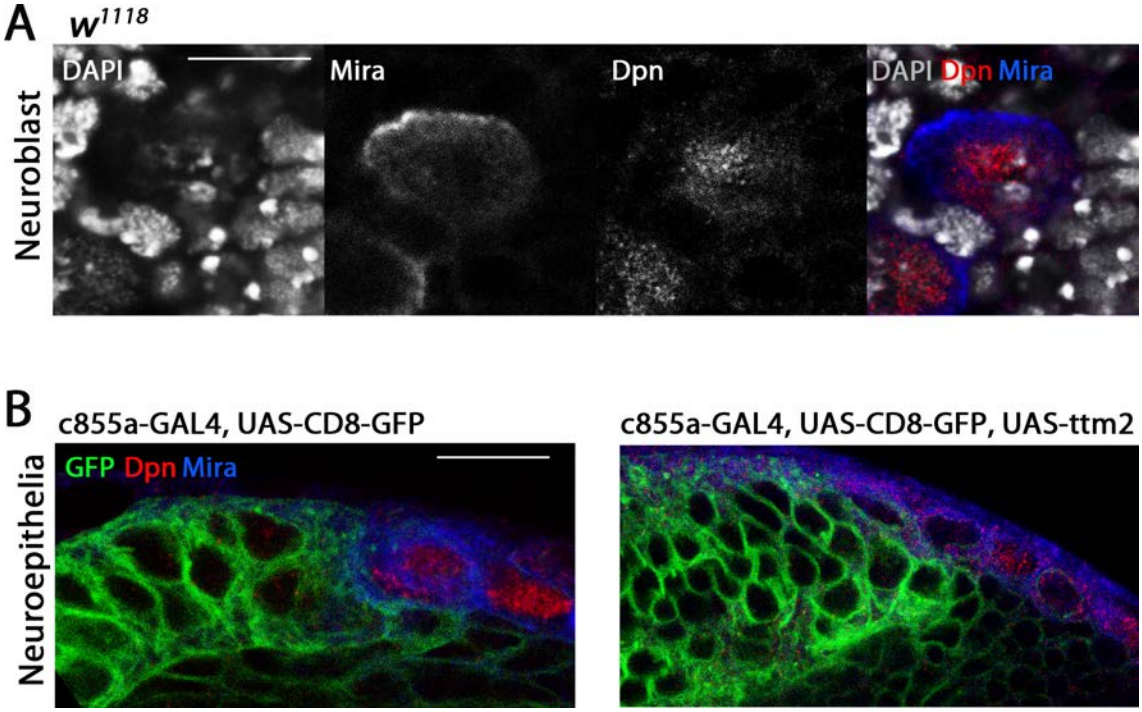

Figure 4.17: The ttm2-GOF amplified cell pool does not express NB cell markers. A) w^{1118} NB dividing cell labeled with Miranda (Mira) and Deadpan (Dpn). Scale bar 5μm. B) GFP-expressing w^{1118} OPC cells and ttm2-GOF OPC cells labeled with Miranda (blue) and Deadpan (red). Scale bar 10μm.

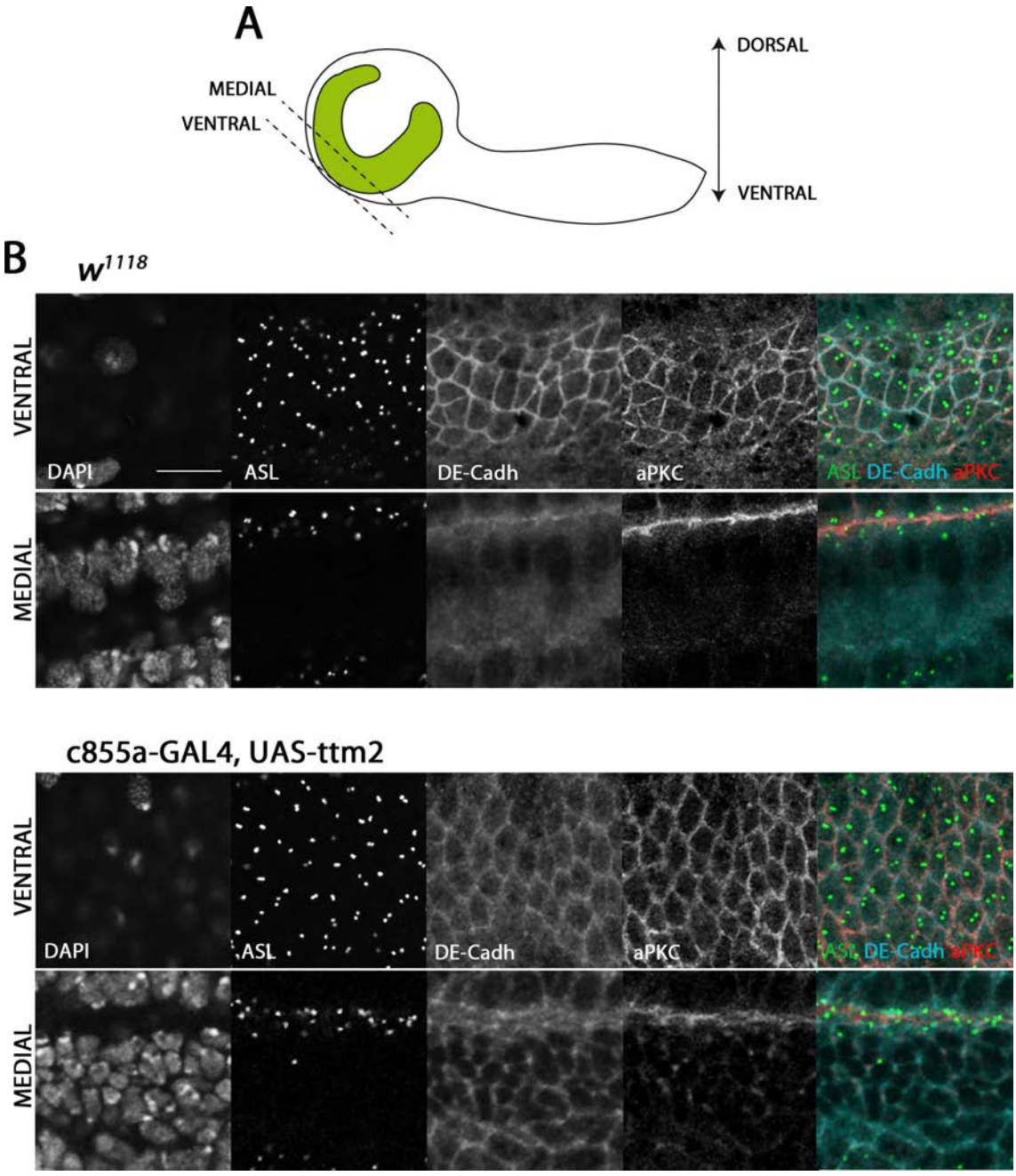

Figure 4.18: The ttm2-GOF amplified cell pool keeps epithelial polarity markers. A) Schematic depiction of the larval brain indicating both ventral and medial sections. B) Images of ventral and medial sections of both w^{1118} OPC cells or *ttm2* overexpressing OPC cells. The brains are stained with DAPI to label DNA, asl-YFP (green) that labels the centrosomes, DE-Cadh (cyan) that labels adherens junctions and aPKC (red) that labels the epithelial apical cortex. Scale bar 10μm.

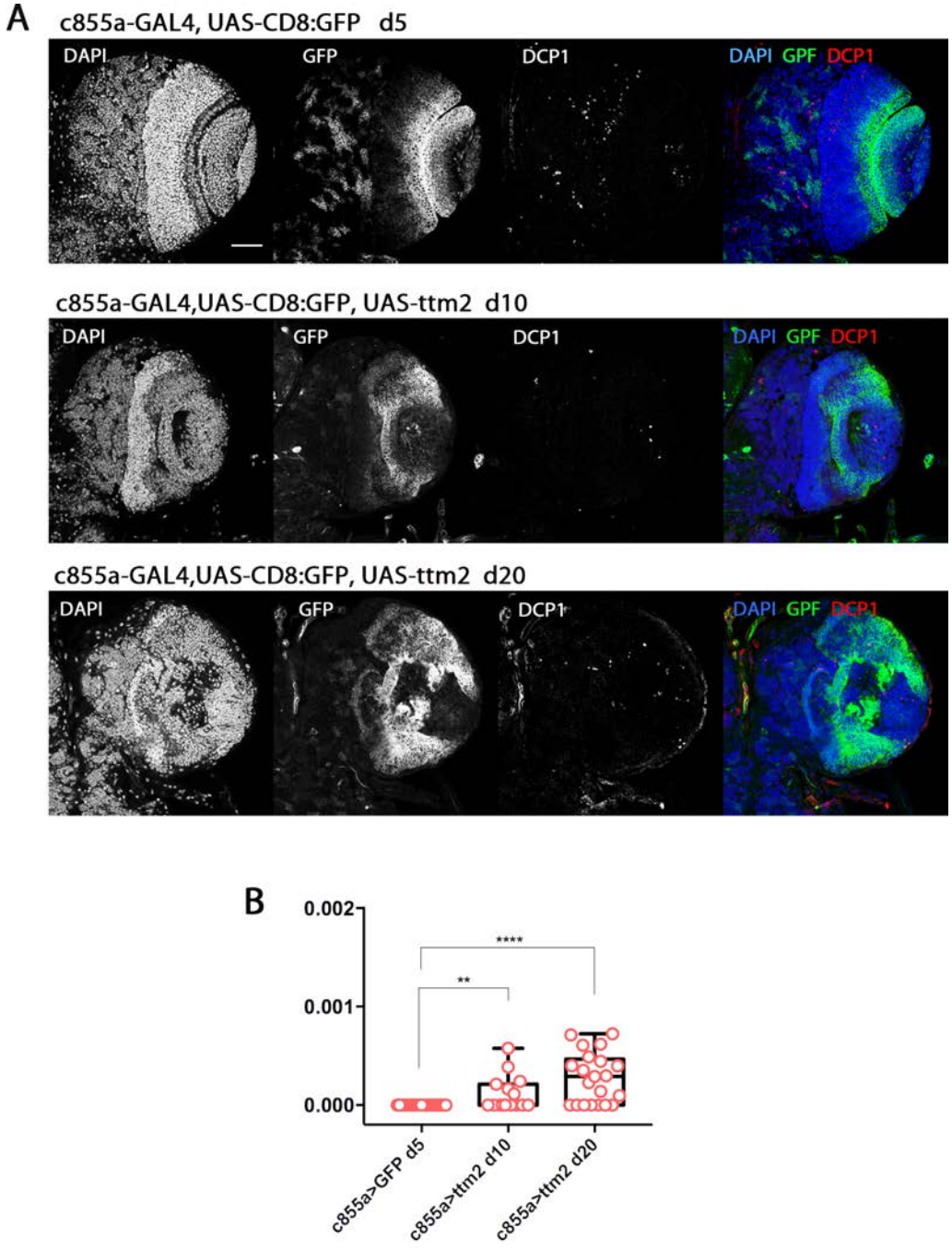

Figure 4.19: Apoptosis is not highly increased in the neuroepithelia of hyperplastic ttm2-GOF brains. A) Images of ventral OL in which UAS-CD8:GFP or UAS-CD8:GFP and UAS-ttm2 were overexpressed with c855a-GAL4. The brains were stained with DAPI to label the DNA and DCP1 to label apoptotic cells. B) Boxplot representing the apoptotic index in the NE region, as quantified by the number of apoptotic cells per NE area. Error bars indicate s.d. $****p < 0.001$; $**p < 0.01$. Scale bar 50μm.

The hyperplasia becomes severe as time progresses, and brains at day 20 show a greatly disorganized mutant anatomy. Interestingly, the level of apoptosis in the overgrown NE region caused by *ttm2* overexpression, although higher than that in the wild-type NE -there were cero apoptotic cells in all wild-type NE analyzed-, is still very low (Fig. 4.19).

As mentioned before, ttm2-GOF larvae have a significant developmental delay. It is known that the developing adult organs, the imaginal discs, regulate the entrance to pupariation (Simpson et al., 1980). Indeed, the c885a-GAL4 driver is as well expressed in the imaginal discs, thus I investigated whether ectopic *ttm2* expression also affects imaginal disc development. I found that wing discs overexpressing *ttm2* have a disorganized epithelia and a notable increase of apoptotic cells as revealed by DCP-1 caspase staining (Song et al., 1997) (Fig. 4.20). This result substantiates that the observed delay in larval pupariation upon *ttm2* expression using the c885a-GAL4 driver might be caused by a defect in the imaginal disc growth.

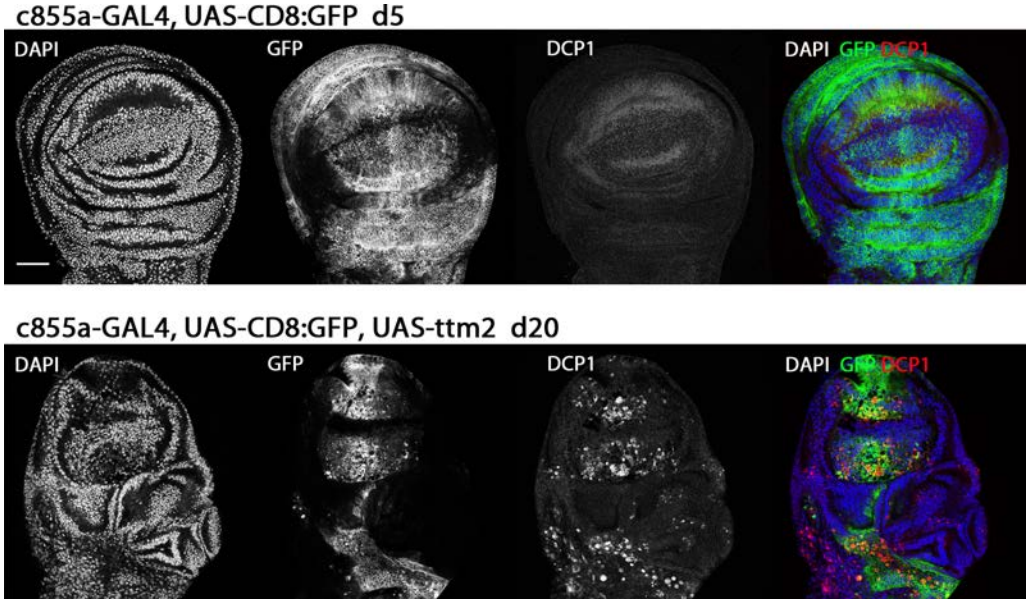

Figure 4.20: *ttm2* overexpression in the wing imaginal discs using c855a-GAL4 disrupts disc development and increases apoptosis. Images of wing imaginal discs in which UAS-CD8:GFP or UAS-CD8:GFP and UAS-ttm2 were overexpressed with c855a-GAL4 disected at 5 days or 20 days AEL respectively. Discs are stained with DAPI to label the DNA and DCP1 to label apoptotic cells. Scale bar 50μm.

In connection with the previous, we then wondered whether the OPC hyperplastic phenotype derived from ttm2-GOF was a consequence of the extended larval stage. To address this issue I overexpressed *ttm2* using nub-GAL4, a wing disc driver that is not expressed in the neuroepithelia (Fig. 4.21A). I found that in these larvae, imaginal discs are abnormal and larval development is also notably extended, up until 10 days AEL, but importantly, the morphology of the brain is not perturbed (Fig.4.21B). These results strongly suggest that the OPC hyperplasia observed upon ttm2-GOF in the NE is not a secondary effect of the developmental delay, but rather a direct consequence of *ttm2* overexpression in the NE.

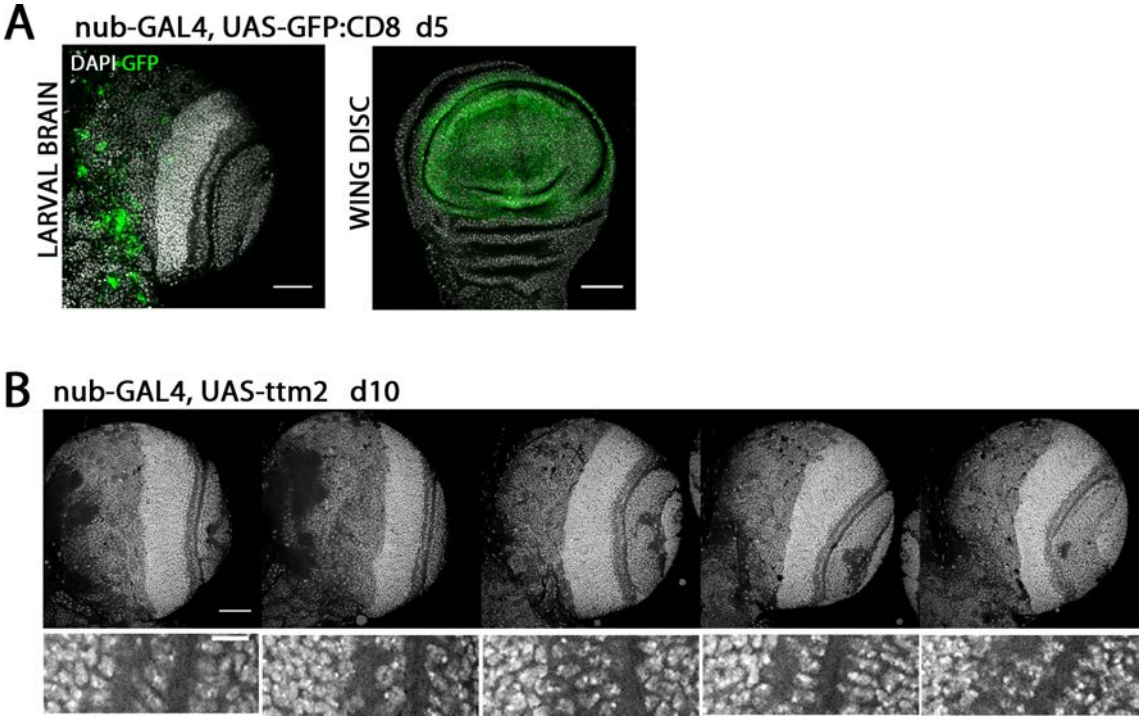

Figure 4.21: *ttm2* overexpression restricted to the imaginal discs causes developmental delay that does not produce hyperplasia in the OPC. A) nub-GAL4 expression pattern in third instar larval brains and imaginal discs shown by UAS-CD8:GFP at 5 days AEL. B) Array of confocal ventral sections of five DAPI stained optic lobes from nub-GAL4, UAS-ttm2 larvae disected at 10 days AEL. An inset of the OPC is shown. Scale bars: *in toto* brains and wing disc 50μm; OPC insets 10μm.

4.8 Ttm2 overexpression disrupts wing imaginal disc development and causes defective adult wing formation

Upon overexpression of *ttm2* with c855a-GAL4, both NE and wing discs are affected. To further investigate the effect of *ttm2* overexpression in wing discs, I used three different well-established wing disc drivers: nub-GAL4, that is expressed in the wing pouch; sal-GAL4, that is expressed in a restricted area of the wing pouch; and hh-GAL4, expressed in the posterior compartment (Fig. 4.22A). Ectopic expression of *ttm2* in the wing disc causes developmental delay that extends the larval stage until day 7-8 AEL in the case of sal-GAL4 and hh-GAL4, and until 10 days AEL using the nub-GAL4 driver. Moreover, *ttm2* overexpression with any of the wing disc drivers mentioned above, caused a dramatic increase in the number of apoptotic cells and a concomitant reduction of the compartment area in which *ttm2* was expressed (Fig. 4.22B and C). However, apoptosis was not restricted to the area of *ttm2* expression, but affected neighboring compartments as well, a phenomena previously described in discs as apoptosis induced apoptosis (AIA) (Pérez-Garijo et al., 2013). Escapers overexpressing *ttm2* either with nub-GAL4 or sal-GAL4 drivers presented wings that are smaller than wild-type and have defective vein formation (Fig. 4.23). These results show that *ttm2* overexpression affects the development of a different type of epithelia besides the OPC. It remains to be tested whether upon apoptotic inhibition, *ttm2* overexpression in the wing discs also produces hyperplasia as observed in the OPC cells. Indeed, overexpression of *ttm50*, the somatic counterpart of *ttm2*, has been published to increase cell proliferation in the larval wing imaginal disc upon co-expression with the baculovirus P35 caspase inhibitor (Sugiyama et al., 2007).

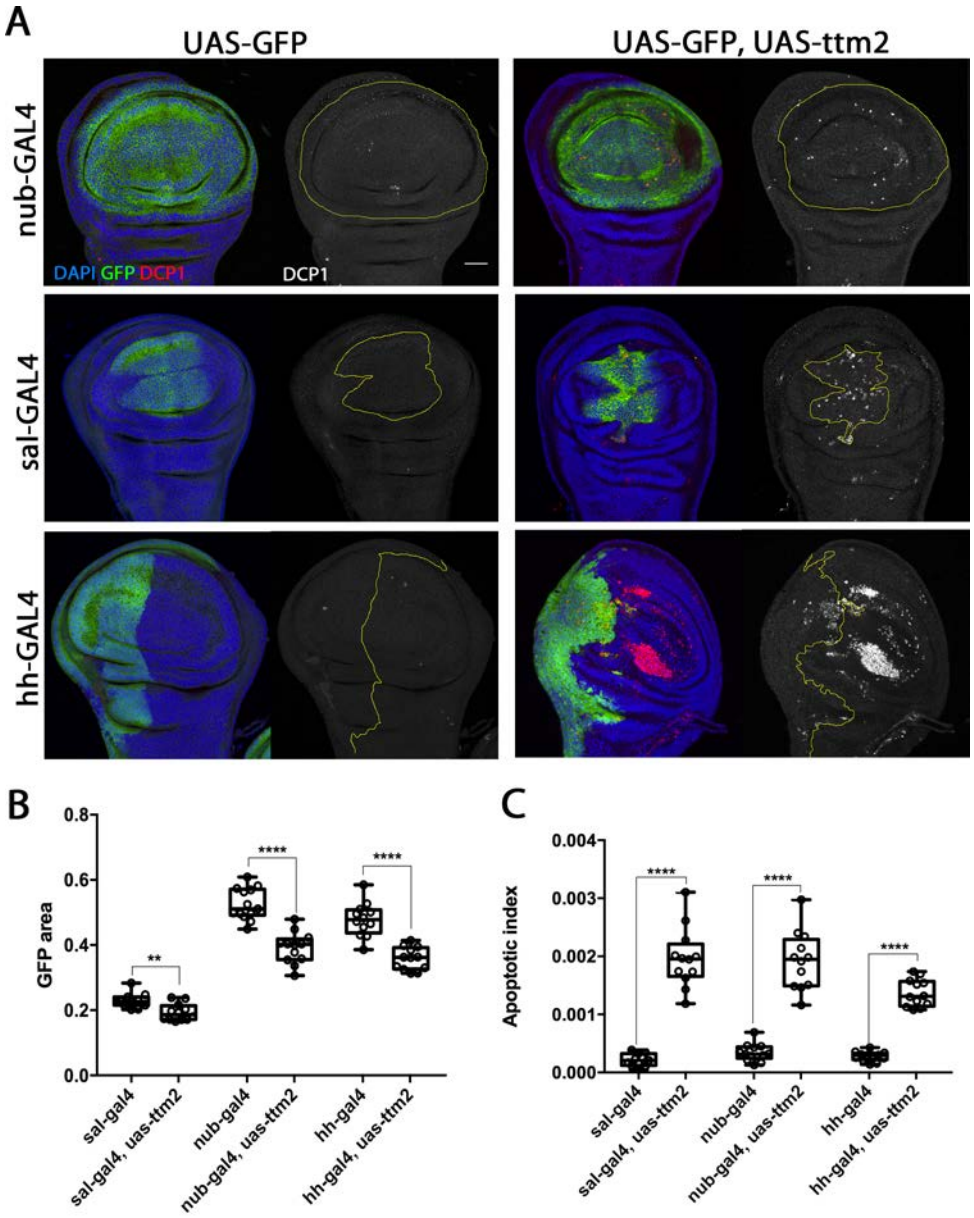

Figure 4.22: *ttm2* overexpression in the wing imaginal discs increases apoptosis. A) Left panel shows the expression pattern of the different imaginal disc drivers upon expression of UAS-GPF. Right panel shows the phenotype of the expression of both UAS-GFP and UAS-ttm2 together. Imaginal discs are labeled with DAPI to stain the DNA and DCP1 to stain apoptotic cells. B) Boxplot representing the relative GFP area of control and ttm2-OE discs. C) Boxplot representing the apoptotic index of control and ttm2-OE discs. Error bars indicate s.d. $^{****}p < 0.001$; $^{**}p < 0.01$. Scale bar 50μm.

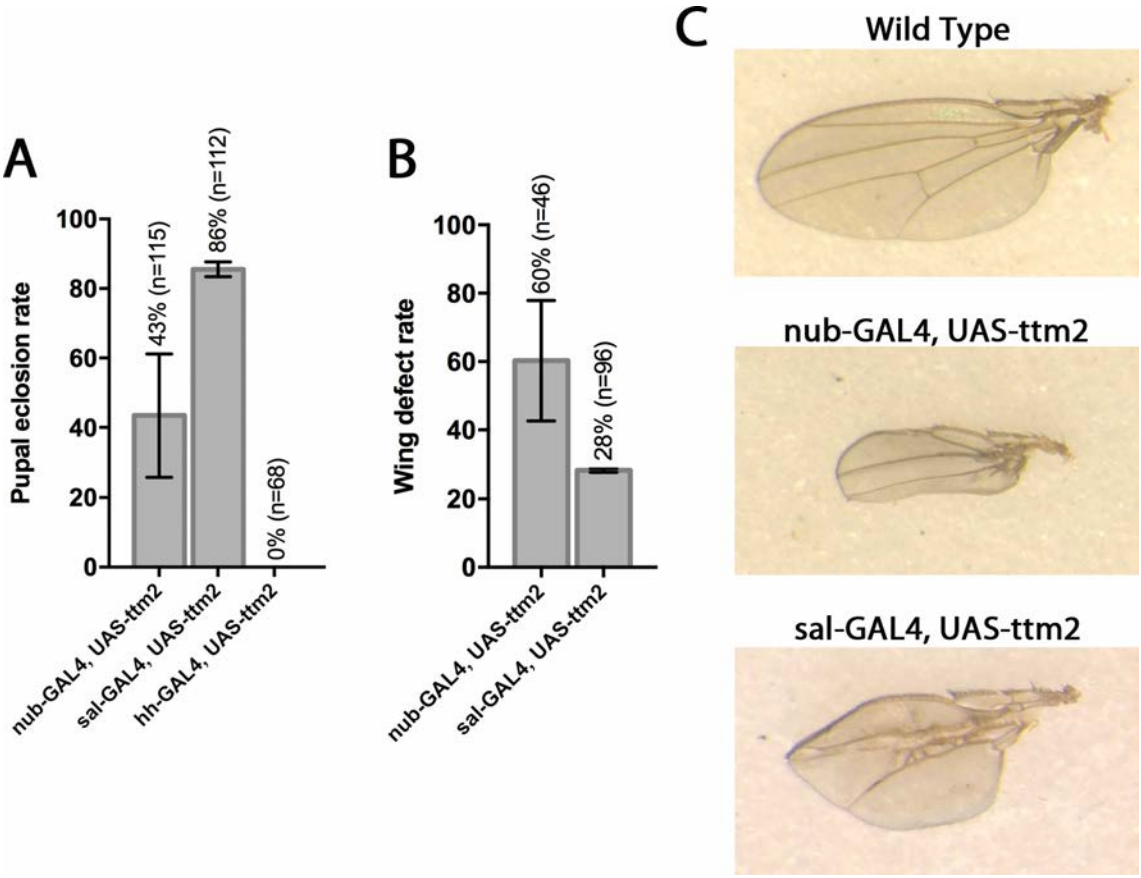

Figure 4.23: *ttm2* overexpression causes adult wing morphology defects. A) Graph showing pupal eclosion rates when *ttm2* is overexpressed using different wing drivers. Average pupal eclosion rate and total number of pupae are specified for each condition. B) Graph representing wing defect rate from the total number of adult flies eclosed when *ttm2* is overexpressed using nub-GAL4 and sal-GAL4 wing disc drivers. Average wing defect rate and total number of flies are specified for each condition. Error bars indicate s.d. C) Images of wild-type; nub-GAL4 UAS-ttm2 and sal-GAL4 UAS-ttm2 adult wings.

5. Discussion

Drosophila has become a valuable model to study human diseases, including cancer. Because of the increasing interest in tumor metabolism, I have interrogated the requirement of several mitochondrial genes for *lethal (3) malignant brain tumor* growth through an in vivo screen. I have found that mbt tumors are dependent on the function of testis-mitochondrial genes. In addition, I have discovered that the testis-mitochondrial gene *ttm2* is not only required but also sufficient to drive hyperplasia in the *Drosophila* larval neuroepithelium. The data presented in this thesis project provide novel information about the critical role of mitochondria controlling cell fate and carcinogenesis.

5.1 Mitochondrial dependence of mbt tumors

l(3)mbt loss of function causes malignant neoplasms in *Drosophila* that recapitulate the upregulation of cancer/testis (CT) genes observed in many human cancers (Janic et al., 2010). In order to address which biological processes are key for mbt and therefore could be targeted to inhibit malignant growth, we have combined the *Drosophila l(3)mbt* experimental brain tumor model and well-established RNAi technology methods. To select for functions whose depletion has a much stronger effect on the tumor than in other tissues of the tumor-bearing animal, we chose to drive RNAi expression ubiquitously, hence filtering out RNAis that cause lethality or severely impair development (Rossi et al., 2017). There are two types of functions that can be expected to meet these criteria: those that are under higher demand in the tumor than in the rest of the body and those that are tumor-specific.

Belonging to the first kind, I found several components of the mitochondrial translation machinery. RNAi inhibition of 9 out of 10 MRPs tested impaired the growth of mbt tumors. Mitoribosomes are essential in the regulation of cellular respiration, as they synthesize the proteins encoded by the mitochondrial DNA, i.e. mostly components of the oxidative phosphorylation machinery. Advances in cancer cell genomics and proteomics have provided remarkable insights into the genetic and metabolic basis of most tumor types. Mitoribosome assembly factors and mitochondrial translation components are modified in numerous human cancers, a trait that has been linked to tumorigenesis and metastasis (Kim et al., 2017).

Indeed, a genome-wide study on human breast cancer cells detected significantly increased transcripts from more than 90 genes that are associated with mitochondrial biogenesis and mitochondrial translation, nearly 40 of them being MRPs (Sotgia et al., 2012).

L(3)mbt acts as a chromatin insulator and it is essential for repressing Salvador-Warts-Hippo (SWH) target genes. Upon *l(3)mbt* loss of function, many SWH genes are dysregulated. In addition, overexpression of *expanded* or the removal of one copy of *yorkie* rescues mbt tumor growth, indicating that the SWH pathway and its target genes are important for *l(3)mbt* tumor formation (Richter et al., 2011). Recent studies in *Drosophila* have discovered that there is a crosstalk between mitochondrial fusion and the SWH pathway. Activation of Yorkie causes direct transcriptional up-regulation of genes that regulate mitochondrial function, such as *optic atrophy 1-like* (*Opa1*) and *mitochondria assembly regulatory factor* (*Marf*). Opa1 and Marf regulate mitochondrial dynamics by promoting mitochondrial fusion (Deng et al., 2008). When mitochondrial fusion is genetically attenuated by the inhibition of *Opa1* or *marf*, the Yorkie-induced tissue overgrowth in the larval eye disc is significantly suppressed (Nagaraj et al., 2012; Deng et al., 2016). Mitochondrial dynamics and bioenergetics reciprocally influence each other, and mitochondrial elongation correlates with high oxidative phosphorylation activity (Mishra & Chan, 2016). These results suggest that there is link between mitochondrial fusion and the Hippo pathway that is essential in controlling cell proliferation and tissue homeostasis in *Drosophila*, that could as well regulate mbt tumor development.

This finding suggests that, as it occurs in several human cancers, mbt tumors might be more sensitive than wild-type tissues to the loss of mitochondria-related functions and that a certain threshold might exist at which normal development can proceed, but tumor growth is severely curtailed. However, it is important to understand the key metabolic differences between cancer and normal cells and the underlying regulatory mechanisms to design proper metabolic intervention strategies and minimize unwanted toxicity in the healthy tissue.

5.2 Human testes-specific isoforms of the mitochondrial electron transport chain

During the course of this project, I also found several testis-mitochondrial genes that belong to the second category of suppressors, i.e., those that exert functions that are specifically required for mbt tumor growth. Out of the 32 testis-mitochondrial genes tested, 10 of them improved *l(3)mbt* viability and brain anatomy traits. The testis-mitochondrial genes found as mbt-SPRs belong to the following gene ontologies related to mitochondrial function: Mitochondrial membrane transport (*Tim17a1, Tomboy20, Tomboy40, Ttm2* and *CG1409*) or Oxidative phosphorylation (*Cyt-c-1L, ND-20L, UQCR11L, CG14077, CGCG1409* and *CG6629*). All these mbt-SPRs are duplicated nuclear mitochondrial genes with a maximum expression in the testes. In *Drosophila*, two or more copies of several mitochondrial genes exist in the genome, and while one is mostly expressed in the soma, the other has acquired testis-specific expression. In contrast, gene duplicates in humans show tissue-biased expression in many tissues, not just in testis, and fall into various functional categories (Eslamieh et al., 2017).

There are, however, some components of the mitochondrial respiratory chain that have isoforms with a testis specific expression in mammals. A testis-specific isoform of CytC is expressed in the germinal epithelial cells of rodents (Goldberg et al., 1977). Although the amino acid sequence of both the testis-specific (T-CytC) and the somatic (S-CytC) isoforms is very similar, its expression pattern and biological functions are distinct. S-CytC is expressed in all cells including those of the testis, however its expression is gradually decreased in the testicular germ cells. As spermatogenesis proceeds, T-Cytc expression increases, becoming the predominant form in mature sperm. T-Cyc knockout mice revealed reduced sperm motility, ATP production, and fertility (Narisawa et al., 2002; Hüttemann et al., 2011). The Cytochrome C Oxidase (COX) complex also displays different isoforms. For COX subunit 6B a testes-specific isoform (COX6B2) was identified in human, bull, rat and mouse. COX6B2 has two potential tyrosine phosphorylation sites that are absent in subunit COX6B1. In bovine sperm, cAMP-dependent protein tyrosine phosphorylation has been demonstrated to be a crucial step in the activation of sperm motility (Hüttemann et al., 2003; Kadenbach & Hüttemann, 2015). Furthermore, a second isoform for subunit COX7B has been annotated in

the GenBank and based on BioGPS GeneAtlas, and testis is the only tissue in mice that expresses COX7B2. If confirmed, this would expand testes-specific expression of electron transport chain proteins Cytochrome C and COX6B to yet another COX subunit pointing to the importance of tissue-specific metabolic adaptation of the male reproductive organ (Kadenbach & Hüttemann, 2015).

Altogether, these data suggest that there may be unique energy demands of spermatozoa that, while in *Drosophila* are achieved through mitochondrial gene duplication, in mammals are addressed through testis-specific isoform expression of ETC components, but in both cases these specific testis-mitochondrial components appear to be essential for proper sperm function and male fertility.

5.3 Testis and brain-restricted human Cancer/Testis genes

Our finding that several testis-mitochondrial genes are required for mbt tumor growth recapitulates the previous observation made by our laboratory regarding the overexpression of germline genes in mbt tumors (Janic et al., 2010). However, mitochondrial-testis genes are neither included in the MBTS nor among the 4000 most expressed proteins in mbt brains.

In humans, genes that are predominantly expressed in germline cells and have little or no expression in somatic adult tissues but become aberrantly activated in various malignancies are known as cancer/testis (CT) (Simpson et al., 2005). In order to classify the increasing number of heterogeneous CT candidates that have appeared in the literature, Hofmann and colleagues analyzed CT gene expression in the different fly tissues (Hofmann et al., 2008). Interestingly, a high number of CT genes were found to be expressed in no somatic tissues except for brain, suggesting the presence of a distinctive transcriptional control mechanism that functions with tissue specificity in germ cells and in brain (Hofmann et al., 2008). In addition, based on quantitative RT-PCR data, mRNA levels of CT genes in somatic tissues are usually less than 1% of their expression in testis (Scanlan et al., 2004). I have found that *ttm2* is expressed in both wild-type testis and brain, although at much lower levels in the later one, and also in mbt tumors. We hypothesize that a similar expression pattern could apply for all the testis-mitochondrial genes that are necessary for mbt tumor growth. If so, this would prove the existence of a group

of genes belonging to a testis-brain restricted expression category in *Drosophila* with a role in tumor formation.

5.4 Mitochondrial Cancer/Testis genes

The aberrant expression of Cancer/Testis (CT) genes by human cancer cells has been proposed to confer a range of germline phenotypic traits that are highly advantageous for the cancer cells (Simpson et al., 2005). Several CT genes are involved in the regulation of energy production in sperm. *COX6B2*, the sperm-specific isoform of complex IV of the electron transport chain, is a promoter of efficient oxidative phosphorylation. *COX6B2* is upregulated in various cancer cell lines and essential for tumor cell viability (Maxfield et al., 2015). The CT gene *Spermatogenesis Associated 19* (*Spata19*) plays an important role in sperm motility by regulating the organization and function of the mitochondria (Mi et al., 2015), and it is frequently expressed in prostate cancer and basal cell carcinoma (Ghafouri-Fard et al., 2009, 2010; Wong et al., 2017). Thus, the two above-mentioned CT genes could be critical to satisfy the energetic demands of sperm motility, but their actual role in cancer remains unknown.

Our results demonstrate that several testis-mitochondrial genes are necessary for the growth of *Drosophila* mbt tumors. Those mbt-SPRs belong to a special set of mitochondrial genes predominantly expressed in the testes that might regulate mitochondrial biogenesis and respiration in order to fulfill the energetic requirements of the sperm. Thus, we hypothesize that mbt tumors rely on a high mitochondrial activity that is achieved by the expression of testis-mitochondrial genes, without which the tumor is unable to grow. In connection with this, the inactivation of mitochondrial CT genes might have tumor-suppressing effects also in human cancer.

5.5 Ttm2 role in wild-type tissue and mbt tumors

One of the testis-mitochondrial genes required for mbt tumor growth is *ttm2*. Ttm2 is a mitochondrial protein essential for male fertility. *Drosophila ttm2* somatic paralog, *ttm50*, is required for fly viability and *ttm50* mutants show decreased mitochondrial membrane potential, whereas *ttm50* overexpression increases mitochondrial membrane potential and apoptosis, and in co-expression with p35 induces overproliferation in the eye disc (Sugiyama et al., 2007). Tim50,

Ttm2 human ortholog, possesses phosphatase activity and it is present in a transmembrane protein complex with human Tim23 (Gevorkyan-Airapetov et al., 2009). When Tim50 is depleted from human cells or zebrafish embryos, the mitochondria lose their ability to import a large number of matrix proteins, many of which are essential for energy production and maintenance of the mitochondrial function (Guo et al., 2004). Loss of Tim50 in vertebrates causes mitochondrial membrane permeabilization and dysfunction followed by cytoplasmic release of Cytochrome C along with other mitochondrial inducers of cell death. Moreover, Tim50 has been described as overexpressed in breast cancer and non-small cell lung carcinoma cell lines and its depletion reduced cellular growth rate (Sankala et al., 2011; Gao et al., 2016). Given the high sequence similarity between Ttm2 and both Ttm50 and Tim50, we speculate that Ttm2 could also be involved in the regulation of mitochondrial membrane transport and oxidative phosphorylation.

Interestingly, I have found that the ectopic expression of *ttm2* is sufficient to cause hyperplasia in an otherwise wild-type larval brain. The results presented show that the sole overexpression of a mitochondrial protein is on its own able to induce hyperproliferation on the neuroepithelial compartment. This is a novel finding that highlights the importance of mitochondrial regulation as a major driving force in tumorigenesis and opens the question to whether the expression of human mitochondrial CTs is not only required but also a fundamental step for malignant transformation.

5.6 Mitochondrial regulation in brain cell types

I have found that overexpression of *ttm2* causes hyperplasia in the neuroepithelial compartment. Prior to third larval instar, most neuroepithelial stem cells predominantly undergo symmetric divisions to expand the stem cell population, forming a C-shaped swath flanked with few neuroblasts at the medial edge bordering the central brain. In the third larval instar, neuroepithelial stem cells progressively transition into neuroblasts from the medial edge toward the lateral edge of the optic lobe, leading to narrowing of the neuroepithelia and widening of the medulla area (Weng & Lee, 2011). In contrast, upon ectopic expression of *ttm2* in the neuroepithelia, there is an increase in the number of neuroepithelial cells and a

decrease in medulla formation, suggesting a disruption in the neuroepithelia to neuroblast transition.

Our results suggest that the hyperplasia is specific of the medial neuroepithelial cells, because both lateral OPC and IPC populations are unaffected upon *ttm2* overexpression. Indeed, the neurogenesis of these two regions is dependent on different regulatory mechanisms. Lateral OPC neuroepithelial cells bypass the neuroblast stage and generate lamina progenitor cells that divide once to produce lamina neurons (Huang & Kunes, 1996). IPC neuroepithelial cells give rise to progenitors that migrate to a second neurogenic domain, where they mature into type I neuroblasts. These progenitors are distinct, because they originate from a neuroepithelium, do not express markers for neuroblasts, INPs, GMCs or postmitotic neurons, and acquire neural stem cell properties after completing their migration (Apitz & Salecker, 2015). In addition, overexpression of *ttm2* in medulla or central brain neuroblast does not cause cell amplification nor impairs asymmetric cell division. These results suggest that metabolic requirements vary throughout the different brain cell types. Indeed, a previous study has shown that in flies the majority of the glial energy demand appears to be satisfied by glycolysis, whereas neurons require the activity of the mitochondrial TCA cycle, which seems to be fueled by glia-derived alanine and lactate (Volkenhoff et al., 2015).

Our results support a recent line of research that suggests that mitochondria are not simply bystanders in the differentiation and developmental process, but rather their activity, shape and localization directly influences nuclear programs and ultimately cell fate.

5.7 Future perspectives

A major line of future research should be the identification of the mechanism of action whereby testis-mitochondrial genes are required for mbt tumor growth. One promising way forward in this direction might be to perform oxygen consumption analysis and metabolome profiling of both mbt and mbt-suppressed brains to check whether the inhibition of testis-mitochondrial genes impacts on mitochondrial function. These analysis are challenging because of the great amounts of tissue that are required, but conclusive results have already been achieved using *Drosophila* larval brains, proving its feasibility (Volkenhoff et al., 2015). In addition, it may be

useful to study the function of those proteins during the process of spermatogenesis to extrapolate a similar role in the tumor. *Drosophila* spermatogenesis is well characterized, the stages of sperm development are easy to examine and a variety of molecular and genetic techniques permit the dissection of the cellular processes involved, therefore studying the phenotypes of testis-mitochondrial mutants should be very approachable.

Another relevant line of research would be to investigate the hyperplasia caused by the overexpression of the testis-mitochondrial gene *ttm2*. In this regard, it would be interesting to check whether other components of the testis mitochondrial membrane transport machinery also cause hyperplasia when overexpressed in the neuroepithelium, as well as their respective somatic counterparts (Fig. 5.1). In connection with the previous, the malignancy of the observed hyperplasia should be assessed by testing the growth capacity of the tissue upon abdomen injection, as well as the phenotype in wing discs when the overexpression of testes-mitochondrial proteins is induced when apoptosis is blocked.

Finally, a most relevant point would be to study how mitochondria orchestrate cell fate and differentiation in specific brain cell types and to demonstrate whether, as shown for glia and neurons, there is a metabolic compartmentalization and coupling between other brain cell types such as the neuroepithelia and the neuroblasts.

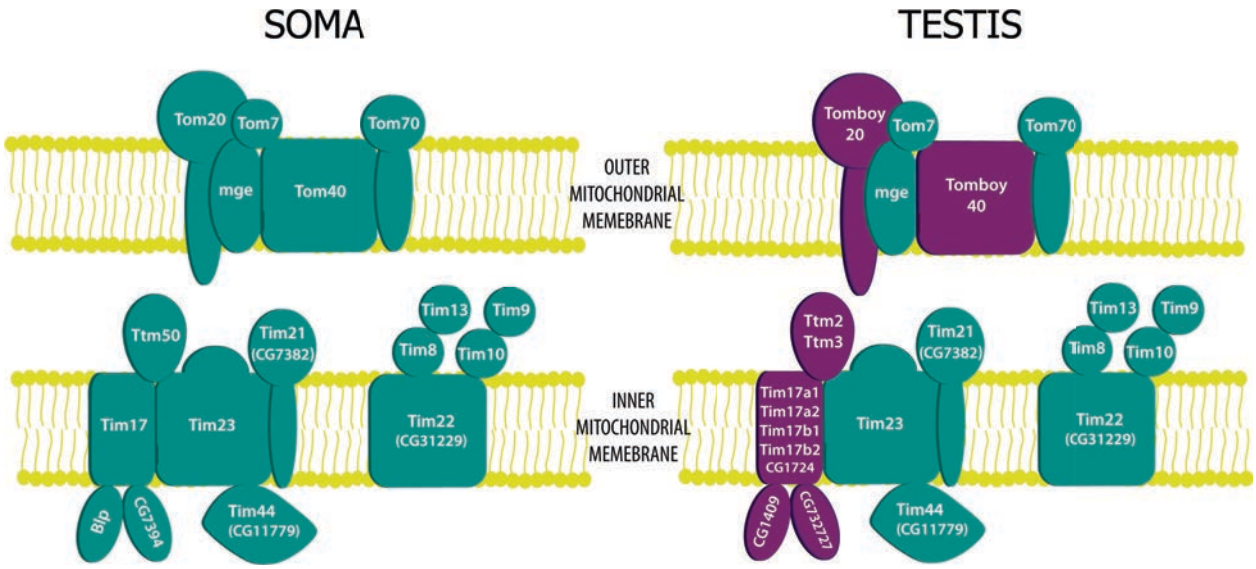

Figure 5.1: Comparison between the somatic and the testis-specific mitochondrial membrane transport machinery. Schematic representation of the components of the *Drosophila* membrane transport machinery and their respective testis counterparts (in purple).

6. Conclusions

- Depletion of the mitochondrial translation machinery affects both wild-type and *l(3)mbt* development.
- The inhibition of several testis-mitochondrial genes impairs the growth of *l(3)mbt* tumors, recovering brain anatomy and viability, without impairing either wild-type or *brat* development.
- Our proteomic profile revealed that one third of the *l(3)mbt* tumor signature genes (MBTS) are also expressed at the protein level in *l(3)mbt* mutant brains.
- The mitochondrial membrane transport component *ttm2* is expressed in both wild-type and *l(3)mbt* brains.
- Ectopically expressed Ttm2 protein localizes to the mitochondria in both neuroepithelial and neuroblast cells.
- Overexpression of *ttm2* in an otherwise wild-type background is sufficient to induce hyperplasia in the medial OPC cells of the larval brain, but does not affect either lateral OPC or IPC cells.
- Overexpression of *ttm2* affects neither the medulla nor the central brain neuroblasts.
- Overexpression of *ttm2* disrupts imaginal wing disc development and induces apoptosis.

References

Adams, M.D., et al. *The genome sequence of Drosophila melanogaster.* Science (New York, N.Y.), 287 (5461), 2185–95, 2000.

Almeida, L.G., et al. *CTdatabase: a knowledge-base of high-throughput and curated data on cancer-testis antigens.* Nucleic Acids Research, 37 (Database), D816–D819, 2009.

Apitz, H. & Salecker, I. *A region-specific neurogenesis mode requires migratory progenitors in the Drosophila visual system.* Nature Neuroscience, 18 (1), 46–55, 2015.

Arama, E., et al. *Mutations in the beta-propeller domain of the Drosophila brain tumor (brat) protein induce neoplasm in the larval brain.* Oncogene, 19 (33), 3706–16, 2000.

Bai, Y., et al. *Comparative genomics reveals a constant rate of origination and convergent acquisition of functional retrogenes in Drosophila.* Genome Biology, 8 (1), R11, 2007.

Bate, M. & Martinez Arias, A. *The Development of Drosophila melanogaster.* Cold Spring Harbor Laboratory Press, 1993.

Becker, S., et al. *The black-pearl gene of Drosophila defines a novel conserved protein family and is required for larval growth and survival.* Gene, 262 (1-2), 15–22, 2001.

Bello, B., et al. *The brain tumor gene negatively regulates neural progenitor cell proliferation in the larval central brain of Drosophila.* Development, 133 (14), 2639–2648, 2006.

Bello, B.C., et al. *Amplification of neural stem cell proliferation by intermediate progenitor cells in Drosophila brain development.* Neural Development, 3 (1), 5, 2008.

Bertet, C. *The Developmental Origin of Cell Type Diversity in the Drosophila Visual System.* In *Decoding Neural Circuit Structure and Function*, 419–435. Springer International Publishing, Cham, 2017.

Betschinger, J., et al. *Asymmetric Segregation of the Tumor Suppressor Brat Regulates Self-Renewal in Drosophila Neural Stem Cells.* Cell, 124 (6), 1241–1253, 2006.

Bilder, D. *Epithelial polarity and proliferation control: links from the Drosophila neoplastic tumor suppressors.* Genes & Development, 18 (16), 1909–25, 2004.

Bonasio, R., et al. *MBT domain proteins in development and disease.* Seminars in Cell & Developmental Biology, 21 (2), 221–230, 2010.

Boone, J.Q. & Doe, C.Q. *Identification of Drosophila type II neuroblast lineages containing transit amplifying ganglion mother cells.* Developmental Neurobiology, 68 (9), 1185–1195, 2008.

REFERENCES

Bowman, S.K., et al. *The Tumor Suppressors Brat and Numb Regulate Transit-Amplifying Neuroblast Lineages in Drosophila.* Developmental Cell, 14 (4), 535–546, 2008.

Brand, A.H. & Perrimon, N. *Targeted gene expression as a means of altering cell fates and generating dominant phenotypes.* Development (Cambridge, England), 118 (2), 401–15, 1993.

Brand, A.H., et al. *Chapter 33 Ectopic Expression in Drosophila.* Methods in Cell Biology, 44, 635–654, 1994.

Brumby, A.M. & Richardson, H.E. *Using Drosophila melanogaster to map human cancer pathways.* Nature Reviews Cancer, 5 (8), 626–639, 2005.

Butler, M.J., et al. *Discovery of genes with highly restricted expression patterns in the Drosophila wing disc using DNA oligonucleotide microarrays.* Development (Cambridge, England), 130 (4), 659–70, 2003.

Calleja, M., et al. *Visualization of gene expression in living adult Drosophila.* Science (New York, N.Y.), 274 (5285), 252–5, 1996.

Cavalli, L.R., et al. *Diminished tumorigenic phenotype after depletion of mitochondrial DNA.* Cell Growth & Differentiation : The Molecular Biology Journal of the American Association for Cancer Research, 8 (11), 1189–98, 1997.

Chen, X., et al. *Trehalase Regulates Neuroepithelial Stem Cell Maintenance and Differentiation in the Drosophila Optic Lobe.* PLoS ONE, 9 (7), e101433, 2014.

Coux, R.X., et al. *L(3)mbt and the LINT complex safeguard cellular identity in the Drosophila ovary.* Development (Cambridge, England), 145 (7), dev.160721, 2018.

Cruz, C., et al. *A gain-of-function screen identifying genes required for growth and pattern formation of the Drosophila melanogaster wing.* Genetics, 183 (3), 1005–26, 2009.

Davidson, S.M., et al. *Environment Impacts the Metabolic Dependencies of Ras-Driven Non-Small Cell Lung Cancer.* Cell Metabolism, 23 (3), 517–528, 2016.

Deng, H., et al. *The Parkinson's disease genes pink1 and parkin promote mitochondrial fission and/or inhibit fusion in Drosophila.* Proceedings of the National Academy of Sciences of the United States of America, 105 (38), 14503–8, 2008.

Deng, Q., et al. *Cross-Talk Between Mitochondrial Fusion and the Hippo Pathway in Controlling Cell Proliferation During Drosophila Development.* Genetics, 203 (4), 1777–1788, 2016.

Dietzl, G., et al. *A genome-wide transgenic RNAi library for conditional gene inactivation in Drosophila.* Nature, 448 (7150), 151–156, 2007.

Dorus, S., et al. *Genomic and functional evolution of the Drosophila melanogaster sperm proteome.* Nature Genetics, 38 (12), 1440–1445, 2006.

Egger, B., et al. *Regulation of spindle orientation and neural stem cell fate in the*

Drosophila optic lobe. Neural Development, 2 (1), 1, 2007.

Egger, B., et al. *Notch regulates the switch from symmetric to asymmetric neural stem cell division in the Drosophila optic lobe.* Development (Cambridge, England), 137 (18), 2981–7, 2010.

Eichenlaub, T., et al. *Warburg Effect Metabolism Drives Neoplasia in a Drosophila Genetic Model of Epithelial Cancer.* Current Biology, 28 (20), 3220–3228.e6, 2018.

Englund, C., et al. *Miple1 and miple2 encode a family of MK/PTN homologues in Drosophila melanogaster.* Development Genes and Evolution, 216 (1), 10–18, 2006.

Eslamieh, M., et al. *Few Nuclear-Encoded Mitochondrial Gene Duplicates Contribute to Male Germline-Specific Functions in Humans.* Genome Biology and Evolution, 9 (10), 2782–2790, 2017.

Feichtinger, J., et al. *Meta-analysis of clinical data using human meiotic genes identifies a novel cohort of highly restricted cancer-specific marker genes.* Oncotarget, 3 (8), 843–853, 2012.

Figueroa-Clarevega, A. & Bilder, D. *Malignant Drosophila Tumors Interrupt Insulin Signaling to Induce Cachexia-like Wasting.* Developmental Cell, 33 (1), 47–55, 2015.

Gallach, M., et al. *Analyses of Nuclearly Encoded Mitochondrial Genes Suggest Gene Duplication as a Mechanism for Resolving Intralocus Sexually Antagonistic Conflict in Drosophila.* Genome Biology and Evolution, 2, 835–850, 2010.

Gao, S.P., et al. *Loss of TIM50 suppresses proliferation and induces apoptosis in breast cancer.* Tumor Biology, 37 (1), 1279–1287, 2016.

García-Bellido, A. *Genetic control of wing disc development in Drosophila.* Ciba Foundation symposium, 0 (29), 161–82, 1975.

Garcia-Bellido, A. & Merriam, J.R. *Parameters of the wing imaginal disc development of Drosophila melanogaster.* Developmental Biology, 24 (1), 61–87, 1971.

Gateff, E. *Malignant neoplasms of genetic origin in Drosophila melanogaster.* Science (New York, N.Y.), 200 (4349), 1448–59, 1978.

Gateff, E. *Tumor suppressor and overgrowth suppressor genes of Drosophila melanogaster: developmental aspects.* The International Journal of Developmental Biology, 38 (4), 565–90, 1994.

Gateff, E., et al. *A temperature-sensitive brain tumor suppressor mutation of Drosophila melanogaster: Developmental studies and molecular localization of the gene.* Mechanisms of Development, 41 (1), 15–31, 1993.

Gevorkyan-Airapetov, L., et al. *Interaction of Tim23 with Tim50 Is essential for protein translocation by the mitochondrial TIM23 complex.* The Journal of Biological Chemistry, 284 (8), 4865–72, 2009.

Ghafouri-Fard, S., et al. *Elevated expression levels of testis-specific genes TEX101*

and SPATA19 in basal cell carcinoma and their correlation with clinical and pathological features. British Journal of Dermatology, 162 (4), 772–779, 2009.

Ghafouri-Fard, S., et al. *Expression of Two Testis-specific Genes, SPATA19 and LEMD1, in Prostate Cancer.* Archives of Medical Research, 41 (3), 195–200, 2010.

Goldberg, E., et al. *Cytochrome c: immunofluorescent localization of the testis-specific form.* Science (New York, N.Y.), 196 (4293), 1010–2, 1977.

Gonzalez, C. *Spindle orientation, asymmetric division and tumour suppression in Drosophila stem cells.* Nature Reviews Genetics, 8 (6), 462–472, 2007.

Gonzalez, C. *Drosophila melanogaster: a model and a tool to investigate malignancy and identify new therapeutics.* Nature Reviews Cancer, 13 (3), 172–183, 2013.

Gonzalez, C. & Glover, D. *Techniques for studying mitosis in Drosophila.* In P. Fantes & R. Brooks, eds., *The cell cycle*, chap. Techniques, 143–175. Oxford University Press, Oxford, UK, 1993.

Gonzalez-Roca, E., et al. *Accurate Expression Profiling of Very Small Cell Populations.* PLoS ONE, 5 (12), e14418, 2010.

Goto, H., et al. *Identification of a novel phosphorylation site on histone H3 coupled with mitotic chromosome condensation.* The Journal of Biological Chemistry, 274 (36), 25543–9, 1999.

Greber, B.J. & Ban, N. *Structure and Function of the Mitochondrial Ribosome.* Annual Review of Biochemistry, 85 (1), 103–132, 2016.

Guo, Y., et al. *Tim50, a Component of the Mitochondrial Translocator, Regulates Mitochondrial Integrity and Cell Death.* Journal of Biological Chemistry, 279 (23), 24813–24825, 2004.

Herranz, H. & Cohen, S. *Drosophila as a Model to Study the Link between Metabolism and Cancer.* Journal of Developmental Biology, 5 (4), 15, 2017.

Hevia, C.F. & de Celis, J.F. *Activation and function of TGFβ signalling during Drosophila wing development and its interactions with the BMP pathway.* Developmental Biology, 377 (1), 138–153, 2013.

Hofmann, O., et al. *Genome-wide analysis of cancer/testis gene expression.* Proceedings of the National Academy of Sciences of the United States of America, 105 (51), 20422–7, 2008.

Homem, C.C.F. & Knoblich, J.A. *Drosophila neuroblasts: a model for stem cell biology.* Development, 139 (23), 4297–4310, 2012.

Huang, Z. & Kunes, S. *Hedgehog, transmitted along retinal axons, triggers neurogenesis in the developing visual centers of the Drosophila brain.* Cell, 86 (3), 411–22, 1996.

Hüttemann, M., et al. *Cytochrome c oxidase of mammals contains a testes-specific isoform of subunit VIb-the counterpart to testes-specific cytochrome c?* Molecular Reproduction and Development, 66 (1), 8–16, 2003.

Hüttemann, M., et al. *The multiple functions of cytochrome c and their regulation in life and death decisions of the mammalian cell: From respiration to apoptosis.* Mitochondrion, 11 (3), 369–381, 2011.

Janic, A., et al. *Ectopic Expression of Germline Genes Drives Malignant Brain Tumor Growth in Drosophila.* Science, 330 (6012), 1824–1827, 2010.

Januschke, J. & Gonzalez, C. *Drosophila asymmetric division, polarity and cancer.* Oncogene, 27 (55), 6994–7002, 2008.

Kadenbach, B. & Hüttemann, M. *The subunit composition and function of mammalian cytochrome c oxidase.* Mitochondrion, 24, 64–76, 2015.

Kim, H.J., et al. *Mitochondrial ribosomes in cancer.* Seminars in Cancer Biology, 47, 67–81, 2017.

Knoblich, J.A. *Mechanisms of Asymmetric Stem Cell Division.* Cell, 132 (4), 583–597, 2008.

Koe, C.T. & Wang, H. *Asymmetric Cell Division in Drosophila Neuroblasts.* In *eLS*, 1–14. John Wiley & Sons, Ltd, Chichester, UK, 2016.

Kwon, Y., et al. *Systemic organ wasting induced by localized expression of the secreted insulin/IGF antagonist ImpL2.* Developmental Cell, 33 (1), 36–46, 2015.

Lawrence, P.A. & Struhl, G. *Morphogens, compartments, and pattern: lessons from drosophila?* Cell, 85 (7), 951–61, 1996.

Lewis, P.W., et al. *Identification of a Drosophila Myb-E2F2/RBF transcriptional repressor complex.* Genes & Development, 18 (23), 2929–40, 2004.

Li, X., et al. *Temporal patterning of Drosophila medulla neuroblasts controls neural fates.* Nature, 498 (7455), 456–462, 2013.

Livak, K.J. & Schmittgen, T.D. *Analysis of Relative Gene Expression Data Using Real-Time Quantitative PCR and the 2−ΔΔCT Method.* Methods, 25 (4), 402–408, 2001.

Masgras, I., et al. *The Chaperone TRAP1 As a Modulator of the Mitochondrial Adaptations in Cancer Cells.* Frontiers in Oncology, 7, 58, 2017.

Maxfield, K.E., et al. *Comprehensive functional characterization of cancer–testis antigens defines obligate participation in multiple hallmarks of cancer.* Nature Communications, 6 (1), 8840, 2015.

Meier, K., et al. *LINT, a Novel dL(3)mbt-Containing Complex, Represses Malignant Brain Tumour Signature Genes.* PLoS Genetics, 8 (5), e1002676, 2012.

Mi, Y., et al. *Spata19 is critical for sperm mitochondrial function and male fertility.* Molecular Reproduction and Development, 82 (11), 907–913, 2015.

Mishra, P. & Chan, D.C. *Metabolic regulation of mitochondrial dynamics.* J Cell Biol, 212 (4), 379–387, 2016.

Mollinari, C., et al. *Miranda, a protein involved in neuroblast asymmetric division, is associated with embryonic centrosomes of Drosophila melanogaster.* Biology of the cell, 94 (1), 1–13, 2002.

REFERENCES

Morais, R., et al. *Tumor-forming ability in athymic nude mice of human cell lines devoid of mitochondrial DNA.* Cancer Research, 54 (14), 3889–96, 1994.

Nagaraj, R., et al. *Control of mitochondrial structure and function by the Yorkie/YAP oncogenic pathway.* Genes & Development, 26 (18), 2027–37, 2012.

Narisawa, S., et al. *Testis-specific cytochrome c-null mice produce functional sperm but undergo early testicular atrophy.* Molecular and Cellular Biology, 22 (15), 5554–62, 2002.

Nériec, N. & Desplan, C. *From the Eye to the Brain: Development of the Drosophila Visual System.* Current Topics in Developmental Biology, 116, 247–71, 2016.

Ngo, K.T., et al. *Concomitant requirement for Notch and Jak/Stat signaling during neuro-epithelial differentiation in the Drosophila optic lobe.* Developmental Biology, 346 (2), 284–295, 2010.

Northcott, P.A., et al. *The miR-17/92 polycistron is up-regulated in sonic hedgehog-driven medulloblastomas and induced by N-myc in sonic hedgehog-treated cerebellar neural precursors.* Cancer Research, 69 (8), 3249–55, 2009.

Ohsawa, S., et al. *Mitochondrial defect drives non-autonomous tumour progression through Hippo signalling in Drosophila.* Nature, 490 (7421), 547–551, 2012.

Pavlova, N.N. & Thompson, C.B. *The Emerging Hallmarks of Cancer Metabolism.* Cell Metabolism, 23 (1), 27–47, 2016.

Pérez-Garijo, A., et al. *Apoptotic cells can induce non-autonomous apoptosis through the TNF pathway.* eLife, 2, 2013.

Porporato, P.E., et al. *Mitochondrial metabolism and cancer.* Cell Research, 28 (3), 265–280, 2018.

Richter, C., et al. *The tumour suppressor L(3)mbt inhibits neuroepithelial proliferation and acts on insulator elements.* Nature Cell Biology, 13 (9), 1029–1039, 2011.

Rossi, F. & Gonzalez, C. *Studying tumor growth in Drosophila using the tissue allograft method.* Nature Protocols, 10 (10), 1525–1534, 2015.

Rossi, F., et al. *An n vivo genetic screen in Drosophila identifies the orthologue of human cancer/testis gene SPO11 among a network of targets to inhibit lethal(3)malignant brain tumour growth.* Open Biology, 7 (8), 170156, 2017.

Roy, S., et al. *Essential role of Drosophila black-pearl is mediated by its effects on mitochondrial respiration.* FASEB journal : official publication of the Federation of American Societies for Experimental Biology, 26 (9), 3822–33, 2012.

Rubin, G.M. & Lewis, E.B. *A brief history of Drosophila's contributions to genome research.* Science (New York, N.Y.), 287 (5461), 2216–8, 2000.

Rubin, G.M., et al. *Comparative Genomics of the Eukaryotes.* Science, 287 (5461), 2204–2215, 2000.

Rudrapatna, V.A., et al. *Drosophila cancer models.* Developmental Dynamics, 241 (1), 107–118, 2012.

Saini, N. & Reichert, H. *Neural Stem Cells in Drosophila: Molecular Genetic Mechanisms Underlying Normal Neural Proliferation and Abnormal Brain Tumor Formation.* Stem Cells International, 2012, 1–10, 2012.

Salomon, R.N. & Jackson, F.R. *Tumors of the testis and midgut in aging flies.* Fly, 2 (6), 265–268, 2008.

Sankala, H., et al. *Upregulation of the mitochondrial transport protein, Tim50, by mutant p53 contributes to cell growth and chemoresistance.* Archives of Biochemistry and Biophysics, 512 (1), 52–60, 2011.

Scanlan, M.J., et al. *The cancer/testis genes: review, standardization, and commentary.* Cancer immunity, 4, 1, 2004.

Schneider, D.T., et al. *Molecular genetic analysis of central nervous system germ cell tumors with comparative genomic hybridization.* Modern Pathology, 19 (6), 864–873, 2006.

Selleck, S.B. & Steller, H. *The influence of retinal innervation on neurogenesis in the first optic ganglion of Drosophila.* Neuron, 6 (1), 83–99, 1991.

Senft, D. & Ronai, Z.A. *Regulators of mitochondrial dynamics in cancer.* Current Opinion in Cell Biology, 39, 43–52, 2016.

Shadel, G.S. & Horvath, T.L. *Mitochondrial ROS signaling in organismal homeostasis.* Cell, 163 (3), 560–9, 2015.

Simpson, A.J.G., et al. *Cancer/testis antigens, gametogenesis and cancer.* Nature Reviews Cancer, 5 (8), 615–625, 2005.

Simpson, P., et al. *The initiation of pupariation in Drosophila: dependence on growth of the imaginal discs.* Journal of Embryology and Experimental Morphology, 57, 155–65, 1980.

Slaninova, V., et al. *Notch stimulates growth by direct regulation of genes involved in the control of glycolysis and the tricarboxylic acid cycle.* Open Biology, 6 (2), 150155, 2016.

Song, Z., et al. *DCP-1, a Drosophila cell death protease essential for development.* Science (New York, N.Y.), 275 (5299), 536–40, 1997.

Sonoda, J. & Wharton, R.P. *Drosophila Brain Tumor is a translational repressor.* Genes & Development, 15 (6), 762–773, 2001.

Sotgia, F., et al. *Mitochondria "fuel" breast cancer metabolism: Fifteen markers of mitochondrial biogenesis label epithelial cancer cells, but are excluded from adjacent stromal cells.* Cell Cycle, 11 (23), 4390–4401, 2012.

Southall, T.D., et al. *Cell-type-specific profiling of gene expression and chromatin binding without cell isolation: assaying RNA Pol II occupancy in neural stem cells.* Developmental Cell, 26 (1), 101–12, 2013.

Srivastava, S., et al. *Magmas functions as a ROS regulator and provides cytoprotection against oxidative stress-mediated damages.* Cell Death & Disease, 5 (8), e1394–e1394, 2014.

REFERENCES

St Johnston, D. *The art and design of genetic screens: Drosophila melanogaster.* Nature Reviews Genetics, 3 (3), 176–188, 2002.

Sugiyama, S., et al. *Involvement of the Mitochondrial Protein Translocator Component Tim50 in Growth, Cell Proliferation and the Modulation of Respiration in Drosophila.* Genetics, 176 (2), 927–936, 2007.

Sullivan, L.B. & Chandel, N.S. *Mitochondrial reactive oxygen species and cancer.* Cancer & Metabolism, 2 (1), 17, 2014.

Tanimoto, H., et al. *Hedgehog Creates a Gradient of DPP Activity in Drosophila Wing Imaginal Discs.* Molecular Cell, 5 (1), 59–71, 2000.

Tripoli, G., et al. *Comparison of the oxidative phosphorylation (OXPHOS) nuclear genes in the genomes of Drosophila melanogaster, Drosophila pseudoobscura and Anopheles gambiae.* Genome Biology, 6 (2), R11, 2005.

Vidal, M. & Cagan, R.L. *Drosophila models for cancer research.* Current Opinion in Genetics & Development, 16 (1), 10–6, 2006.

Vincent, J.P. *Compartment boundaries: where, why and how?* The International Journal of Developmental Biology, 42 (3), 311–5, 1998.

Volkenhoff, A., et al. *Glial Glycolysis Is Essential for Neuronal Survival in Drosophila.* Cell Metabolism, 22 (3), 437–447, 2015.

Vyas, S., et al. *Mitochondria and Cancer.* Cell, 166 (3), 555–566, 2016.

Wallace, D.C. *Mitochondria and cancer.* Nature Reviews Cancer, 12 (10), 685–698, 2012.

Wang, C.W., et al. *In vivo genetic dissection of tumor growth and the Warburg effect.* eLife, 5, 2016.

Wang, W., et al. *Notch signaling regulates neuroepithelial stem cell maintenance and neuroblast formation in Drosophila optic lobe development.* Developmental Biology, 350 (2), 414–428, 2011.

Warburg, O. *On the origin of cancer cells.* Science, 123 (3191), 309–314, 1956.

Wasbrough, E.R., et al. *The Drosophila melanogaster sperm proteome-II (DmSP-II).* Journal of Proteomics, 73 (11), 2171–2185, 2010.

Weinberg, S.E., et al. *Mitochondria in the Regulation of Innate and Adaptive Immunity.* Immunity, 42 (3), 406–417, 2015.

Weinhouse, S. *On respiratory impairment in cancer cells.* Science (New York, N.Y.), 124 (3215), 267–9, 1956.

Wen, S., et al. *Targeting cancer cell mitochondria as a therapeutic approach.* Future Medicinal Chemistry, 5 (1), 53–67, 2013.

Weng, M. & Lee, C.Y. *Keeping neural progenitor cells on a short leash during Drosophila neurogenesis.* Current Opinion in Neurobiology, 21 (1), 36–42, 2011.

Weng, M., et al. *Changes in Notch signaling coordinates maintenance and differentiation of the Drosophila larval optic lobe neuroepithelia.* Developmental Neurobiology, 72 (11), 1376–1390, 2012.

Wong, K.K., et al. *Cancer/testis antigen SPATA19 is frequently expressed in benign prostatic hyperplasia and prostate cancer.* APMIS, 125 (12), 1092–1101, 2017.

Yasugi, T. & Nishimura, T. *Temporal regulation of the generation of neuronal diversity in Drosophila.* Development, Growth & Differentiation, 58 (1), 73–87, 2016.

Yasugi, T., et al. *Drosophila optic lobe neuroblasts triggered by a wave of proneural gene expression that is negatively regulated by JAK/STAT.* Development (Cambridge, England), 135 (8), 1471–80, 2008.

Yasugi, T., et al. *Coordinated sequential action of EGFR and Notch signaling pathways regulates proneural wave progression in the Drosophila optic lobe.* Development, 137 (19), 3193–3203, 2010.

Yohn, C.B., et al. *l(3)malignant brain tumor and three novel genes are required for Drosophila germ-cell formation.* Genetics, 165 (4), 1889–900, 2003.